

EFFECTS OF COMPOUNDING ON STRESS-STRAIN
BEHAVIOUR OF NATURAL RUBBER VULCANIZATES

THESIS

presented for the degree of

MASTER OF PHILOSOPHY

in the

UNIVERSITY OF LONDON

and

DIPLOMA OF MEMBERSHIP

of the

IMPERIAL COLLEGE OF SCIENCE AND TECHNOLOGY

by

ALIAS BIN OTHMAN

Malaysian Rubber Producers' Research Association,
Brickendonbury,
Hertford, Hertfordshire

and

Dept of Chemical Engineering and Chemical Technology,
Imperial College of Science and Technology,
London.

April 1983

ABSTRACT

A study was carried out to determine the effects of compounding on the stress-strain behaviour of rubbers. The study was based on a model which expresses a nominal stress as a function of a strain invariant, I_1 and three material constants, A, B and C. Parameter A is the limiting modulus at high strain, the reciprocal of C is the difference between the limiting moduli at low and high strains while B determines the change in modulus between the two limits. In tension, lubricated compression and simple shear, parameters A, B and C for a rubber vulcanizate were the same. The dependence of A, B and C on the types and concentrations of carbon black and crosslink are discussed.

The presence of carbon black has been found to alter the crosslinking efficiency of the vulcanizing systems. When the crosslink density of the peroxide cured rubber was assumed to be unaffected by the presence of carbon black, results showed that the crosslink density of the corresponding rubber crosslinked using the sulphur vulcanizing system increases linearly with the volume fraction of black. A correction to the Guth-Gold type of the hydrodynamic equation used for predicting the modulus of filled rubber, to account for the change in crosslink density of the rubber matrix is proposed.

ACKNOWLEDGEMENTS

The author wishes to express his sincere gratitude to Datuk Haji (Dr.) Ani Arope, the Director of the Rubber Research Institute of Malaysia, for his secondment to the Malaysian Rubber Producers' Research Association, (MRPRA), Brickendonbury, England.

The work described in this thesis was carried out at the Tun Abdul Razak Laboratories, MRPRA and the programme of research was registered at the Imperial College of Science and Technology, University of London. The author is greatly indebted to Dr. M.J. Gregory of MRPRA, his Research Supervisor, Dr. J.S. Higgins, his University Supervisor and Dr. P.B. Lindley, the Head of Engineering Group, MRPRA for their help.

The typing of this thesis by Mrs A. Bland and J.E. Davies is gratefully acknowledged.

CONTENTS

	<u>Page</u>
TITLE PAGE	1
ABSTRACT	2
ACKNOWLEDGEMENTS	3
CONTENTS	4
LIST OF FIGURES	8
LIST OF TABLES	11
NOTATION	13
SECTION 1	GENERAL INTRODUCTION
	17
1.1	Objective and scope of the present investigation
	18
1.2	Natural rubber
	19
1.2.1	Chemical structure
	19
1.2.2	Vulcanization
	20
1.2.3	Compounding
	20
1.2.4	Crosslinks
	22
SECTION 2	ELASTICITY OF UNFILLED AND FILLED RUBBERS
	27
2.1	Theories of Rubber-Like Elasticity
	28
2.1.1	Introduction
	28
2.1.2	The statistical theory of Elasticity
	28
2.1.3	Phenomonological Theories of Elasticity
	39
2.1.3.1	The Theory of Mooney
	40
2.1.3.2	The Theory of Rivlin
	43
2.1.3.3	Alternative Forms of Stored Energy Function
	48

		<u>Page</u>
2.2	Effects of carbon black on rubber vulcanizates	53
2.2.1	Introduction	53
2.2.2	The nature and classification of carbon black	53
2.2.3	The stiffening effects of carbon black	59
2.2.3.1	Hydrodynamic effects	59
2.2.3.2	Interaggregate interactions	63
SECTION 3	EXPERIMENTAL	68
3.1	Experimental techniques	69
3.1.1	Materials	69
3.1.2	Preparation of test specimens	71
3.1.2.1	Tensile test-pieces	72
3.1.2.2	Compression test-pieces	74
3.1.2.3	Shear test-pieces	75
3.1.3	Instrumentation	77
3.1.4	Stress-strain measurements	81
3.1.4.1	Uniaxial extension	81
3.1.4.2	Lubricated compression	82
3.1.4.3	Simple shear	86
3.1.5	Equilibrium swelling measurements	87
3.2	Experimental discussions	89
3.2.1	Uniaxial extension	89
3.2.1.1	Effects of measurement techniques	89
3.2.1.2	Effects of types of test-piece	95
3.2.1.3	Effects of anisotropy	97
3.2.2	Lubricated compression	97

		<u>Page</u>
3.2.2.1	Effects of types of test-piece	97
3.2.3	Simple shear	102
3.2.3.1	Effects of types of test-piece	102
3.3	Conclusions	105
SECTION 4	STRESS-STRAIN RELATIONSHIP FOR FILLED AND UNFILLED RUBBERS	107
4.1	Introduction	108
4.2	A form of stress-strain relationship	122
4.3	Verification of stress-strain relationship	125
4.3.1	The correlation between stress and strain	125
4.3.2	Comparisons between experimental and predicted values	130
4.4	Physical significance of parameters A, B and C	139
SECTION 5	EFFECTS OF COMPOUNDING ON PARAMETERS A, B AND C	141
5.1	Introduction	142
5.2	Parameter A	142
5.2.1	Effects of crosslink density	142
5.2.2	Effects of carbon black	148
5.2.3	The enhancement of crosslink density	164
5.3	Parameter C	169
5.3.1	Effects of crosslink density	169
5.3.2	Effects of interparticle distance	173
5.3.3	A combined function of crosslink density and interparticle distance	175
5.4	Parameter B	177

	<u>Page</u>
SECTION 6 SUMMARY AND CONCLUSIONS	184
APPENDIX	188
REFERENCES	191

		<u>Page</u>
Figure		
1.1	Structural features of an accelerated sulphur vulcanizate of natural rubber.	23
2.1	Effects of chain deformation	31
2.2	Types of strain (a) unstrained unit cube (b) simple extension (c) uniaxial compression (d) simple shear.	36
2.3	Comparison between the experimental curve with the theoretical form for simple extension (24).	38
2.4	Mooney-Rivlin plot for data of simple extension and uniaxial compression (28).	42
2.5	Variations of $\frac{\partial W}{\partial I_1}$ and $\frac{\partial W}{\partial I_2}$ with I_1 and I_2 (31).	47
2.6	Idealized plot of shear modulus as a function shear strain.	64
3.1	Tensile test-pieces: (a) parallel sided dumbell (or bongo) and (b) type C dumbell.	73
3.2	Shear test-pieces: (a) Double and (b) quadruple.	76
3.3	Grips for tensile-test (a) spring loaded (b) pulley.	79
3.4	Grips for shear-test (a) collar (b) notched.	80
3.5	Pull test.	84
3.6	Coefficients of sliding friction, μ , as a function of applied load.	85
3.7	Effects of modulus on techniques of measurement for parallel sided dumbell samples.	92
3.8	Effects of modulus on techniques of measurement for ring samples.	96
3.9	Effects of modulus on types of test-piece.	98
3.10	Effects of modulus on sample geometry for moulded samples.	100
3.11	Effects of modulus on sample geometry for plied-up samples.	101
3.12	Effects of shear modulus on types of test-piece.	104

	<u>Page</u>
Figure	
4.1	Relation between λ_1 and λ_2 at constant I_1 and I_2 (28). 111
4.2	Shear, tensile and compressive moduli as a function of $(I_1-3)^{\frac{1}{2}}$. 113
4.3	Effects of cyclic deformation on tensile modulus of 40 pphr N347 black filled rubbers. 117
4.4	Shear, tensile and compressive moduli as a function of $(I_1-3)^{\frac{1}{2}}$ for 25 pphr N330 black filled rubber. 119
4.5	Shear, tensile and compressive moduli as a function of $(I_1-3)^{\frac{1}{2}}$ for 60 pphr N347 black filled rubbers. 120
4.6	Shear stress as a function of shear strain for rubbers filled with 25 pphr N330 black. 123
4.7	$(H-A)^{-1}$ as a function of $(I_1-3)^{\frac{1}{2}}$ for rubbers filled with 20 pphr N347 black. 127
4.8	$(H-A)^{-1}$ as a function of $(I_1-3)^{\frac{1}{2}}$ for rubbers filled with 60 pphr N347 black. 128
4.9	Comparison between experimental and predicted tensile moduli. 135
4.10	Comparison between experimental and predicted compressive moduli. 136
4.11	Comparison between experimental and predicted shear moduli. 137
5.1	Parameter A as a function of (phr S) for unfilled and rubbers filled with N347 black. 143
5.2	Parameter A as a function of (phr S) for rubbers filled with N550 black. 144
5.3	Parameter A as a function of (phr DCP) for unfilled and rubbers filled with N347 black. 146
5.4	Parameter A as a function of (phr DCP) for rubbers filled with N550 black. 147
5.5	$\left(\frac{A}{A_0} - 1 \right)$ as a function of ϕ for rubbers filled with 150
	$\frac{\quad}{\phi}$
	different blacks and crosslinked using different vulcanizing systems.

Figure		<u>Page</u>
5.6	$\frac{Q}{Q_0}$ as a function of e^{-z} for rubbers filled with N347 black.	157
5.7	Values of $\frac{\eta}{\eta_0}$ as a function of ϕ for rubbers filled with N347 black and crosslinked using different vulcanizing systems.	161
5.8	$\frac{\left(\frac{A}{A_m} - 1\right)}{\phi}$ as a function of ϕ for N347 black filled rubbers crosslinked using the four different vulcanizing systems.	165
5.9	$\frac{\left(\frac{A}{A_m} - 1\right)}{\phi'}$ as a function of ϕ' for the N347 black filled rubbers crosslinked using the four different vulcanizing systems.	168
5.10	Variations of $\frac{C_0}{C\left(\frac{A}{A_m}\right)}$ with crosslink density for rubbers filled with N347 black.	174
5.11	$\frac{C_0}{C\left(\frac{A}{A_m}\right)}$ as a function of reciprocal of interparticle distance for rubbers crosslinked using the sulphur vulcanizing system.	176
5.12	$\frac{C_0}{C\left(\frac{A}{A_m}\right)}$ as a function of $n\left(\frac{1}{d}\right)^{2.5}$ for rubbers of different types and concentrations of crosslink.	178
5.13	Parameter B as a function of $S\left(\frac{\phi}{1-\phi}\right)$ for rubbers filled with different types of black crosslinked using the sulphur vulcanizing systems.	181
5.14	Parameter B as a function of $S\left(\frac{\phi}{1-\phi}\right)$ for rubbers filled with different types of black and crosslinked using the peroxide system.	182

LIST OF TABLES

<u>Table</u>		<u>Page</u>
1.1	The proportion of sulphur and accelerator for conventional, semi-EV and EV systems (4).	23
1.2	Approximate types of crosslink present in accelerated sulphur systems at optimum cure.	25
2.1	Second digit classification in ASTM system.	58
3.1	Grades of carbon black used.	69
3.2	Formulations	70
3.3	Natural rubber cement	74
3.4	Values of creep calculated from stress-relaxation using conversion factor α at $t = 2$ minutes.	90
3.5	Effects of sample slippage on modulus.	93
3.6	Effects of sample contraction (Quadruple shear).	103
4.1	Relative contribution of the terms given by the James and Green formula for simple extension.	115
4.2	Values of A, B and C for unfilled rubbers.	129
4.3	Values of A, B and C for the sulphur cured N550 black filled rubbers.	131
4.4	Values of A, B and C for the sulphur cured N347 black filled rubbers.	132
4.5	Values of A, B and C for the peroxide cured N550 and N347 black filled rubbers.	133
5.1	Experimental and calculated values of A.	148
5.2	Values of $F'(\phi)$ for the sulphur cured (semi-EV) rubbers.	153

<u>Table</u>		<u>Page</u>
5.3	Influence of carbon black on crosslink density of rubbers crosslinked using different vulcanizing systems.	159
5.4	Influence of carbon black on experimental values of A and of the rubber matrix, A_m .	166
5.5	Effects of crosslink density and black loading on parameter C for rubbers filled with N550 black.	170
5.6	Effects of crosslink density and black loading on parameter C for rubbers filled with N347 black.	171
5.7	Values of $\frac{C_o}{CX}$ for rubbers crosslinked using different vulcanizing systems.	172

NOTATION

A, A_0	limiting modulus at high strain for filled and unfilled rubber; constants in the proposed equation 4.15.
A_m	limiting modulus at high strain for the rubber matrix.
A_0, A_1, a_0, a_1, a_2	constants for the Obata's equation (equation 4.3).
a	constant representing the contribution due to chain entanglements (equation 4.3).
a	constant in the Lorenz and Park's equation (equation 5.11).
a_n, a_1, a_2, a_3	constants in the Odgen's stored energy function.
B, B_0	constants in the proposed equation (4.15) representing values for filled and unfilled rubbers.
b	constant in equation 2.1, characterizing the chain geometry.
b	constant in the Lorenz and Park's equation.
C, C_0	constants in the proposed equation (4.15), representing values for filled and unfilled rubbers.
C	constant in equation 2.4.
C	constant in equation 2.53.
C	volume concentration of filler particles (equation 2.58).
C_1, C_2	the Mooney constants.
C_{ij}	constant in the Rivlin's equation.
C_R	rate of creep.
c	a filler constant (equation 5.10)
D	diameter of black particle
d	interparticle distance

e	change in length divided by the original length (or strain).
E, E_0	Young's Modulus of filled and unfilled rubbers.
F	Pull force (section 3.1.4.2a).
f	shape factor of filler particle/aggregate
G	shear modulus
G_0, G_∞	limiting shear modulus at low and high strains
H	tensile or compressive modulus.
H_0, H_∞	limiting tensile/compressive modulus at low and high strains
I_1, I_2, I_3	the strain invariants
k	the Boltzmann constant
k	constant in equation 4.8
k_1, k_2, k_3	reaction rate constants
l	bond length
M	molecular weight of rubber network
M_c	molecular weight between crosslinks
N	total number of chains in a unit volume
n	number of links or bonds
p	hydrostatic pressure
p	probability
Q, Q_0, Q_m	weights of solvent imbibed per unit weight of rubber for filled, unfilled and that of rubber matrix.
R	gas constant
r_0, r	vectors representing end to end distances of undeformed and deformed chains

S_0, S	entropy of a single chain before and after deformation
S_R	rate of stress relaxation
T	temperature
t	time
t_i, t_1, t_2, t_3	true stress or stress per unit strained area
V	molar volume of solvent/swelling agent
V_{r_0}, V_r	volume fraction of swollen unfilled and filled rubbers
W	stored energy function
W	normal stress
w	function of strain (equation 2.49)
X	scaling factor for filled rubber
x, y, z	axes of the rectangular co-ordinate system
z	weight of filler per unit weight of rubber
α	Gent's conversion factor (equation 3.1)
α, β	constants associated with shape factor and occluded volume (equation 5.4)
α, β, γ	constant for the Tobisch equation (equation 2.57)
γ	shear strain
η_0, η	crosslink density of unfilled and filled rubbers
η_0, η	viscosity of liquid and suspension (equation, 2.58)
ρ	density of rubber
ρ_s	density of n-decane
σ	stress per unit unstrained area or nominal stress
μ_n	constant for the Odgen's equation
μ	coefficient of sliding friction
λ	extension ratio
χ	rubber-solvent interaction parameter

ϕ	volume fraction of filler
ϕ'	effective volume fraction of filler
ϕ_{occ}	volume fraction of occluded rubber
ϕ	angle of shear (equation 2.2.1)
$\bar{\phi}, \bar{\phi}_1, \bar{\phi}_2$	functions of strain invariants for the Rivlin equation

SECTION 1: GENERAL INTRODUCTION

1.1 Objective and scope of the present investigation

1.2 Natural rubber

1.2.1 Chemical structure

1.2.2 Vulcanization

1.2.3 Compounding

1.2.4 Crosslinks

SECTION 1 GENERAL INTRODUCTION

1.1 Objective and scope of the present investigation

In engineering applications, rubbers are mostly subjected to low to moderate strains. In compression, for instance, rubbers are generally deformed to about 15%, while in shear, strains of up to 100% are sometimes employed. There are various theories which provide the relationships between stress and strain for low to moderate strains but in general they are not applicable to filled rubbers. Thus, a satisfactory prediction of a stress at any defined strain or vice-versa of components made from filled rubber cannot be made.

The objective of the studies described in this thesis is to find a relationship between stress and strain which is applicable to both filled and unfilled rubbers and to determine the effects of compounding on the stress-strain behaviour, so that an adequate description of the elastic behaviour of rubbers can be made.

The experimental work carried out is discussed in section 3. The effects of measurement techniques and types of test-piece on the stress-strain measurements were investigated using three simple modes of deformation viz. simple extension, lubricated compression and simple shear at low to moderate strains.

Section 4 gives the derivation of a relationship between the stress and strain for different modes of deformation and the verification of the proposed relationship.



The effects of compounding on the stress-strain behaviour are discussed in section 5. The variables investigated were the effects of types and concentrations of crosslink and carbon black.

The conclusions of the studies described in this thesis are given in section 6.

1.2 Natural rubber

Natural rubber comes from the latex of many plants, the major source being *Hevea Brasiliensis*, a large tree which is indigenous to South America and which is cultivated mainly in South East Asia and West Africa. The coagulum, obtained by treatment of the latex with acid, followed by washing and drying, contains a high proportion of hydrocarbon mixed with proteins, resins and other constituents. The non-rubber contents are usually characterised analytically as "acetone soluble", nitrogen and ash. A typical analysis of the raw rubber on weight basis being: hydrocarbon 94.5%, acetone soluble 2.8%, nitrogen 0.4% (in a form of protein), ash 0.2%, with the rest being moisture (1).

1.2.1 Chemical Structure

Natural rubber hydrocarbon consists of linear chain cis-1,4, polyisoprene having a number average molecular weight of about 10^6 . It has the same empirical formula as Gutta-percha, $(C_5H_8)_n$, having one carbon-carbon double bond for each C_5H_8 unit, the difference being solely in the arrangement of the carbon-carbon bond adjacent to the double bond. In natural rubber, the single bonds both lie on the same side of the double bond (ie ) forming the cis-configuration, whilst in Gutta-percha, the single bonds lie on the opposite sides of the double bond (ie ) to form the trans-configuration (2). These differences give markedly different physical properties for the two materials, with natural rubber being rubbery at room temperature while Gutta-percha is a crystalline solid.

1.2.2 Vulcanization

Raw rubber is a mass of soft-flexible material. It shows viscoelastic properties since the molecules interact strongly with their neighbours through the attractive forces and physical entanglements. Being uncrosslinked, the rubber does not exhibit wholly elastic properties. Unvulcanized rubber is tacky when hot and slowly crystallises to a rather hard and tough material when stored at low temperature ($<15^{\circ}\text{C}$). In the unvulcanized state, raw rubber has rather limited uses but it can be transformed from its predominantly plastic state to a highly elastic state through a process called vulcanization.

Vulcanization consists, essentially, of chemical crosslinking of rubber molecules to form a three dimensional network. It is generally carried out under pressure at high temperature (normally $>100^{\circ}\text{C}$). Vulcanized rubber is generally referred to simply as "rubber", a term which is used in this thesis.

1.2.3 Compounding

Commercial rubber, in its usual form, requires compounding prior to vulcanization. This is a process of blending the rubber with vulcanizing agents and other substances to produce a homogeneous mix. The compounding ingredients, may be classified, in the approximate order of importance as:

- (a) Vulcanizing agents
- (b) Accelerators
- (c) Accelerator modifiers
- (d) Fillers
- (e) Processing aids
- (f) Protective agents
- (g) Others

Any chemicals which are capable of forming crosslinks between the rubber chains can act as vulcanizing agents, but the preferred agent is still sulphur.

When sulphur and rubber are heated together, a very slow crosslinking reaction takes place. In order to speed up the reaction processes, organic accelerators are used, and the major functions of the accelerators (when used in conjunction with auxiliary agents) are:

- (a) To increase the rate of sulphur reacting with rubber
- (b) To increase the efficiency of the utilization of sulphur as a crosslinking agent and thereby producing a simpler network structure.

Various types of accelerator are available and the types used depend mainly on the processing stages involved. The sulphenamide (N-cyclobenzothiazole sulphenamide) was used for this thesis because it gives a fairly long (>20 minutes at 120°C) scorch time (i.e. time before onset of crosslinking) thus allowing a reasonable length of time for the mixing processes.

The organic accelerator used in the sulphur vulcanizing systems requires Zinc oxide and a fatty acid (normally Stearic acid) as auxiliary agents or accelerator modifiers. The Zinc oxide-fatty acid system are also known as activators. Their function in the crosslinking process is mainly to interact with the accelerator to form an active sulphurating complex prior to the attack on the rubber chain. When dicumyl peroxide is used as the vulcanizing agent, no activator is required.

Unfilled or pure gum rubbers are not suitable for most practical applications because they are too soft. Fillers are therefore added

to stiffen the product. Carbon black is the most popular type of filler which is used to increase the rubber stiffness.

When fillers are mixed with rubber, the use of process oils is necessary. These are hydrocarbon oils and their presence reduces the frictional energy generated during mixing.

Protective agents are added to protect the rubber from degradation. The types of protective agent used depend on the use of the finished product. Waxes, for instance, are incorporated to protect the rubber against ozone attack while chemicals such as 1,2-dihydro 2,2,4-trimethyl 6-phenyl quinoline are used to protect against oxidative degradation.

Apart from the compounding ingredients discussed above, there are other substances which are added for certain specific purposes, where their presence does not significantly alter the physical properties or the service life of the products. Among these substances are the colouring pigments, used to make articles look attractive and deodorant used for imparting a pleasant scent.

Mixing of the compounding ingredients with rubber is usually carried out on an open two roll mill or in an internal mixer, details of which are discussed in section 3.

1.2.4 Crosslinks

Different types of vulcanization system produce different types of crosslink. The accelerated sulphur vulcanizing system produces three different types of crosslink, namely the mono-, di- and polysulphidic types (3). The structural features of vulcanizates of rubber crosslinked using an accelerated sulphur system may be represented pictorially in figure 1.1. Apart from crosslinks,

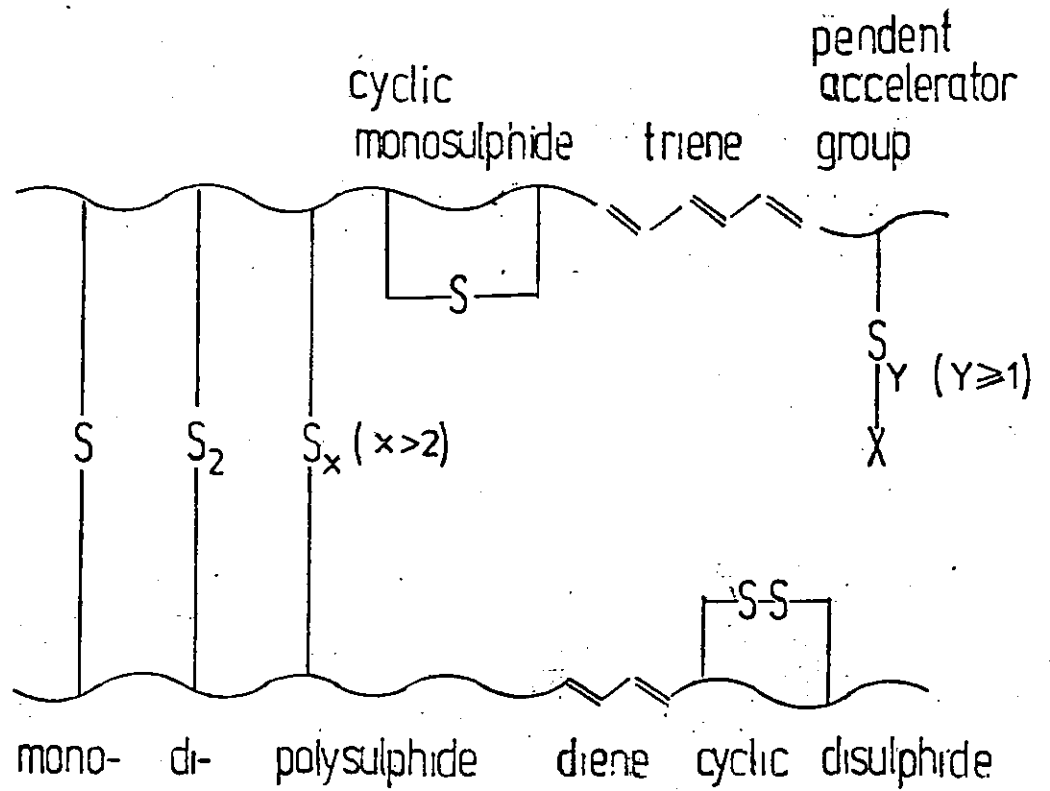


Figure 1.1. Structural features of an Accelerated Sulphur Vulcanizate of Natural Rubber.

cyclic mono- and di-sulphides, pendent sulphide groups containing accelerator fragments and conjugated diene and triene units are also present.

There is an accepted terminology for the accelerated sulphur vulcanizing system. Conventional systems contain much higher concentrations of sulphur than accelerator, efficient vulcanization systems (EV) contain a much lower concentration of sulphur than accelerator and semi-efficient vulcanization systems (semi-EV) are between the first two extremes. Typical concentrations of sulphur and accelerator used for the above three systems in parts per hundred parts by weight of rubber (pphr) are given in table 1.1.

Table 1.1 The proportions of sulphur and accelerator used for conventional, Semi-EV and EV systems (4)

Curing Systems	Sulphur (pphr)	Accelerator (pphr)
Conventional	2.0 - 3.5	0.4 - 1.0
Semi-EV	1.0 - 1.7	1.6 - 2.5
EV	0.3 - 0.8	2.5 - 6.0

The relative proportion of different types of sulphidic crosslink present in an accelerated vulcanizing system depends on the concentrations of sulphur and accelerator. A higher concentration of sulphur in relation to accelerator (i.e. conventional systems) gives a higher proportion of di- and polysulphidic crosslinks while those containing a lower concentration of sulphur relative to the concentration of accelerator give a higher yield of monosulphidic

crosslinks. The approximate proportion of these crosslinks present in the three different systems are given in table 1.2.

Table 1.2 Approximate types of crosslink present in the
accelerated sulphur systems at optimum cure

Vulcanization system Crosslinks	Conventional	Semi-EV	EV	Peroxide
	Poly and di-sulphidic ($-\text{S}_x-$, $-\text{S}_2-$)	95%	50%	20%
Monosulphidic ($-\text{S}-$)	5%	50%	80%	-
Carbon-carbon (C-C)	-	-	-	100%

Polysulphidic crosslinks are thermally less stable than mono or di-sulphidic types of crosslink. Thus, variation in time and temperature of vulcanization also changes the proportion of different types of crosslink (5).

Organic peroxides, such as dicumyl peroxide form carbon to carbon crosslinks. The crosslinks are formed without the use of any catalyst or accelerator, so normally their formation requires high temperature or long cure times.

Different vulcanizing systems impart different properties to the rubber vulcanizates. Conventional systems give rubber with higher tensile and tear strengths than rubber cured with an EV system and these in turn are stronger than rubbers crosslinked using the peroxide vulcanizing system. These differences are due to variation in bond energies for the rupture of the crosslinks, with

the S-S < C-S < C-C bonds; the weakest bond gives the strongest rubber because it is labile and able to break under stress, thus giving a yield mechanism for the dissipation of stress at the critical point of incipient failure (6).

The ranking of vulcanized rubbers to heat resistance is the reverse order to that based on its strength properties. This is because the C-C crosslinks are more stable to heat than the monosulphidic crosslinks, and the polysulphidic crosslinks are the least stable. The order of heat resistance for rubbers crosslinked using different vulcanizing systems is as follows:

Conventional < Semi EV < EV < Peroxide .

The crosslink density (or number of crosslinks per unit volume) also affects the physical properties of rubbers (6). The modulus and hardness, for instance, both increase with crosslink density because more network chains are available to bear the stresses. The tensile strength, on the other hand, initially increases with crosslink density for the same reason as that of the modulus and hardness, but it reaches a maximum and finally starts to decrease as the network chains become shorter and less extensible. Hence, the network is prone to rupture before appreciable orientation has occurred and ultimately the loss in extensibility is accompanied by a loss in strength.

SECTION 2: ELASTICITY OF UNFILLED AND FILLER RUBBERS

- 2.1. Theories of Rubber-like Elasticity
 - 2.1.1. Introduction
 - 2.1.2. The Statistical Theory of Elasticity
 - 2.1.3. Phenomenological Theories of Elasticity
 - 2.1.3.1. The Theory of Mooney
 - 2.1.3.2. The Theory of Rivlin
 - 2.1.3.3. Alternative Forms of Stored Energy Function

- 2.2. Effects of carbon black on rubber vulcanizates
 - 2.2.1. Introduction
 - 2.2.2. The nature and classification of carbon black
 - 2.2.3. The stiffening effects of carbon black
 - 2.2.3.1. Hydrodynamic effects
 - 2.2.3.2. Interaggregate interactions

2.1 Theories of Rubber-like Elasticity

2.1.1 Introduction

Rubber-like materials (7) are long chain molecules with chemical structures permitting free rotation of segments of molecules about their chemical bonds in many places and sufficiently small intermolecular forces to take up random configurations. The linear distances between the ends of the molecules form a normal distribution about the most probable value (8-14). Irrecoverable deformation or flow is prevented by some permanent connections between molecules such as the chemical crosslinks introduced during vulcanization. The interlocking of the molecules at few places along the chain length forms a three dimensional network.

The kinetic theory of elasticity of rubber-like materials was put forward by Meyer, Von Susich and Valko (8). It was based on the concept that the rubber-like materials can take up various conformations by virtue of the independent vibrations and rotations of the individual atoms of the chain due to thermal Brownian motion. Of all the conformations which may arise as a result of these random rotations, the great majority will be of the highly irregular kinked forms. When the chain is straightened out by an application of a force to its ends the entropy decreases because the freedom of the chains to take up different configurations is limited, but on removal of the force the chain will return in the course of time to one of its original form i.e. it will exhibit the property of elasticity. This forms the fundamental concept of the now generally accepted theory of rubber elasticity.

2.1.2 The Statistical Theory of Elasticity

The statistical treatment requires the calculation of the entropy of the whole assembly of chains as a function of the microscopic state

of strain in the sample and the derivation of the free energy or work of deformation from that. The work done in deforming the rubber elastically is considered to arise from the decrease in entropy when the molecules are forced by deformation to take up less probable configurations (8-14). From the work of deformation, corresponding to a given state of strain, the associated stresses are then readily derived from the application of mechanics.

The development of the theory for a crosslinked rubber has been carried out by a number of workers (8-14) and the assumptions made are listed in the appendix.

The quantitative analysis of the change of entropy with deformation and network structure has been successfully carried out using a modified molecular model consisting of hypothetical chains of freely jointed links about which there is a complete freedom of rotation; other than by the crosslinks, no interaction occurs between elements of the chains (assumption a).

The configuration of the freely jointed chain resembles the path described by a diffusing gas molecule. If one end of a chain containing n links each of length l is considered to be at the origin of the coordinate system (x, y, z) and the other held in a small volume element $\Delta\mathcal{V}$ ($=\Delta x\Delta y\Delta z$) at a point (x_0, y_0, z_0) , the probability of such positions for the chain ends is given by,

$$p(x_0, y_0, z_0)\Delta x\Delta y\Delta z = \left(\frac{b}{\pi^2}\right)^3 \exp[-b^2(x_0^2 + y_0^2 + z_0^2)]\Delta x\Delta y\Delta z \quad (2.1)$$

where $b^2 = \frac{3}{2nl^2}$. The function $p(x_0, y_0, z_0)$ is the probability function or probability per unit volume (sometimes referred to as the probability density).

The entropy of a system (S_o) is related to the number of possible configurations by Boltzmann's relation,

$$S_o = k[\ln p(x_o, y_o, z_o)\Delta\tau] \quad (2.2)$$

where k is the Boltzmann constant. Substituting (2.1) into (2.2) gives

$$\begin{aligned} S_o &= k\left[\ln\left(\frac{b}{\pi^{\frac{1}{2}}}\right)^3 \exp(-b^2 r_o^2)\Delta\tau\right] \\ &= k\left[\ln\left(\frac{b}{\pi^{\frac{1}{2}}}\right)^3 - b^2 r_o^2 + \ln\Delta\tau\right] \end{aligned} \quad (2.3)$$

where $r_o (= \sqrt{x_o^2 + y_o^2 + z_o^2})$ is a vector representing the end-to-end distance of an undeformed chain. Since the volume element $d\tau$ is assumed constant, then equation (2.3) may be written as

$$S_o = C - kb^2 r_o^2 = C - kb^2 (x_o^2 + y_o^2 + z_o^2) \quad (2.4)$$

where C is an arbitrary constant which includes the volume element $d\tau$. Equation (2.4) shows that the entropy of the chain is maximum when the two ends of the chain are coincident (i.e. $r = 0$) and decreases continuously with increasing distance between the ends.

When the chain is subjected to a pure homogeneous strain^{*}, the coordinate of the free end of the chain changes from (x_o, y_o, z_o) to (x, y, z) and the vector representing the end-to-end distance correspondingly changes from r_o to r (Figure 2.1). The affine

*In a pure homogeneous strain, the principal extension ratios λ are along the three mutually perpendicular axes. Under such strain, a cube is transformed into a rectangular parallel piped having three unequal lengths $\lambda_1, \lambda_2, \lambda_3$. These extension ratios may either be greater than 1 corresponding to a stretch or less than 1, corresponding to a compression, provided that the volume is constant, i.e. $\lambda_1 \lambda_2 \lambda_3 = 1$ (assumption C).

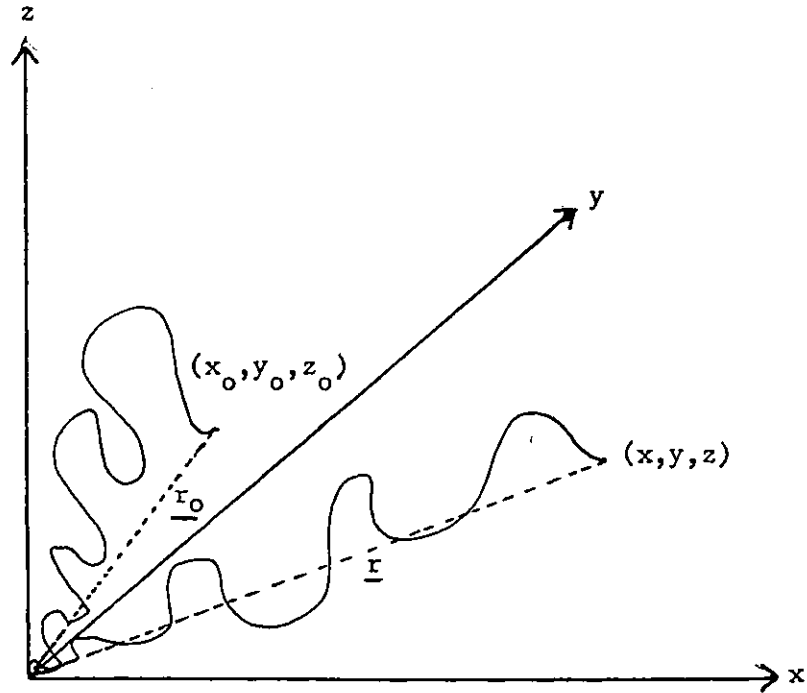


Figure 2.1 Effects of chain deformation

deformation assumption implies that the relative displacement of the chain ends is defined by the macroscopic deformation (assumption d). Thus on deformation, when the axes of coordinates are chosen to coincide with the principal axes of strain, then

$$\begin{aligned}
 x &= \lambda_1 x_0 \\
 y &= \lambda_2 y_0 \\
 z &= \lambda_3 z_0
 \end{aligned}
 \tag{2.5}$$

where λ_1 , λ_2 and λ_3 are the three principal extension ratios referred to the unstrained state. The entropy of the chain before deformation is given by equation (2.4) and the corresponding entropy of the chain after deformation will be

$$S = C - kb^2(\lambda_1^2 x_o^2 + \lambda_2^2 y_o^2 + \lambda_3^2 z_o^2) \quad (2.6)$$

The change in entropy from an undeformed to a deformed state of strain will be

$$\Delta S = S - S_o = -kb^2[(\lambda_1^2 - 1)x_o^2 + (\lambda_2^2 - 1)y_o^2 + (\lambda_3^2 - 1)z_o^2] \quad (2.7)$$

The total entropy for all N chains contained in a unit volume of network is obtained by summation of all the changes in entropies for the individual chains (assumption e). Thus, the total entropy change is given by

$$\Delta S = -kb^2[(\lambda_1^2 - 1)\sum x_o^2 + (\lambda_2^2 - 1)\sum y_o^2 + (\lambda_3^2 - 1)\sum z_o^2] \quad (2.8)$$

The terms $\sum x_o^2$, $\sum y_o^2$ and $\sum z_o^2$ are the sums of squares of the x, y and z components respectively in the unstrained state of the network for the assembly of N chains. Since the directions of the chain vectors r_o in the unstrained state are entirely random, there were no preferences for the x, y and z directions. Hence, remembering that,

$$\sum x_o^2 + \sum y_o^2 + \sum z_o^2 = \sum r_o^2 \quad (2.9)$$

we may write

$$\sum x_o^2 = \sum y_o^2 = \sum z_o^2 = \frac{1}{3}\sum r_o^2 \quad (2.10)$$

$$\text{Therefore, } \Delta S_N = -\frac{1}{3}kb^2 \sum r_o^2 (\lambda_1^2 + \lambda_2^2 + \lambda_3^2 - 3) \quad (2.11)$$

$$\text{By definition, } \langle r_o^2 \rangle = \frac{\sum r_o^2}{N} \quad (2.12)$$

where $\langle r_o^2 \rangle$ is the mean square end-to-end distance of the chains in the unstrained state. Rearranging (2.12) and substituting into equation (2.11) gives

$$\Delta S_N = -\frac{1}{3} Nkb^2 \langle r_o^2 \rangle (\lambda_1^2 + \lambda_2^2 + \lambda_3^2 - 3) \quad (2.13)$$

If we introduce the assumption that the mean-square end-to-end distance in the unstrained state is the same as for a corresponding set of free chains (assumption f), we have $\langle r_o^2 \rangle = \frac{3}{2b^2}$, which on insertion into equation (2.19) gives

$$\Delta S_N = -\frac{1}{2} Nk(\lambda_1^2 + \lambda_2^2 + \lambda_3^2 - 3) \quad (2.14)$$

Equation (2.14) does not contain the parameter b , which is a function of the contour length. It follows that, the same formula could be applied to chains having different contour lengths, such as randomly crosslinked rubber. Assuming, in accordance with the basic principles of the kinetic theory, that there is no change in internal energy on deformation (15-17) then the work of deformation (or Helmholtz free energy) is given by

$$W = \frac{1}{2}G (\lambda_1^2 + \lambda_2^2 + \lambda_3^2 - 3) \quad (2.15)$$

where $G = NkT$ and T is the absolute temperature. W represents the elastically stored free energy per unit volume of rubber and is also known as the strain energy function. The elastic constant, G , is related to the number average molecular weight, M_c of the chains (i.e. segment of molecules between successive crosslinks) by,

$$G = \frac{\rho RT}{M_c} \quad (2.16)$$

where ρ is the density of the rubber and R is the gas constant.

Equation (2.16) assumes that the rubber network is perfect in that all chains in the network are effective in giving rise to the elastic stress. Ideally each crosslink connects four network chains. In reality however, a number of imperfections are possible. Even if

the molecules are all connected by crosslinks, each chain with molecular weight M must give rise to two terminal chains that are incapable of supporting stress. Thus the number of effective chains must not include the imperfections due to chain ends. Taking the terminal chains or loose ends into consideration, Flory (18) expressed G as

$$G = \left(\rho \frac{RT}{M_c} \left(1 - \frac{2M_c}{M} \right) \right) \quad (2.17)$$

where the second term in the bracket represents the contribution from the loose ends. Note, however, that if we assume that the initial molecular weight of polymer is infinite or sufficiently large, equation (2.17) reduces to equation (2.16) (ie as $\frac{1}{M} \rightarrow 0$).

Another type of deviation from an ideal network structure is the effect of chain entanglements (18). The effects would impose additional conformational restrictions on the network chains, and thus produce the effect of quasi-crosslinks in increasing the elastic stress. Since in reality, the chains are rather closely packed together, one might expect that several entanglements would occur between the crosslinks. Thus their contribution to the stress may be quite significant, especially for chains that are long enough to permit a number of such entanglements. The effects of entanglements on the elastic stress have been studied by a number of authors (18-22) and empirical methods have been proposed to account for the effects. In the absence of an effective way to calculate the number of entanglements, we could in general add its contribution to the shear modulus (22) as

$$G = \left(\rho \frac{RT}{M_c} + a \right) \left(1 - \frac{2M_c}{M} \right) \quad (2.18)$$

where a represents the entanglement contribution.

In addition to terminal chains and entanglements, there are other types of network imperfection which do not contribute to the elastic stress such as inter-chain loops (18). Unfortunately owing to its complexity, it is at present impossible to characterise completely the network structure of a rubber.

In simple extension (figure 2.2b) whereby during deformation one dimension of the specimen is increased in the ratio λ_1 and the other two dimensions are correspondingly reduced by $1/\sqrt{\lambda_1}$ (since the volume was assumed to be constant), the strain energy function is given by

$$W = \frac{1}{2} G (\lambda_1^2 + \frac{2}{\lambda_1} - 3) \quad (2.19)$$

The force required to extend the network chain in the direction λ_1 will be

$$\sigma = \frac{dW}{d\lambda_1} = G(\lambda_1 - \lambda_1^{-2}) \quad (2.20)$$

where σ is the force per unit cross-section area measured in the unstrained state (or nominal stress).

Uniaxial compression (figure 2.2c) is a reverse of simple extension and the compression ratio λ_c is less than one. The extension ratios of the lateral dimensions are also $1/\lambda_c$ and σ_c is negative. The stress-strain relation for rubber under compression is similarly given by equation (2.20).

Simple shear (figure 2.2d) may be represented by the sliding of planes which are parallel to a given plane through a distance proportional to their distances from a given plane. Shear deformation transformed a cube into parallelograms and a sphere into ellipsoids. The amount of shear is measured by the tangent of the angle ϕ through

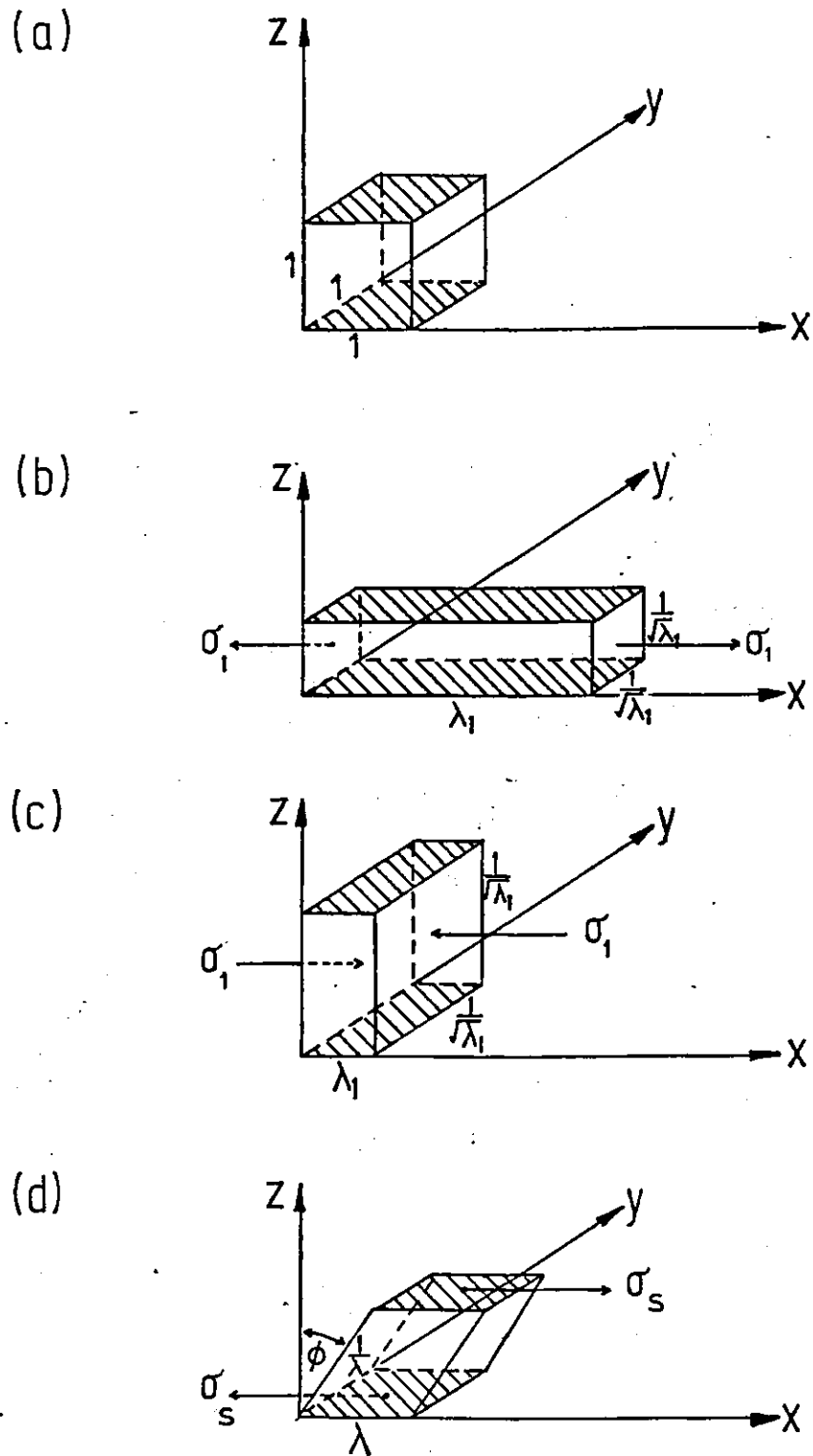


Figure 2.2. Types of strain (a) Unstrained unit cube
 (b) simple extension (c) Uniaxial compression
 (d) simple shear

which a vertical edge is tilted and there is no strain in the plane normal to the plane of shear. Since the volume of the material is constant the three principal extension ratios may therefore be expressed in terms of the major axis of strain λ_1 by $\lambda_1 = \lambda_1$, $\lambda_2 = 1$ and $\lambda_3 = 1/\lambda_1$ and the shear strain, γ , is related to the angle ϕ , or to the principal extension ratio (23) by

$$\gamma = \tan \phi = \lambda_1 - \frac{1}{\lambda_1} \quad (2.21)$$

The strain energy per unit volume has the form.

$$\begin{aligned} W &= \frac{1}{2} G \left(\lambda_1^2 + \frac{1}{\lambda_1^2} - 2 \right) \\ &= \frac{1}{2} G \gamma^2 \end{aligned} \quad (2.22)$$

If the work done on the body is entirely due to the shear force, then the shear stress will be given by

$$\sigma_s = \frac{dW}{d\gamma} = G\gamma \quad (2.23)$$

Equation (2.23) thus predicts that Hooke's Law will be obeyed in simple shear.

Experimental examination of the stress-strain relationships however, reveals significant deviations between the theoretical and experimental results. In simple extension for instance (figure 2.3) there are two distinct deviations (24). First at moderate strains, the experimental curve falls below the theoretical values, and secondly, at very large strains, the stresses tend to rise sharply and may eventually exceed the theoretical predictions.

The deviations from the statistical theory are also observed in shear deformations (24). The theory predicts that shear stress

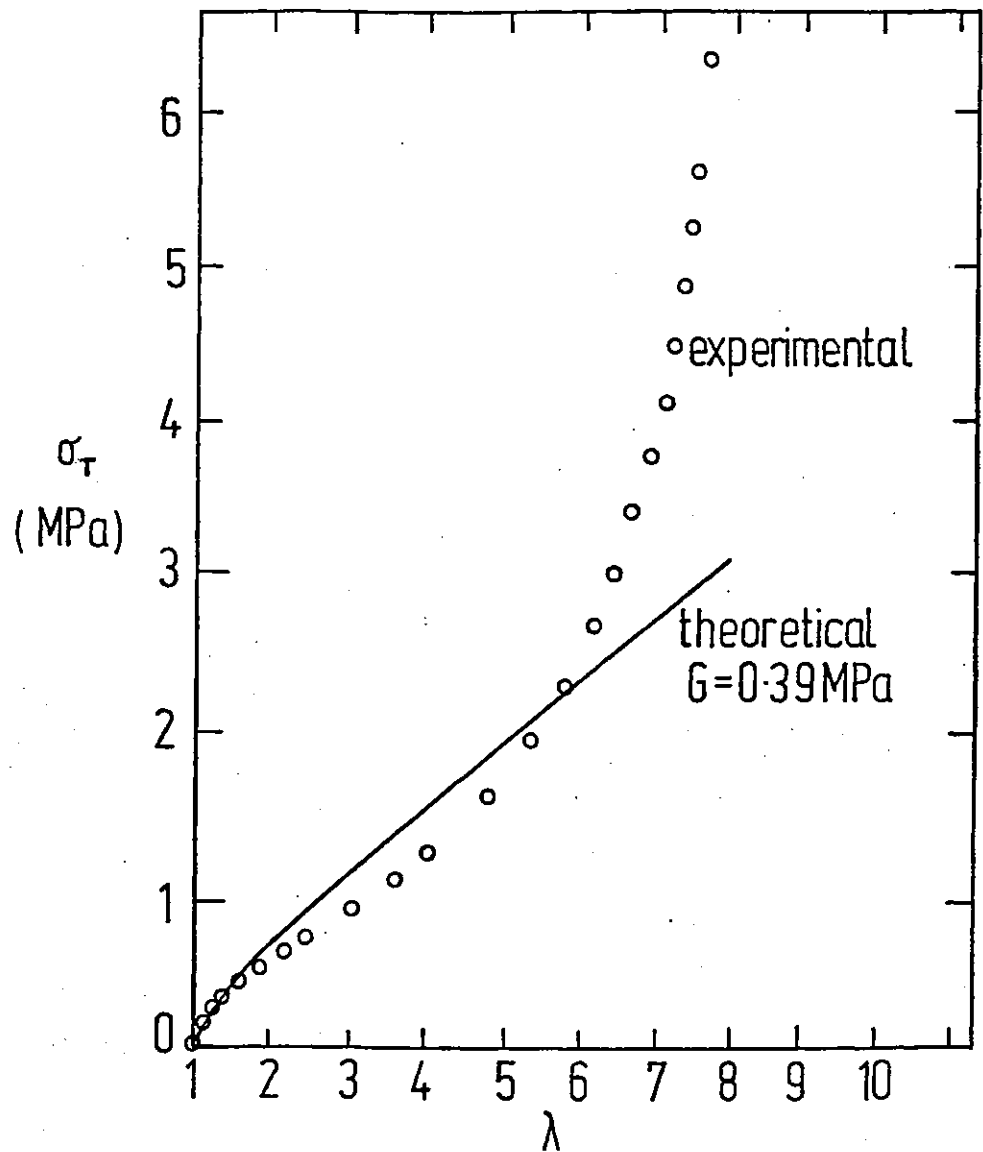


Figure 2.3. Comparison between the experimental curve with the theoretical form for simple extension (Treloar (24))

is proportional to shear strain but results showed that the shear stress falls initially below the predicted value at low strain and subsequently rises sharply. The deviations observed with shear deformations are similar to those observed for simple extension.

The deviations discussed above suggest that the statistical theory, which only involves a constant G , is inadequate to describe the stress-strain behaviour of a real rubber. There is as yet no satisfactory explanation for the deviation in the region of intermediate or moderate strains. At high strains though, the deviation observed has been attributed to the finite maximum extensibility of the network chains (11,13). It arises because a Gaussian type of probability distribution is used to describe the end-to-end distances between the rubber chains. The use of a Gaussian distribution is only justified when the end-to-end distance is much smaller than the fully extended length of the chain. Hence, the departure from the theory is expected to become more prominent at higher strains.

The range of validity of the statistical theory also depends on the degree of vulcanization. Between a comparatively highly and lightly vulcanized rubber, the former will have long enough chain segments for the probability distribution to be valid up to a much higher strain than the latter since the statistical argument will fail with the highly crosslinked rubber after a small amount of deformation. This follows because a short molecule is more likely to be found near its maximum length compared to a long molecule (11).

2.1.3 Phenomenological Theories of Elasticity

In an effort to describe the mechanical properties of rubber, a number of purely phenomenological theories have sprung up over the years. The theories are based not on the molecular or structural

concept, but on purely mathematical reasoning i.e. they are concerned with the way of describing the properties of the material not with their explanation or interpretation in the molecular or physical sense.

2.1.3.1 The Theory of Mooney

One of the earliest and most widely applied of the phenomenological theories is that due to Mooney (25). The theory appeared some years before the statistical theory and its evolution obviously has no relation to deviations from the latter theory. Mooney was concerned with the problem of developing a general theory for large elastic deformations. Making use of the assumptions that a rubber is incompressible and isotropic in the unstrained state, and that Hooke's Law is obeyed in simple shear, Mooney derived by purely mathematical argument based on the considerations of symmetry, the stored energy function,

$$W = C_1(\lambda_1^2 + \lambda_2^2 + \lambda_3^2 - 3) + C_2\left(\frac{1}{\lambda_1} + \frac{1}{\lambda_2} + \frac{1}{\lambda_3} - 3\right) \quad (2.24)$$

which contained two elastic constants, C_1 and C_2 . The first term on the left hand side of equation (2.24) corresponds to the form derived from the statistical theory with $2C_1 = NkT$. The statistical theory is therefore a particular case of the Mooney theory corresponding to $C_2 = 0$.

For a simple extension or uniaxial compression, where $\lambda_2 = \lambda_3 = 1/\sqrt{\lambda_1}$ equation (2.24) becomes,

$$W = C_1\left(\lambda_1^2 + \frac{2}{\lambda_1} - 3\right) + C_2\left(\frac{1}{\lambda_1} + 2\lambda_1 - 3\right) \quad (2.25)$$

and the nominal stress is given by

$$\bar{\sigma} = 2(\lambda_1 - \lambda_1^{-2})\left(C_1 + \frac{C_2}{\lambda_1}\right) \quad (2.26)$$

For a case of simple shear, where the shear strain, $\gamma = \lambda_1 - 1/\lambda_1$ and the principal extension ratios are $\lambda_1 = 1/\lambda_3, \lambda_2 = 1$, equation (2.24) becomes

$$W = (C_1 + C_2)\gamma^2 \quad (2.27)$$

The shear stress, $\bar{\sigma}_s$, is therefore given by

$$\bar{\sigma}_s = 2(C_1 + C_2)\gamma \quad (2.28)$$

which corresponds to Hooke's Law, where the shear modulus G is given by $2(C_1 + C_2)$.

The term C_1 was found to be dependent on the crosslink density and was consequently related to the elastic constant of the statistical theory (26). The origin of the C_2 term is still obscure, but it can be regarded as a measure of the departure of the observed stress-strain relationship from the form suggested by the statistical theory.

Numerous experiments have been carried out which give support to the applicability of the Mooney equation in simple extension for natural rubber and other polymers (26,27). However, the data of Rivlin and Saunders (28) for equibiaxial extension (which is equivalent to uniaxial compression) showed marked deviation from the Mooney relationship. In the extension region ($1/\lambda < 1$) the Mooney line (Fig. 2.4) corresponds to a value of $C_2/C_1 \approx 0.8$, but in compression ($1/\lambda > 1$), C_2 was found to be about zero. Thus, when considering the extension and compression data together, it is clear that the Mooney equation is no improvement over the statistical theory.

In simple shear, deviations from linearity of the same kind and of a similar order of magnitude to the deviation from the statistical theory in the case of simple extension were observed (24). The

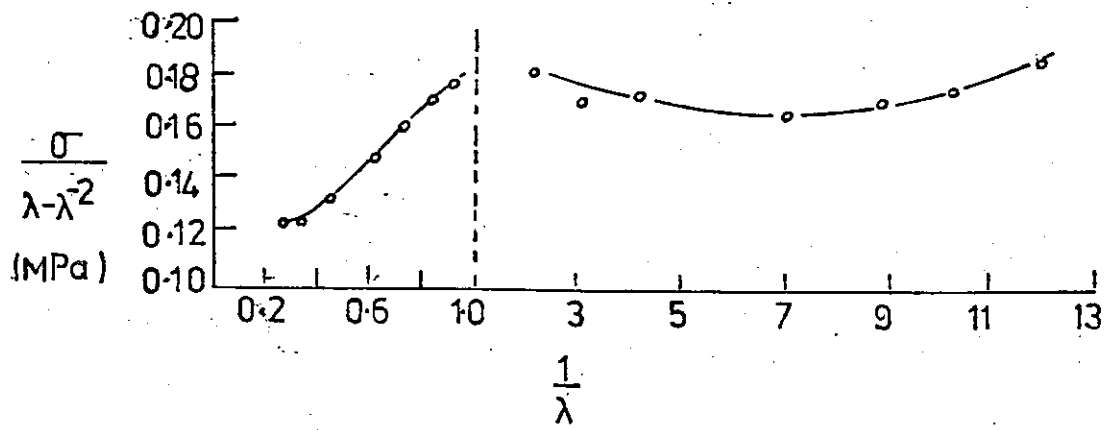


Figure 2.4. Mooney-Rivlin plot for data of simple extension and uniaxial compression (28)

deviation from the basic postulate of the Mooney theory (ie obeys Hooke's Law in simple shear) is thus of the same order as the deviation in simple extension which this theory is being used to interpret.

Taken as a whole, the Mooney equation does not seem to give a closer fit to the experimental data than the statistical theory. The interpretation of experimental data using the Mooney equation must be treated with caution since the Mooney form of the stored energy function cannot be adequately used to describe the mechanical properties of rubber for all possible types of strain, particularly those in compression.

2.1.3.2 The Theory of Rivlin

In 1948 Rivlin (29) argued that for a material that is incompressible and isotropic in the unstrained state, the strain energy must be a symmetrical power function of the three principle extension ratios. The stored energy function (W) was quoted as

$$W = W(I_1, I_2, I_3) \quad (2.29)$$

where I_1 , I_2 , and I_3 are the strain invariants given by

$$\begin{aligned} I_1 &= \lambda_1^2 + \lambda_2^2 + \lambda_3^2 \\ I_2 &= \lambda_1^2 \lambda_2^2 + \lambda_2^2 \lambda_3^2 + \lambda_3^2 \lambda_1^2 \\ I_3 &= \lambda_1^2 \lambda_2^2 \lambda_3^2 \end{aligned} \quad (2.30)$$

The incompressibility requires that $I_3 = 1$. In the undeformed state, $\lambda_1 = \lambda_2 = \lambda_3 = 1$, so $I_1 = I_2 = 3$. Thus, according to Rivlin and Saunders (28) the most general form of the stored energy function has the

form of a double-infinite series in (I_1-3) and (I_2-3) viz

$$W = \sum_{i=0, j=0}^{\infty} C_{ij} (I_1-3)^i (I_2-3)^j \quad (2.31)$$

where C_{ij} 's are constants.

Purely from consideration of mathematical simplicity, Rivlin (28,29) argued that the lowest member of the series would predominate. Thus by putting $i = 1, j = 0$, he obtained

$$W = C_{10} (I_1-3) \quad (2.32)$$

which represents the form of the stored energy function derived from the statistical theory. The other possible simple form takes the value of $i = 0, j = 1$. This gives

$$W = C_{01} (I_2-3) \quad (2.33)$$

but it has no obvious application to rubber. The combination of equations (2.32) and (2.33), however yield the Mooney equation, viz.

$$W = C_{10} (I_1-3) + C_{01} (I_2-3) \quad (2.34)$$

For an incompressible material, equation (2.29) becomes,

$$W = W(I_1, I_2) \quad (2.35)$$

By partial differentiation, Rivlin (3,31) expressed equation (2.35) in terms of the principal stresses corresponding to a pure homogeneous strain of $d\lambda_1, d\lambda_2$ and $d\lambda_3$ as

$$t_i = 2\left(\lambda_i^2 \frac{\partial W}{\partial I_1} - \frac{1}{\lambda_i^2} \frac{\partial W}{\partial I_2}\right) + p \quad (2.36)$$

where p is an arbitrary hydrostatic stress. Equation (2.36) indicates that for a material which is incompressible, the stresses are

indeterminate to the extent of an arbitrary hydrostatic stress, p . Only the differences between any two of the principal stresses which of course are unaffected by the addition of a hydrostatic stress are determinate. They are given by

$$\begin{aligned} t_1 - t_2 &= 2(\lambda_1^2 - \lambda_2^2) \left(\frac{\partial W}{\partial I_1} + \lambda_3^2 \frac{\partial W}{\partial I_2} \right) \\ t_2 - t_3 &= 2(\lambda_2^2 - \lambda_3^2) \left(\frac{\partial W}{\partial I_1} + \lambda_1^2 \frac{\partial W}{\partial I_2} \right) \\ t_3 - t_1 &= 2(\lambda_3^2 - \lambda_1^2) \left(\frac{\partial W}{\partial I_1} + \lambda_2^2 \frac{\partial W}{\partial I_2} \right) \end{aligned} \quad (2.37)$$

where t_1, t_2 and t_3 are the stresses per unit strained area (true stress).

In simple extension, or uniaxial compression, Rivlin's equation becomes

$$\sigma_T = 2(\lambda_1 - \lambda_1^{-2}) \left(\frac{\partial W}{\partial I_1} + \frac{1}{\lambda_1} \frac{\partial W}{\partial I_2} \right) \quad (2.38)$$

The corresponding shear stress is given by

$$\sigma_s = 2 \left(\frac{\partial W}{\partial I_1} + \frac{\partial W}{\partial I_2} \right) \gamma \quad (2.39)$$

where $\gamma^2 = \lambda_1^2 + 1/\lambda_1^2 - 2 = I_1 - 3 = I_2 - 3$. When $\frac{\partial W}{\partial I_1} = C_1$ and $\frac{\partial W}{\partial I_2} = C_2$ equation (2.39) reduces to

$$\sigma_s = 2(C_1 + C_2)\gamma \quad (2.40)$$

which is the Mooney relationship for simple shear.

The determination of $\frac{\partial W}{\partial I_1}$ and $\frac{\partial W}{\partial I_2}$ involves biaxial strain measurements, the values of which can be related to the true stresses (ie stress per unit strained area) and extension ratios by the equations below

$$2 \frac{\partial W}{\partial I_1} = \left(\frac{\lambda_1^2 t_1}{\lambda_1^2 - \lambda_3^2} - \frac{\lambda_2^2 t_2}{\lambda_2^2 - \lambda_3^2} \right) (\lambda_1^2 - \lambda_2^2)^{-1} \quad (2.41)$$

$$2 \frac{\partial W}{\partial I_2} = - \left(\frac{t_1}{\lambda_1^2 - \lambda_3^2} - \frac{t_2}{\lambda_2^2 - \lambda_3^2} \right) (\lambda_1^2 - \lambda_2^2)^{-1}$$

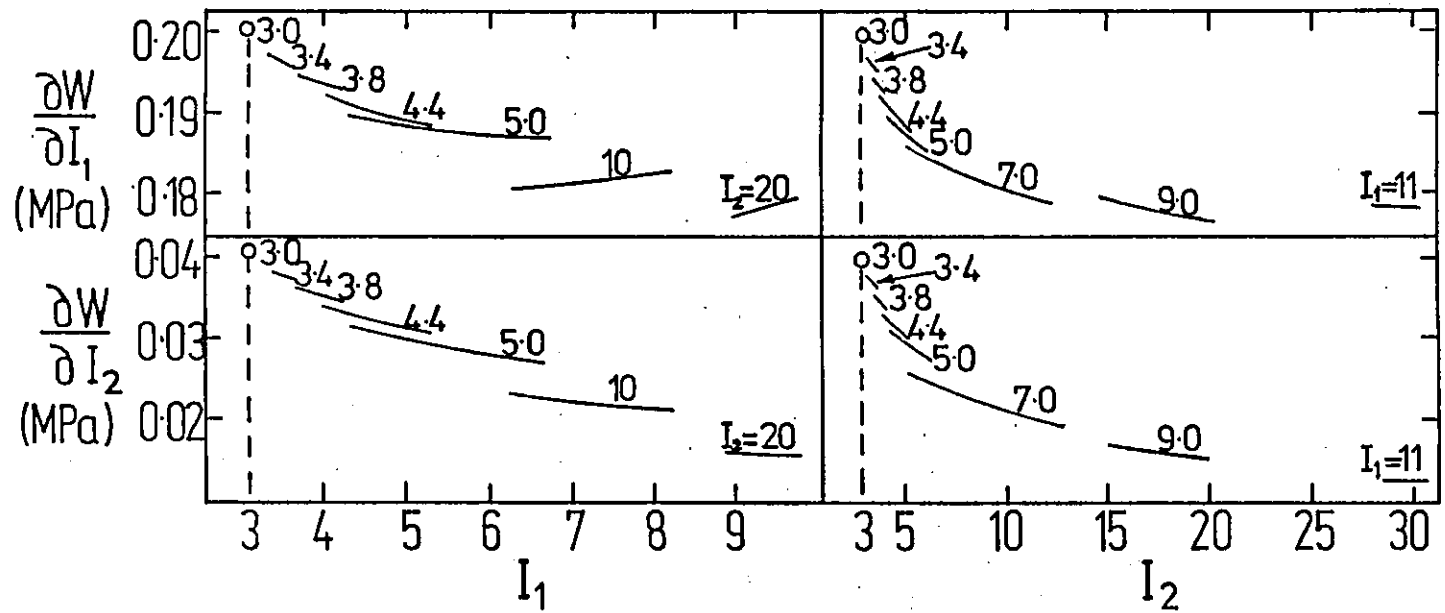
In their analyses, Rivlin and Saunders (28) observed that the term $\frac{\partial W}{\partial I_1}$ was independent of both I_1 and I_2 but $\frac{\partial W}{\partial I_2}$ varies with I_2 but was independent of I_1 (for a given I_2). It was suggested that the strain energy function has the general form of

$$W = C_1 (I_1 - 3) + \Phi (I_2 - 3) \quad (2.42)$$

where C_1 is a constant and Φ is a function whose slope diminishes continuously with increasing I_2 . Other workers (30,31) later showed that neither $\frac{\partial W}{\partial I_1}$ nor $\frac{\partial W}{\partial I_2}$ was constant. Obata et al (30) for instance showed that $\frac{\partial W}{\partial I_1}$ initially decreases with I_2 and subsequently tends toward a constant, but increases with I_1 . The behaviour of $\frac{\partial W}{\partial I_2}$ was found to be directly opposite to that of $\frac{\partial W}{\partial I_1}$ (in contrast to that of Rivlin and Saunders), namely, it increases with increasing I_2 but decreases with increasing I_1 . Jones and Treloar (31) on the other hand suggested that neither $\frac{\partial W}{\partial I_1}$, nor $\frac{\partial W}{\partial I_2}$ was constant, but that each depends on both I_1 and I_2 . The variations in $\frac{\partial W}{\partial I_1}$, were relatively much less important than the variations in $\frac{\partial W}{\partial I_2}$, the extreme variations amounting to only about 10% in the case of $\frac{\partial W}{\partial I_1}$, compared with about 70% for $\frac{\partial W}{\partial I_2}$ (fig. 2.5). Obata et. al. and Jones and Treloar observed that the values of $\frac{\partial W}{\partial I_2}$ were much smaller than $\frac{\partial W}{\partial I_1}$.

Since both $\frac{\partial W}{\partial I_1}$ and $\frac{\partial W}{\partial I_2}$ are not constants, then equation (2.42) may be more appropriately written as

Figure 2.5: Variations of $\frac{\partial W}{\partial I_1}$ and $\frac{\partial W}{\partial I_2}$ with I_1 and I_2 (Jones and Treloar (31))



$$W = \bar{\Phi}_1 (I_1 - 3) + \bar{\Phi}_2 (I_2 - 3) \quad (2.43)$$

where $\bar{\Phi}_1$ and $\bar{\Phi}_2$ are functions which vary with both I_1 and I_2 . It therefore appears that the deviation of the experimental data from both the statistical and Mooney theories may be associated with the terms $\bar{\Phi}_1$ and $\bar{\Phi}_2$, which according to Jones and Treloar, bear no relation to the empirical Mooney constants, C_1 and C_2 . The stored energy function as expressed by equation (2.43) for unfilled rubbers may therefore be a more appropriate form compared to the statistical or the Mooney theory.

2.1.3.3 Alternative Forms of Stored Energy Function

There have been a number of attempts to represent the stored energy function by incorporating the terms in I_1 and I_2 higher than the first and also cross terms in I_1 and I_2 . These include among others that due to Isihara et. al. (32), Alexander (33), Tschaegl (34) and Gent & Thomas (35), but these formulae raised no new principal since they utilise the basic formula of Rivlin.

New departures from Rivlin and Saunders formulae, were made by Ogden (36) and Valanis and Landel (37). Their equations were based on a power function of the extension ratios, but not of an invariant form.

Ogden in his treatment, discarded the requirement that the strain energy function shall be a power function of the extension ratios, as implied by Rivlin (28) and expressed the stored-energy function in terms of the λ 's directly, which can be written as,

$$W = \sum_n \frac{\mu_n}{a_n} (\lambda_1^{a_n} + \lambda_2^{a_n} + \lambda_3^{a_n} - 3) \quad (2.44)$$

in which a_n may have any values, positive or negative and are not

necessarily integers, and μ_n is a constant.

The statistical theory is thus a special case corresponding to $a_n = 2$, while the Mooney equation contains two terms, corresponding to $a_1 = 2$ and $a_2 = -2$. The principal stresses corresponding to the stored energy function expressed in equation (2.44) take the form

$$t_i = \sum_n \mu_n (\lambda_i)^{a_n} - p \quad (2.45)$$

while the difference in the principal stresses is given by

$$t_1 - t_2 = \sum_n \mu_n (\lambda_1^{a_n} - \lambda_2^{a_n}) \quad (2.46)$$

For simple extension of uniaxial compression, the true stress is given by

$$t_1 = \sum_n \mu_n (\lambda_1^{a_n} - \lambda_1^{-\frac{a_n}{2}}) \quad (2.47)$$

and the corresponding nominal stress, σ or t/λ is

$$\sigma_1 = \sum_n \mu_n (\lambda_1^{a_n - 1} - \lambda_1^{-\frac{a_n}{2} - 1}) \quad (2.48)$$

In simple extension, Ogden showed that the predicted and the experimental stress-strain values are in good agreement except at very high strains ($\lambda > 6$), where the latter gets progressively higher than the former. Thus by using an appropriate number of terms, the stress-strain behaviour of a rubber may be represented to any desired degree of accuracy using Ogden formula. The main advantage of the formula is that it is mathematically simple to handle.

Valanis and Landel put forward a more radical hypothesis, which states that the strain energy function may be expressed as the sum of three separate functions of the three principal extension ratios. Thus we have

$$W = w(\lambda_1) + w(\lambda_2) + w(\lambda_3) \quad (2.49)$$

in which, from the consideration of symmetry, the separate functions $w(\lambda_i)$ is of identical form for each of the extension ratios. The corresponding principal stresses are given by

$$t_i = \lambda_i \left(\frac{\partial W}{\partial \lambda_i} \right) - p \quad (2.50)$$

or

$$\sigma_i = \frac{\partial W}{\partial \lambda_i} - \frac{p}{\lambda_i} \quad (2.51)$$

where σ_i is the nominal stress and p is the arbitrary hydrostatic stress. The principal stress differences are,

$$\begin{aligned} t_1 - t_2 &= \lambda_1 w'(\lambda_1) - \lambda_2 w'(\lambda_2) \\ t_2 - t_3 &= \lambda_2 w'(\lambda_2) - \lambda_3 w'(\lambda_3) \\ t_3 - t_1 &= \lambda_3 w'(\lambda_3) - \lambda_1 w'(\lambda_1) \end{aligned} \quad (2.52)$$

where $w'(\lambda) = \frac{\partial W}{\partial \lambda_i}$ ($i = 1, 2, \text{ or } 3$), which can be determined by experiment, in pure shear.

In the case of pure shear, when $\lambda_2 = 1$,

$$(t_1 - t_2)_{\lambda_2=1} = \lambda_1 w'(\lambda_1) - C \quad (2.53)$$

where C is a constant and equal to $w'(1)$. According to Valanis and Landel, without loss of generality, $w'(1)$ may be considered to be zero.

Subsequently therefore, from equation (2.53) the form of $w'(\lambda_1)$ could be determined from the plots of $t_1 - t_2$ Vs $1/\lambda_1$. Based on the experiments in pure shear, Valanis-Landel claimed that the function $w'(\lambda)$ has the form

$$w'(\lambda) = 2\mu \ln \lambda \quad (2.54)$$

where μ is a constant. However, according to Treloar (38), the assumption that $w'(1) = 0$ (ie. C in equation 2.53) is incorrect and the author subsequently proposed an improved form of equation (2.54) namely

$$w'(\lambda) = 2\mu \ln \lambda + C/\lambda \quad (2.55)$$

Based on the studies carried out by Obata, Kawabata and Kawai (30) the forms of $w'(\lambda)$ given by both equations (2.54) and (2.55) were found to be inadequate ie. the function could not fit Obata's data. Later, two different forms of $w'(\lambda)$ were proposed. The first was that due to Jones and Treloar (31). Their proposal was based on the fact that the Valanis-Landel hypothesis is consistent with the Ogden formula, and combining the two formulae, the authors obtained

$$\lambda w'(\lambda) - C = \mu_1 (\lambda_1^{a_1} - 1) + \mu_2 (\lambda_2^{a_2} - 1) + \mu_3 (\lambda_3^{a_3} - 1) \quad (2.56)$$

where $\mu_1, \mu_2, \mu_3, a_1, a_2, a_3$ are constants which were determined by trial and error methods. Tobisch (39) also introduced a new form of $w'(\lambda)$. It involves three parameter constants and takes the form,

$$w'(\lambda_i) = 2 \gamma (e^{\alpha(\lambda_i^2 - 1)} - \beta \lambda_i^{-3}) \quad (2.57)$$

where α, β and γ are constants. The constant γ was said to be equal to $1/3$ of the Young's modulus and $\beta = 1/3 \alpha$. Both equations (2.56) and (2.57) were said to be able to represent all the experimental data satisfactorily.

To date, it is fair to say that no satisfactory form of $w'(\lambda)$ appears to be generally acceptable. Different authors obtained different forms of $w'(\lambda)$, which were the results of curve fitting exercises (31,39). However without the knowledge of $w'(\lambda)$, the hypothesis of Valanis-Landel could still be verified. The verification takes the form of plotting t_1-t_2 as a function of λ_1 (or for $-t_2$ as a function of λ_3) for pure shear deformations. The hypothesis is verified if all the curves obtained are superimposable since equation (2.53) implies that all curves differ from one another only by an additive constant. In a variety of cases (40) verification was indeed made for $\lambda_1 < 3.0$ suggesting that equation (2.52) is valid. However, when the strains were in excess of $\lambda_1 \approx 3.0$, the hypothesis was shown to be unreliable (41).

In general, the Valanis-Landel hypothesis has been verified experimentally but unless an accurate form of $w'(\lambda)$ is obtained, the hypothesis cannot be used to predict other types of strain. Consequently it will not be useful in practice.

2.2 Effects of carbon black on rubber vulcanizates

2.2.1 Introduction

The use of fillers in rubbers ranks as one of the two most important processes in rubber technology - only vulcanization can be considered to surpass it in its universal application.

Carbon black is the principal filler used in rubbers. Generally the incorporation of carbon black alters the properties of rubber; some show an improvement while others deteriorate (42). In this thesis, we are concerned with the effects of carbon black on the modulus of rubber.

2.2.2 The nature and classification of carbon blacks

Carbon black is formed by incomplete combustion of many organic substances: solid, liquid and gaseous. Its production is so simple that it was known in ancient times. The Chinese and Hindus used carbon black as colourants in ink in the third century A.D.

The generic term of carbon black now refers to a group of industrial products consisting of furnace blacks, channel blacks, thermal blacks and lamp blacks.

Furnace black is the most widely used black today. It is made by the incomplete combustion of hydrocarbons in steel furnaces. The black produced is separated from the combustion gases by means of cyclones and filter bags. The yield of carbon black varies from about 25% to 70% of the available carbon and the particle diameter ranges from about 20 nm to 80 nm (43).

Channel black is manufactured by impingement process. The process essentially involves piping the feedstock to thousands of small burners and impinging the small flames on to a large rolling drum or on to a slowly reciprocating channel irons. The deposited

black is taken off by scrapers and collected. The process is very inefficient (5% or less yield) but fine blacks, of particle diameters ranging from 9 nm to 30 nm can be made.

Thermal black is produced by thermal decomposition of natural gas in the absence of air at 1300°C in cylindrical furnaces filled with an open checkerwork of silica bricks. Two furnaces are used, the process being cyclic. Natural gas is admitted to one which has already been heated by firing a mixture of hydrogen and air; carbon and hydrogen are formed. The carbon is collected as carbon black and hydrogen is used to heat the other furnace. The recovery is about 40-50% of the available carbon and the black obtained range in particle diameter from about 120 nm to 500 nm.

Carbon blacks are essentially (90-99%) composed of elemental carbon in the form of non-spherical particles of colloidal size. The carbon atoms are in layer planes, which by parallel alignment and overlapping gives the particles their semi-graphitic nature. The other elements in carbon black which are of significance are hydrogen, oxygen and sulphur (44).

Hydrogen is always found, as part of the hydrocarbons from which the black is formed. The hydrogen content may vary depending on the feed stock and process used but it is generally less than 1%.

Oxygen is introduced in the flame during particle formation. The proportion of oxygen present varies depending on the process of formation involved. Thermal blacks have less oxygen than other blacks, usually below 0.5%, while furnace blacks contain up to 1.2%. Channel blacks contain a rather high proportion of oxygen (about 3% or more).

Sulphur is present generally in both free and chemically bound forms. Thermal and channel blacks have very low sulphur content

(~0.01%), while furnace blacks may contain about 0.2 to 0.8% sulphur.

Carbon blacks rarely exist as separate individual particles but generally as aggregates of coalesced, fused elementary particles (45). An exception is found with thermal black where the particles mostly exist as individual units (44). The particles of black are not closely packed, but loosely coalesce leaving considerable empty spaces or voids in between the particles.

The aggregates of black particles have a tendency to be attracted to one another by the London-Van der Waals forces of attraction to form more complex chains or agglomerates. These agglomerated structures, which vary in geometric form from clustered grape-like assemblies to more bulky branched and filamentous forms, can be broken up by an application of shear, but reagglomerate on standing. The aggregated black on the other hand needs a larger force than that required by the agglomerates to be broken up and once broken, the network is permanently changed.

The term "structure" when used by the carbon black producers refers to the combination of both the aggregated and agglomerated structures. The "structure" is measured by absorption of a liquid (dibutyl phthalate, DBP) up to a point where the dry crumbly carbon black suddenly starts to cohere (46). At this point the liquid is supposed to have filled the voids within the agglomerates and most of the void spaces within the aggregates. The amount of the absorbed liquid, which reflects the "structure" of the carbon black is normally expressed in cm^3 DBP absorbed per 100 gram carbon black (or DBPA number).

The particle size is an important property of carbon black. Normally particle sizes are determined using an electron microscope, where data are obtained from photomicrographs of known enlargement.

Alternatively the particle size of carbon black particles can be calculated from the specific surface area since the latter is roughly inversely proportional to the particle diameter.

The specific surface areas are determined by gas or liquid adsorption. For non-porous black, the surface area can be determined accurately by an adsorption of nitrogen, using a procedure developed by Brunauer, Emmett and Teller (47) (BET procedure) for calculating the monolayer adsorption from the data at several partial pressures which give coverage in the vicinity of a monolayer. Most rubber grade carbon blacks are non-porous; however if micropores (generally slit-shaped a few angstroms in width) are present, the external surface area can be determined by adsorption of large molecules, such as cetyltrimethylammonium bromide (CTAB) from aqueous solution (48).

It is common technical practice to measure, not the surface area, but the iodine number (49) or number of milligrams of iodine adsorbed per gram of black because the determination is rapid and simple to perform. For this method, carbon black is shaken with an aqueous solution of iodine in potassium iodide. The black is then settled by centrifuging and the iodine concentration of the supernatant liquid is determined by titration with a thiosulphate solution. The results are normally expressed as weight of iodine (mg) per gram of carbon black. The iodine number is generally within 10% of the area as measured by the nitrogen or CTAB adsorption, but there can be systematic differences depending on the supplier and technology of manufacture (50). The iodine number is also affected by the tars (toluene-extractable material) present on the surface of the black and by surface oxygen groups (51). In view of these limitations, the iodine number is of limited significance and as a result, the most

frequent use of this method is in the production control.

There are over fifty different types of rubber grade carbon blacks available. They were classified previously, using a system of letters, but the system was found to be inadequate and cumbersome. This led the American Standard for Testing and Materials (ASTM) committee on carbon black to establish a new classification system (52).

The basic distinguishing characteristics of the new system are the particle sizes and their effects on cure. The classification (D 1765) is given by a four character nomenclature system (e.g. N330). The first character is a letter indicating the effect of carbon black on the cure rate of a typical rubber vulcanizate containing the black. The letter "N" is used to indicate a normal curing rate (for neutral or basic black) relative to that of the unfilled vulcanizate while the letter 'S' indicates a slow-curing rate (for acidic black). The second character (first digit) designates the typical average particle size of carbon black as determined by electron microscopic measurements. The particle sizes of the carbon black has been divided into ten arbitrary groups and each has been assigned a digit to describe the group (table 2.1). The third and fourth characters in the system are arbitrarily assigned digits.

Table 2.1 Second digit classification in ASTM System.

Second digit	Particle diameter (nm)	Old Code
0	1-10	
1	11-19	Super Abrasion Furnace (SAF)
2	20-25	Intermediate SAF
3	26-30	High Abrasion Furnace (HAF)
		Easy and Medium Processing Channel (EPC, MPC)
4	31-39	Fine Furnace (FF)
5	40-48	Fast Extrusion Furnace (FEF)
6	49-60	General Purpose Furnace (GPF)
		High Modulus Furnace (HMF)
7	61-100	Semi-reinforcing Furnace (SRF)
8	101-200	Fine thermal (FT)
9	201-500	Medium thermal (MT)

2.2.3 The stiffening effects of carbon black

The use of fillers in rubber has been known since the discovery of rubber but the first serious investigation of the effects of fillers on the physical and chemical properties of rubber was made by Heizerby and Pehl (53) in 1892. However the authors experiments were not well designed and comparison between results was difficult. The first recognition of the stiffening effect was only made following subsequent investigations by Dittma (54), the works of whom are considered to be the first milestone in the study of stiffening effects of filling materials. Today a voluminous literature on the stiffening effect of fillers exists (55-60) but the phenomena involved in the stiffening effect still remains the subject of considerable controversy.

One of the principal effects of carbon black is to increase the stiffness or modulus of unfilled rubbers. The mechanisms involved have been attributed to two different phenomena (a) hydrodynamic effects of filler and (b) interaggregate interactions.

2.2.3.1 Hydrodynamic effects

In the hydrodynamic theory, the rubber is regarded as a continuum and attention is focussed on the effects of carbon black without concern for the behaviour of the rubber at molecular level. The mechanism proposed was derived mainly from the formally identical problem of the increase in viscosity of a liquid caused by a suspension of solid particles. For rigid particles at concentrations sufficiently small for interaction between particles to be neglected, the viscosity of the suspension is given by the Einstein equation (61)

$$\eta = \eta_0 (1 + 2.5C) \quad (2.58)$$

where η and η_0 are the viscosities of the suspension and liquid respectively and C is the volume concentration of particles.

Use of the viscosity relationship given by equation (2.58) was proposed for the analogous elastic problem of rubber containing fillers, with the viscosity η replaced by Young's modulus, E . Smallwood (62) showed that the stress-strain data of several large particle size fillers at low concentration fitted the relationship,

$$E = E_0 (1 + 2.5 \phi) \quad (2.59)$$

where E and E_0 are the Young's Modulus of filled and unfilled rubbers respectively and ϕ is the volume fraction of filler. To take into account higher concentration of fillers by considering the hydrodynamic interactions between pairs of particles, Guth and Gold (63) added an extra term involving the square of concentration of fillers to the Smallwood equation, namely

$$E = E_0 (1 + 2.5 \phi + 14.1 \phi^2) \quad (2.60)$$

Guth (64) found that equation (2.60) fitted the data for fine thermal black (P33 - which consist of essentially spherical particles) up to a volume fraction ϕ of 0.3. Equation (2.60) however could not be used to predict the modulus of rubbers containing fillers which exist as cluster or particles to form asymmetric aggregates. To take into account the asymmetric nature of carbon black aggregates, Guth proposed a modified equation,

$$E = E_0 (1 + 0.67f \phi + 1.62 f^2 \phi^2) \quad (2.61)$$

where f is the ratio of the length to diameter of the aggregate (or shape factor). With a proper choice of the value of f , equation (2.61) was able to account for the variation of modulus E for several

rubber-filler systems. For systems containing up to 30% volume concentration of N330 black, a shape factor of 6.5 was required (65). However later studies of shapes of carbon black particles and aggregates using electron microscope (66) indicated that the shape factors of most blacks are somewhat less than 6.5; they are usually in the range of about 2-3. Thus if the value of the shape factor f is taken as between 2-3, then the predicted value of E will be much lower than the experimental values given by Mullins and Tobin (65).

With rubbers filled with carbon black, the void spaces which are present within carbon black aggregates/agglomerates are filled with rubber. These rubbers are occluded within the interstices of the carbon black structures. When subjected to stress, this occluded rubber is shielded to a significant extent from deformation which the bulk of the rubber undergoes and it thus acts as part of filler rather than as part of rubber matrix (67-69).

Sambrook (70) proposed that the effective volume fraction of carbon black, ϕ' , i.e. volume fraction of carbon black plus volume fraction of occluded rubber, should be used in equation (2.60) instead of the volume fraction of filler, ϕ . The value of ϕ' could be calculated from the value of ϕ and DBPA values using the relationship given by Medalia (67),

$$\frac{\phi'}{\phi} = \frac{46.75 + \text{DBPA}}{68.26} \quad (2.62)$$

Using ϕ' in equation (2.60), Sambrook observed that the values of Young's modulus obtained were about 20% higher than experimental values, suggesting that the use of equation (2.62) in conjunction with equation (2.60) does not adequately describe the stiffening effects of carbon black.

Later Medalia (71) observed that the effective volume fraction of carbon black is equal to the volume fraction of carbon black plus about half of the occluded volume of rubber i.e.

$$\phi' = \phi + 0.5 \phi_{\text{occ}} \quad (2.63)$$

where ϕ_{occ} is the volume fraction of the occluded rubber. This signified that only about half of the total occluded rubber (as calculated from the DBPA values) is shielded from deformation and acts as filler. Using the new effectiveness factor (equation 2.63) in equation (2.60), Medalia (72) showed that the experimental and calculated values of the shear modulus at 10% strain amplitude for several filled rubbers were in reasonably good agreement.

Carbon black aggregates undergo limited breakdown during incorporation into rubber. Depending on the grades of rubber and types of black, after mixing processes, about 30 to 50% (on weight average basis) of the aggregate structure of free blacks are broken down (73,74). The void volume within the aggregates also reduces after mixing or fracture and this is revealed by the "24M4 crush test" (75) in which carbon black is crushed for four times before the measurement of DBPA values. Based on that information, Kraus (76) suggested that the effective volume of carbon black should be more appropriately related to the 24M4 DBPA values rather than the "uncrushed" DBPA values. The author subsequently proposed that,

$$\frac{\phi'}{\phi} = \frac{24 + \text{DBPA (24M4)}}{55} \quad (2.64)$$

For several blacks, Medalia (71) observed that the calculations based on the relationship due to Kraus (equation 2.64) were not quantitatively too different from that using his own equation.

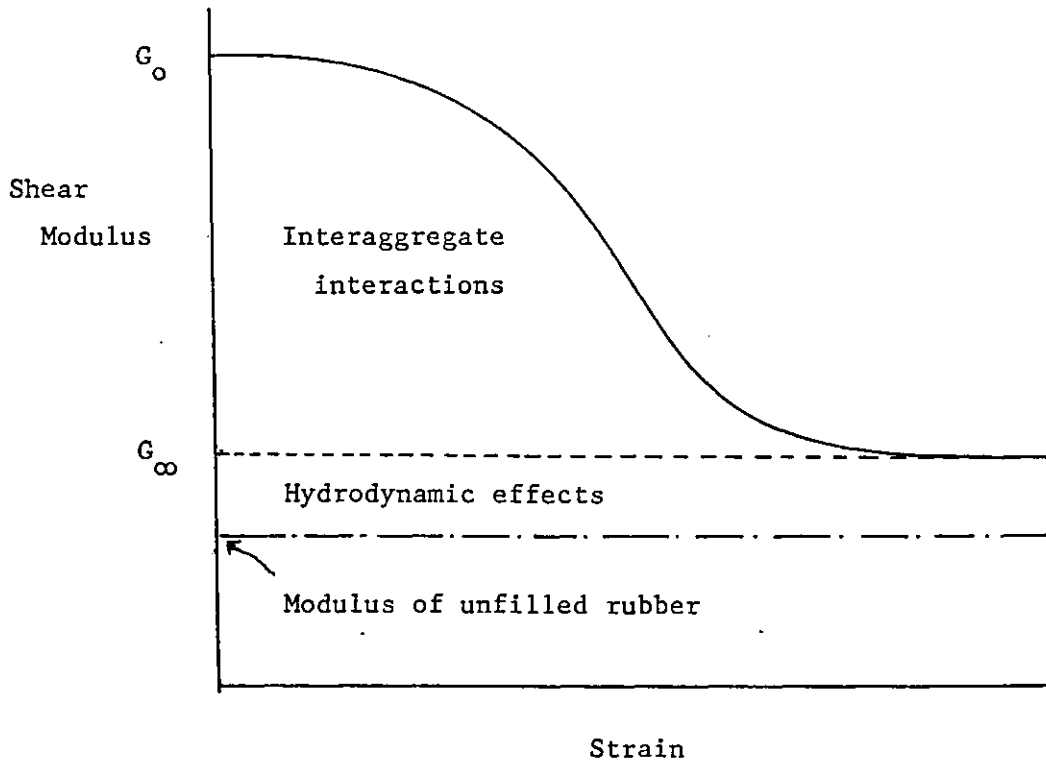
For measurements made at moderate deformations (10% dynamic strain amplitude) Medalia (77) obtained a good prediction of the moduli of rubbers containing carbon black when the effective volume of filler obtained using equation (2.63) was used with the equation by Guth and Gold (equation 2.60). At low strains however, an additional contribution to the modulus was observed. The additional contribution was shown to be a function of particle diameter, details of which are discussed below.

It may be noted that the development of the hydrodynamic theory was based on the measurement of Young's modulus. For an elastomer, in the absence of vacuole formation, the Poisson's ratio is approximately 0.5 (78) and the relation $E = 3G_0$ (where G_0 is the limiting shear modulus at low strain) is approximately valid. Thus any equation relating E for filled and unfilled rubbers has equal validity for the shear modulus G_0 .

2.2.3.2 Interaggregate interactions

According to Payne (79), the shear modulus of filled rubbers is a maximum at low strains (ca 1%) but decreases as the strain increases until at a sufficiently high strain the modulus becomes independent of strain. The idealized form of shear modulus against shear strain plots may be represented by fig. 2.6.

Fig. 2.6: Idealized plot of shear modulus as a function of shear strain



The limiting modulus at low strain was referred to as G_0 while that at high strain was referred to as G_∞ . The corresponding modulus for unfilled rubber is represented by the lower horizontal line. According to Payne, the maximum elastic modulus at low strain, G_0 , is caused by a maximum development of the carbon-black agglomerates. At higher strains, the carbon black agglomerates are broken down and the elastic modulus attains a low value G_∞ , resulting from the contribution of the rubber matrix and the aggregated black (by hydrodynamic effect). The value $G_0 - G_\infty$, therefore characterises the maximum effects of carbon black agglomeration in rubber, and this constitutes the additional contribution to the modulus at low strain which was not accounted for by the hydrodynamic equations.

Payne (79) referred to the effects of black agglomeration as the structural effects i.e. $G_0 - G_\infty$ arises from carbon black agglomerate structures. The author's argument was supported by the results (80) obtained from other two phase systems, such as carbon black in oil and bentonite or stockalite clay in water, one phase of which easily forms agglomerates structure when left undisturbed. When the two phase systems were sheared in a manner similar to that of rubber and carbon black system, similar reductions in modulus with strain were observed. As a further demonstration, Harwood and Payne (81) dissolved crystals of phenyl- β -naphthylamine (PBN) in benzene and swelled it into an unfilled vulcanizate of natural rubber. The benzene was evaporated off and the three dimensional fern-like structures of PBN crystals in rubber vulcanizates were clearly visible by an optical microscope. On deforming the PBN-rubber system, results similar to that of the rubber plus carbon black systems were also obtained.

In view of the fact that the origin of carbon black agglomeration is the mutual particle attraction, Voet, Cook and Hogue (82) argued that the most important parameter in determining $G_0 - G_\infty$ is the interparticle distance. In order to verify the dependence of the black agglomeration (or $G_0 - G_\infty$) on interparticle distances, Voet et. al. prepared samples by swelling uncured mixtures of carbon black and rubber in a high boiling solvent, decahydronaphthalene (decalin), followed by vulcanizing the swollen mixture. The solvent was removed by extraction with a low boiling solvent and the latter was subsequently eliminated by heating in vacuum. In this manner, the authors obtained a series of isotropically shrunken vulcanizates. For varying degrees of swelling, results showed that $(G_0 - G_\infty)$ decreases with the content of the decalin, indicating that the interparticle

distance is a critical quantity in determining the effects of black agglomeration. When $\log (G_0 - G_\infty)$ was plotted against interparticle distance, a linear relationship giving $\log (G_0 - G_\infty)$ as inversely proportional to interparticle distances was obtained. Thus $(G_0 - G_\infty)$ may be expressed as an exponential function of the interparticle distances. This, according to the authors is consistent with the London-Van der Waals forces of attraction which are normally represented by a reciprocal of a high power law of the distance ($\sim R^{-6}$) and therefore confirmed the view that the black agglomeration is attributed to the mutual particle attraction due to London-Van der Waals forces.

Chemical methods have been used to remove the effects due to black agglomeration in rubber (80). The material used are generally known as chemical promoters, usually organic nitroso compounds, the coupling agents added to the unvulcanized during heat treatment, promoting the black-elastomer interaction and greatly improving the dispersion of carbon black. When the chemical promoters [e.g. N-(2-methyl-2-nitropropyl)-4-nitrosoaniline (Nitrol)] are added black to filled rubbers, the $(G_0 - G_\infty)$ values are found to decrease considerably.

Modification of carbon blacks can be achieved by severe attrition through ball or two roll (rubber) milling (83). It has been shown that attrition increases the surface area of carbon black. The increase in surface area was attributed partly to the breakage of the agglomerate structures and partly due to abrasion and fragmentation occurring at the surfaces of the individual particle. The use of attrited black in rubber led to an decrease in the values of $(G_0 - G_\infty)$ compared to the use of the unattrited black and the attrition combined with hot milling treatment almost entirely eliminates the low strain structural effects (80,84).

The increase in surface area of carbon black normally arises from a reduction in the particle size. It follows that, if the particle size decreases, $G_o - G_{\infty}$ will increase (82) and this appears to be contrary to that observed with attrited black. However, the process of attrition changes the nature of carbon black surfaces by abrasion and fragmentation and it is likely that the increase in surface area of the attrited black over that of the corresponding unattrited black is due to the increase in the surface roughness rather than the reduction in particle size. Such an effect produces a reduction in $G_o - G_{\infty}$ value in a similar manner to that of the chemical promoters because the process of attrition resulted with the increase in the oxygen content of the black (80).

The nature of polymers was also found to alter the effects of agglomeration of carbon black (85). Polymers like Nitrile Butadiene rubber (NBR) appeared to possess high $(G_o - G_{\infty})$ values compared to polymers like Natural rubber, Butadiene rubber, or Polyisoprene.

The values of $(G_o - G_{\infty})$ increase with black loading (80) since the presence of more black increases the tendency for the aggregates to form agglomerates. However, it was reported that $(G_o - G_{\infty})$ was independent of the crosslink density (86), and these results were confirmed by the small differences observed between the modulus of vulcanized and unvulcanized rubbers. This finding implies that any change in the rubber matrix does not affect the agglomerate structures of carbon black.

SECTION 3 : EXPERIMENTAL

- 3.1 Experimental techniques
 - 3.1.1 Materials
 - 3.1.2 Preparation of test specimens
 - 3.1.2.1 Tensile test-pieces
 - 3.1.2.2 Compression test-pieces
 - 3.1.2.3 Shear test-pieces
 - 3.1.3 Instrumentation
 - 3.1.4 Stress-strain measurements
 - 3.1.4.1 Uniaxial extension
 - 3.1.4.2 Lubricated compression
 - 3.1.4.3 Simple shear
 - 3.1.5 Equilibrium swelling measurements
- 3.2 Experimental discussion :
 - 3.2.1 Uniaxial extension
 - 3.2.1.1 Effects of measurement techniques
 - 3.2.1.2 Effects of types of test-piece
 - 3.2.1.3 Effects of anisotropy
 - 3.2.2 Lubricated compression
 - 3.2.2.1 Effects of types of test-piece
 - 3.2.3 Simple shear
 - 3.2.3.1 Effects of types of test-piece
- 3.3 Conclusions

SECTION 3 EXPERIMENTAL3.1 Experimental techniques3.1.1 Materials

The base polymer used was Natural rubber. Several grades of Natural rubber are available, but a high quality, light coloured Standard Malaysian Rubber, SMRL, was used. No further purification or treatment of the rubber was carried out.

The grades of carbon black used, together with their relevant properties, are listed in table 3.1.

Table 3.1 Grades of Carbon black used

Types of black (ASTM designation)	Particle diameter (nm)	E.M. Surface Area (m ² /gm)
N110	11-19	125-155
N347	26-30	80-100
N330		70-90
N326		75-105
N500	40-48	36-52
N762	61-100	17-33

Vulcanizates were prepared from a series of masterbatches containing commercial grade ingredients as shown in table 3.2.1. Sulphur (flowers of sulphur) and accelerator (table 3.2.2) were added to the masterbatches to give the sulphur vulcanizing system. Zinc oxide and stearic acid are auxiliary agents used in conjunction with an organic accelerator (N-cyclohexyl benzothiazole-2-sulphenamide, CBS) to speed up the vulcanization processes.

Table 3.2 Formulations

	<u>Ingredients</u>	<u>Filled vulcanizates</u> *	<u>Unfilled vulcanizates</u> *
3.2.1	Natural rubber (SMRL)	100	100
	Carbon black ^a	5-80	-
	Zinc oxide ^b	5	5
	Stearic acid ^c	1.5	1.5
	Flectol H ^d	1.0	1.0
	Process oil ^e	0.5-8	-
3.2.2	Sulphur ^f	0.17-3.75	0.17-3.75
	C.B.S.	0.3-7.5	0.3-7.5
3.2.3	Dicumyl peroxide	1-4.5	1-4.5

Note: * in parts per hundred parts of rubber by weight (pphr)

a - Cabot Corporation

b - Durham Chemical Ltd., 99.9% pure (dry basis)

c - Anchor Chemical Company Ltd., England

d - Monsanto Ltd., London.

Poly 2,2,4-trimethyl 1,2-dihydroquinoline; 98.3% active

e - Shell U.K; Dutrex 729

f - Anchor Chemical Company Ltd., England

g - Monsanto Ltd., N-cyclohexyl benzothiazole-2-sulphenamide

h - Hercules Powder Company Ltd., Dicap R, 99% pure

Peroxide based system consisted of a masterbatch and dicumyl peroxide, (> 99% pure). Although Zinc oxide and stearic acid play no part in the crosslinking processes, they were used to avoid any variation between the masterbatches of the sulphur and peroxide based systems.

An antioxidant, poly 2,2,4-trimethyl 1,2-dihydroquinoline was used to protect the vulcanizate against oxidative degradation during processing, storage and testing. To facilitate mixing, a hydrocarbon oil (Dutrex 729) was used.

3.1.2 Preparation of test-specimens

The masterbatches were mixed in a laboratory internal mixer of one-litre capacity. The mixer rotor speed was 116 revolutions per minute and the starting temperature was approximately 60°C. To avoid any serious overheating during mixing, the temperature of the mixer chamber was controlled and maintained at below 120°C using cooling water. The mixing cycles were as follows:

<u>Time (Minutes)</u>	<u>Operations</u>
0	Add raw rubber
1	Add Zinc oxide, stearic acid and antioxidant
2	Add half carbon black
3.5	Add hydrocarbon oil and rest of black
5	Sweep
6	Dump and Sheet

The weights of masterbatches were checked after mixing. Generally, losses of not more than 1% in weight of the ingredients were observed.

An open two-roll mill, having rollers 330 mm long and 152 mm diameter was used for the incorporation of vulcanizing agents into the rubber masterbatches. The temperature of the mill was thermostatically maintained at about 60°C and the friction ratio of the front to back roll was 1:1.25.

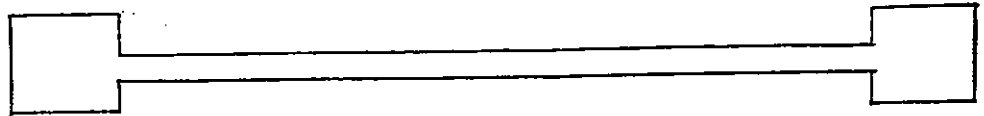
Vulcanizing agents were added to 300 gm portions of the masterbatches. With sulphur vulcanizing systems, the accelerator was added to the rubber masterbatch prior to the addition of sulphur. The rubber mixes were rolled and passed through a tight nip (~ 0.5 mm) three times before being allowed to run at normal nip setting (~ 2 mm gap) to ensure the breakdown of any large undispersed ingredients. The total time taken for the incorporation of vulcanizing agents into rubber masterbatches was about 5 to 7 minutes. While on the mill, the rubber mixes were regularly cut and rolled and not allowed to run uncut for more than 30 seconds.

Vulcanizates were cured a day after the addition of vulcanizing agents in steam heated presses at 150°C. Sulphur based vulcanizates were cured for the time required to develop maximum torque on a Monsanto rheometer at 150°C, while for peroxide based systems, the vulcanization time was 90 minutes.

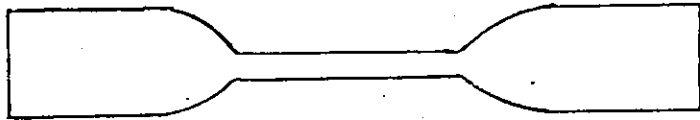
3.1.2.1 Tensile test-pieces

Rubber sheets of various thicknesses (1 to 2 mm) were prepared by moulding the vulcanizates in a square frame mould, 228 x 228 mm². All tensile test-pieces were diestamped from moulded sheets using appropriate dies.

The tensile-pieces were either parallel sided dumbbells, type C dumbbells (B.S. 903, part A2) or rings. The parallel sided dumbbell (fig. 3.1a) consists of a strip (100 mm long, 3.8 mm wide)



(a)



(b)

Figure 3.1. Tensile test-pieces: (a) parallel sided dumbbell (or bongo) and (b) type C dumbbell

having square shoulders ($12.7 \times 12.7 \text{ mm}^2$) at the opposite ends. Type C dumbbells (fig. 3.1b) consists of a test length 25.4 mm long and 4 mm wide between widened ends. The rings have an internal diameter of 44.6 mm and external diameter of 52.6 mm giving a radial width of 4 mm.

3.1.2.2 Compression test-pieces

Compression samples were disks of various diameters having a thickness of about 8 mm, prepared by compression moulding.

Compression samples (termed "cold bonded" sample) were also made by plying up 2 mm thick disks diestamped from moulded sheet. These were bonded together to form 8 mm thick compression samples using a two-part fast-curing rubber cement having the following formulation (in parts per hundred parts of rubber by weight, pphr)

Table 3.3 Natural rubber cement

	<u>A</u>	<u>B</u>
Natural rubber (SMRL)	100	100
Zinc oxide	5	5
Stearic acid	0.5	0.5
Sulphur	4	-
ZIX ^a	-	1.25
DDCN ^b	-	0.5

a - Zinc isopropyl xanthate;

b - Diethyl ammonium di-ethyl dithiocarbamate

The rubber cement was prepared by dissolving mixes A and B separately in toluene to give about 15% solid contents, which were thoroughly mixed immediately before use. The surfaces of rubber which were to be bonded were roughened using a medium grade of sandpaper. Bonding of rubber to rubber was achieved by applying a layer of the adhesive to the roughened surfaces, keeping the bonded surfaces under light pressure for at least 48 hours.

3.1.2.3 Shear test-pieces

The shear test-pieces used were either double or of a quadruple type (fig. 3.2). Double shear test-pieces consist of two rubber disks, 25.4 mm in diameter and of various thicknesses, bonded between three cylindrical metal pieces. Quadruple shear test-pieces consist of four identical parallel sided rubber elements, about 22 mm long, 12.7 mm wide and of various thicknesses, bonded to four rigid plates to form a symmetrical double sandwich arrangement. With both types of shear test-piece, bonding was achieved during moulding or with methyl cyanoacrylate.

Prior to moulding, metal pieces were sandblasted, degreased in 1,1,1 trichloroethane and painted with the proprietary bonding agents, Chemlok 205 (primer coat) and 220 (top coat). An interval of about 15 minutes was allowed between the painting of the primer and top coats, and a further 20 minutes was allowed for the painted metals to dry before moulding.

Moulding was carried out in a transfer mould consisting of two sections, an upper chamber which held a rubber blank and the sample cavity, which held the shear test-pieces. The rubber blank was transferred into the sample cavities from the upper chamber with the use of an integral ram via appropriate nozzles.

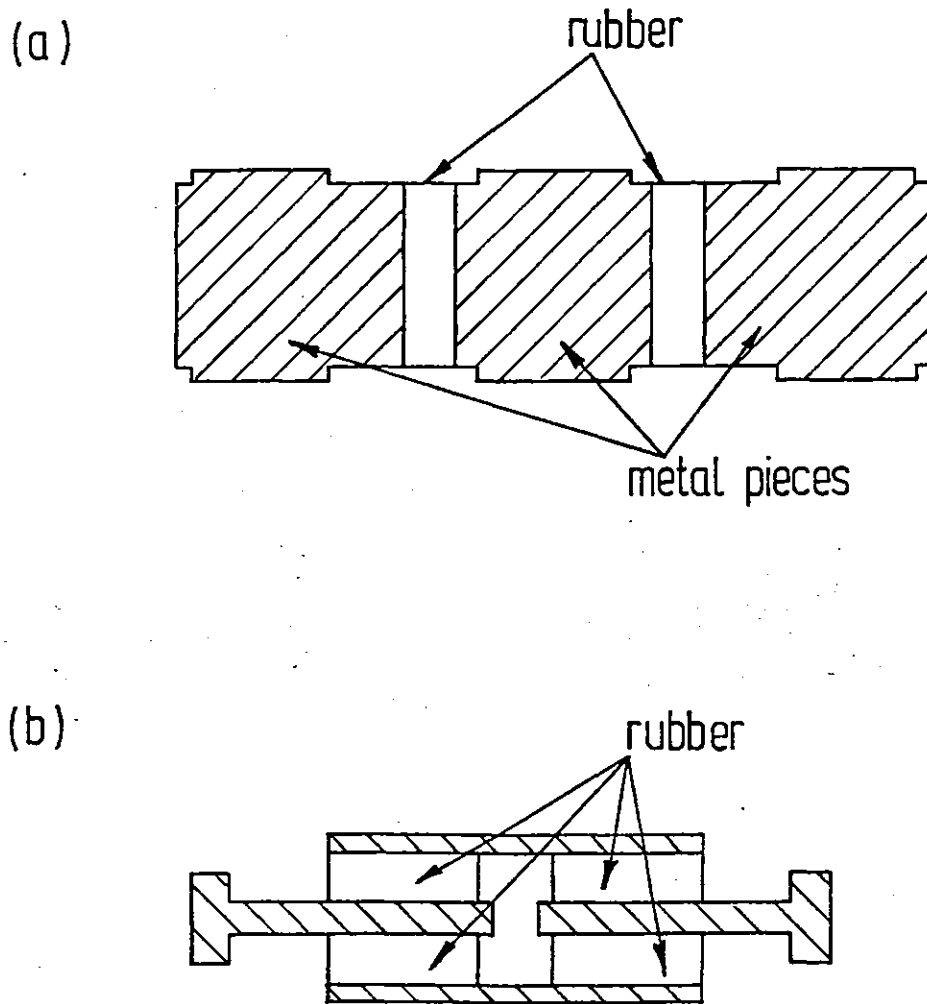


Figure 3.2. Shear test-pieces: (a) Double and (b) quadruple

Prior to room temperature bonding, the metal pieces were cleaned as described above and the rubber surfaces were cleaned with ethanol. The rubber samples for double shear test-pieces were either moulded disks (similar to the compression disks) or disks diestamped from moulded sheets. For quadruple shear, parallel sided rubber elements, diestamped from sheets, were bonded to the metal pieces using methyl cyanoacrylate. Bonding occurred within 30 seconds of contact but the bonded samples were not tested for at least 24 hours after preparation.

3.1.3 Instrumentation

Stress-strain measurements were mostly carried out on Instron testing machines, Models 1115 and 1122. Each instrument is comprised of a loading frame and a moving crosshead operated at a constant rate by two vertical drive screws. Strain gauge load cells were mounted either on the crosshead (Model 1122) or the frame base.

The capacities of the load cells used were 20N, 5 kN or 100 kN, depending on the loads required during deformation. The outputs from load cells were fed into recorders via amplifiers which were calibrated in steps of 1,2,5,10,20,50 and 100. The full scale sensitivity of the load cells were as follows:

<u>Load cells capacity (N)</u>	<u>Ranges of full scale sensitivity (N)</u>
20	0-1 to 0-20
5000	0-10 to 0-5000
100,000	0-2000 to 0-100,000

The accuracy of the load was $\pm 0.5\%$ of the indicated load or $\pm 0.25\%$ of the recorder scale used, whichever was greater for all load ranges.

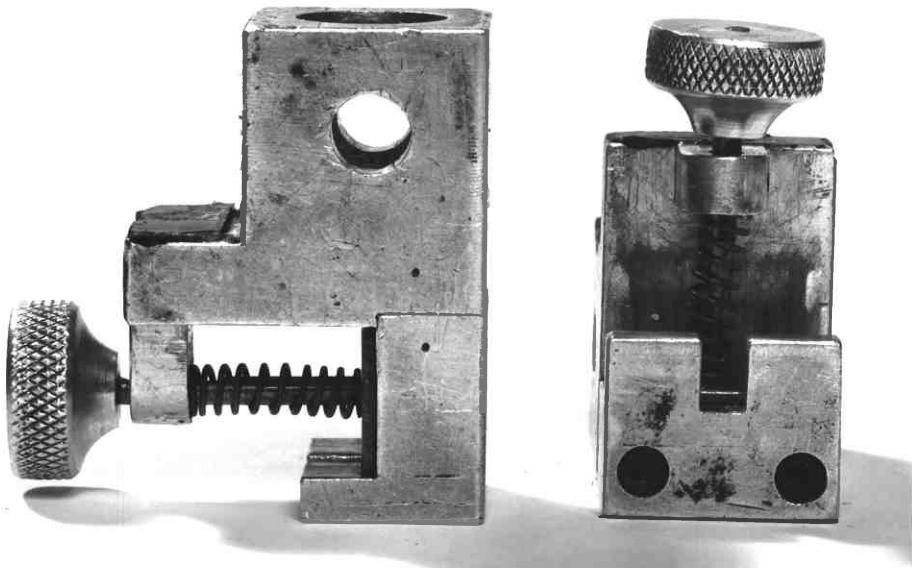
The recorder chart and crosshead were both driven at a constant rate, enabling the crosshead movement and grip separation to be measured. The accuracy of displacement readings (or grip separation) depends on the ratio of crosshead to chart speeds. A ratio of crosshead to chart speed of 1:100 enabled a crosshead movement of 0.01 mm to be measured with reasonable accuracy.

The above technique of measuring displacement assumed the test equipment was rigid. The accuracy of the results may be affected if there is any machine deflection, the amount of which depends on the machine stiffness. The stiffness of the large capacity machine was 50 kN/mm. For most tests, loads of < 5 kN were required, for which the machine deflection gave less than 5% error. In certain cases, in particular for compression tests, an error due to machine deflection may be appreciable because of the high load required (> 10 kN). Corrections were therefore made for machine deflection where necessary.

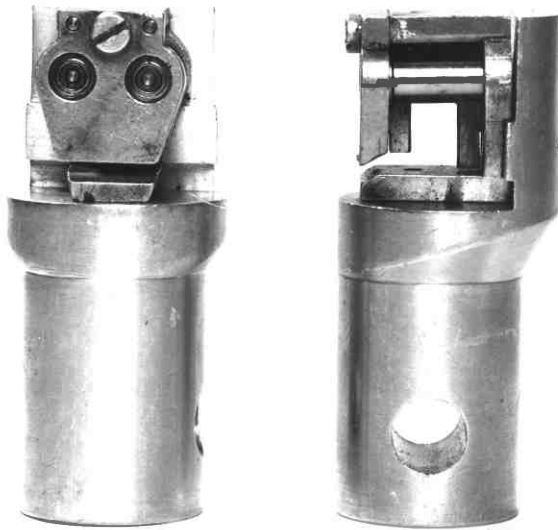
In tension tests carried out on the testing machine, two different types of grips were used. The grips used for parallel sided dumbbells consisted of spring loaded pads (fig. 3.3a).

Lubricated pulleys were used to hold ring samples. A pulley consisted of two smooth aluminium cylinders, about 8 mm in diameter, which were secured to a metal plate (fig. 3.3b). Rings were laid down with the inner diameter in contact with the cylinders, which rotated freely when the sample was stretched.

Double shear samples were held in screw tightened collar grips (fig. 3.4a) by the three metal pieces. The middle section was attached to the moving crosshead while the two end pieces were attached to the frame via the load cell.

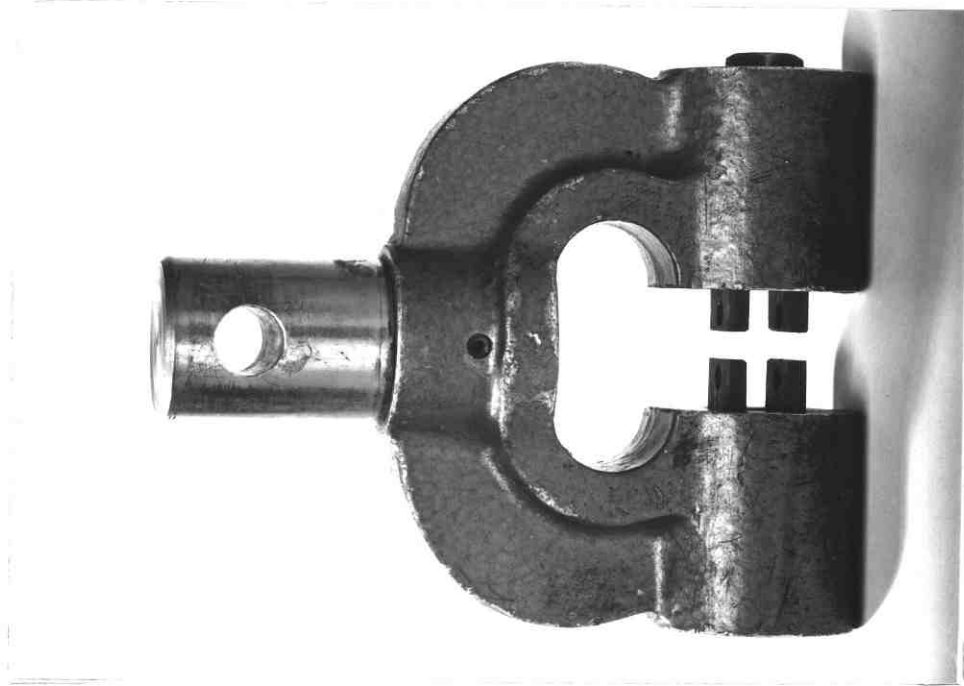


(a)

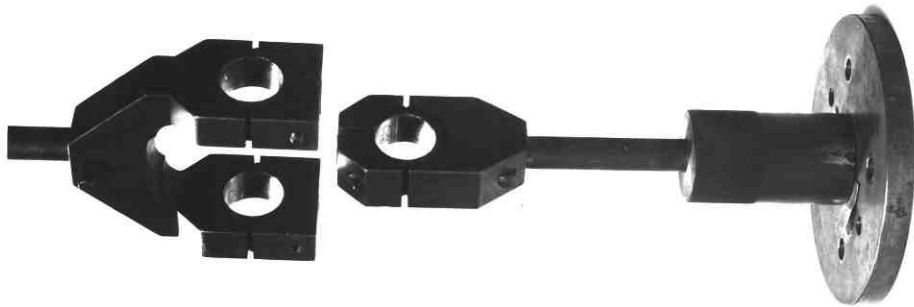


(b)

Figure 3.3. Grips for tensile test (a) spring loaded
(b) pulley



(b)



(a)

Figure 3.4. Grips for shear test (a) Collar
(b) Notched

Quadruple shear test-pieces were held at their T-piece plates in the notched grips (fig. 3.4b).

Compression tests were carried out between two polished circular metal plates (ca. 10 mm diameter). One plate was mounted on the load cell which was fixed to the machine base while the other was fixed to the moving crosshead.

For measurements carried out using dead loading techniques, the parallel sided and type C dumbbells were held by screw tightened brass clamps. With the rings and shear test-pieces, the grips used for dead loading tests were the same as those used on the testing machines.

3.1.4 Stress-strain measurements

All measurements were carried out on samples which were conditioned at least 24 hours at room temperature (23°C) after vulcanization. Except where indicated, all measurements of force and deflection were carried out on previously undeformed samples at room temperature. Where a testing machine was used, the recorder chart speed was 200 mm per minute and zero deflection was taken as the zero load position.

The extension ratio, λ , was taken as the ratio of the deformed length to the original undeformed length of the sample for simple extension and compression while for simple shear, it was taken as the ratio of sample deflection to the undeformed thickness. The nominal stress was obtained by dividing the applied load by the appropriate cross-section area of the sample.

3.1.4.1 Uniaxial extension

For tests carried out using the testing machines, all extensions were at 20 mm per minute until the sample broke or, in the case of parallel sided dumbbells, until the sample slipped out of the grips.

On extension, the parallel sided dumbbells gave fairly clear strain origins (i.e. no tailing or soft lead-in of the load-deflection curve). With the rings, no clear origin was obtained and the load-deflection curves appeared to give a tailing effect at low strains before it rises. Zero deflection and load positions were obtained by extrapolating the linear region of the load-deflection curve to the base line.

For dead loading techniques of measurement, two reference lines about 25 mm apart, were drawn mid-way between the two gripped ends. Extension of the test piece hanging vertically was measured by following the movement of the reference lines using a cathetometer. The position of the reference line was measured to ± 0.01 mm. To standardise and reduce the errors in measurement, three readings were taken after each load increase. The first reading (upper reference line) was taken at 60 seconds after adding the weights. It was immediately followed by reading the lower reference line (second reading) and a repeat reading of the upper reference line (third reading). The average of the first and third readings gave the position of the top reference line.

The increment of load varied, depending on the stiffness of the rubber, so as to result in a 2 to 3% change in strain at low strain region and about 10 to 20% change in strain at high strains. The maximum load added was about 120N or that giving about 300% extension, whichever was achieved first.

3.1.4.2 Lubricated uniaxial compression

(a) Evaluation of suitable lubricant for compression test

In lubricated compression, the role of lubricants is to reduce the friction between the rubber block and compression plates so as to

ensure homogenous deformation. An evaluation of the most suitable lubricant to be used, based on the coefficients of sliding friction between the rubber block and metal plate was carried out.

The lubricants evaluated were water/teepol mixtures and silicone oils. Tests were carried out on two rubber disks (25.4 mm diameter, 8.0 mm thick) bonded to a polished circular metal plate (50 mm diameter, 5 mm thick) using methyl cyanoacrylate (fig. 3.5).

Lubricants were applied to the unbonded surfaces of the rubber, and the laminate was placed between compression plates. A compressive load was applied and a steady pull force required to slide the sample noted. The laminate was removed, fresh quantity of lubricant applied and the process was repeated with different loads and lubricants. The load was increased by an arbitrary amount and the maximum load applied was determined by the magnitude of pulling force, the latter not exceeding 200N.

Results obtained were expressed as μ , the coefficient of sliding friction μ (= pull force \div load) Vs Load (N) (fig. 3.6). Water appeared to be a comparatively poor lubricant, but as indicated by the coefficients of friction, the 1:1 volume:volume water-teepol mixture proved to be the best lubricant, particularly at low loads, although at high loads, silicone oil of 1000 c/s viscosity appeared to be comparable to the water-teepol mixture. Concentrated teepol and the water-teepol mixtures showed comparable coefficients of friction at low loads but at high loads, the water-teepol mixture gave a much lower coefficient of sliding friction. Therefore, in subsequent studies, the 1:1 volume:volume water-teepol mixture was used as a lubricant.

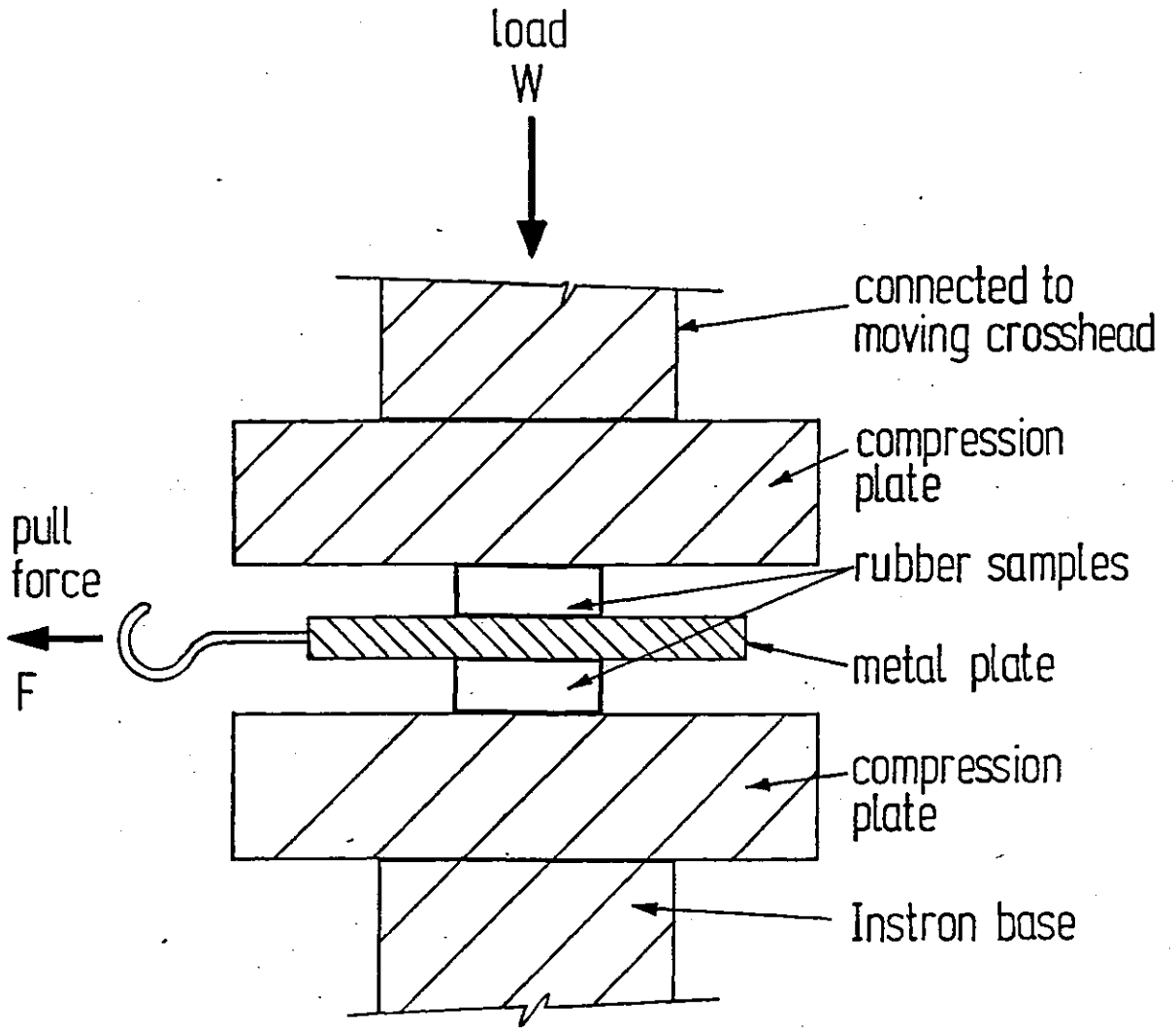


Figure 3.5. Pull test

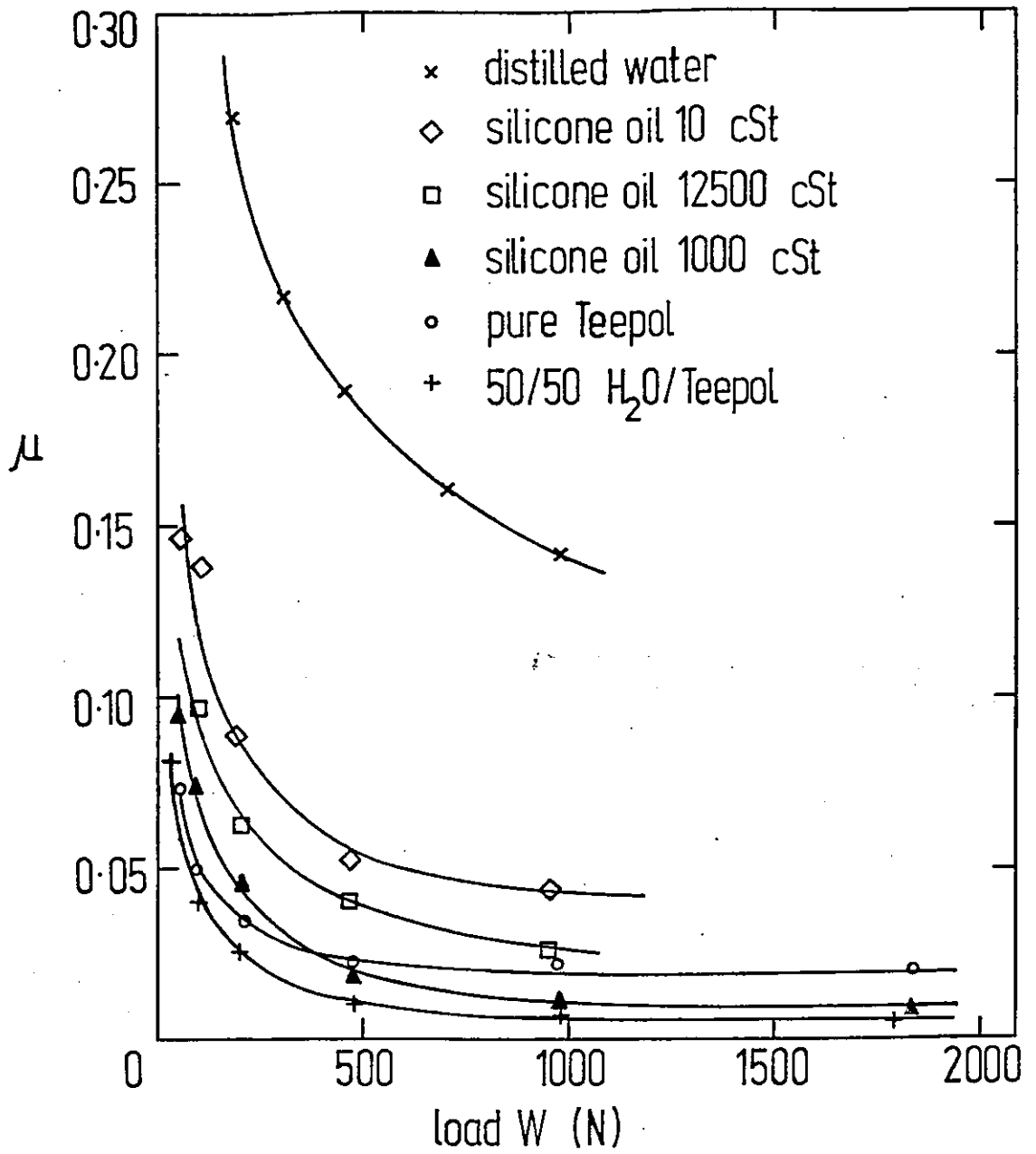


Figure 3.6. Coefficients of sliding friction, μ , as a function of applied load

(b) Compressive stress-strain measurements

Rubber disks which were lubricated with a water-teepol mixture were placed between two compression plates. Displacement was applied by lowering the upper compression plate onto the samples at 2 mm per minute, up to a maximum of about 80% strain.

3.1.4.3 Simple shear

All shear tests carried out on the testing machine were at 2 mm per minute until the samples broke. Failures occurred mainly at the rubber-metal bonds but occasionally within the rubber. For dead loading techniques, samples were deformed to about 50% shear strain.

(a) Double shear tests

The two ends of the samples were held firmly in a jig which was suspended freely from a load cell while the lower grip holding the central section was secured to the crosshead. Deformation was applied by displacing the central section of the test-piece.

For dead loading techniques of measurement, two reference lines were drawn opposite each other on one end and the central section of the test-piece. Samples were firmly gripped at the two ends and loads were applied to the central section of the test-piece. The separation of the two reference lines was followed as described in section 3.1.4.1. The load increment was chosen so as to give a strain increment of about 2% at low strain region and about 10% increment at high strain. The maximum load added was about 220N.

(b) Quadruple shear tests

Samples were suspended on by upper grip and deformation was achieved by applying a displacement to the lower grip. The outer metal plates were free to move horizontally and the contraction of the sample was monitored using a Vernier caliper.

For dead loading techniques, two reference lines were drawn at the centre of the unbonded faces on the metal T-plates. The separation of the reference lines on deformation was followed as described in section 3.1.4.1 and the load increment was as described above (section 3.1.4.3a).

3.1.5 Equilibrium swelling measurements

The tests were carried out to determine the amount of swelling agent/solvent imbibed at equilibrium swelling by both unfilled and filled rubbers. The samples were prepared from masterbatches (table 3.2) which contained no process oil, as this was leached out during swelling, causing an undesirable variation in the results. The products of sulphur and accelerator concentrations for EV, Semi-EV and conventional vulcanizing systems used were kept constant so as to maintain approximately the same crosslink density using weight ratios of CBS:S of 6.0:0.3, 1.0:1.8, and 0.6:3.0 respectively. For the peroxide vulcanizing system, a 3.0 pphr dicumyl peroxide was used because it gave comparable moduli to that of the sulphur vulcanizing system.

The solvent used was n-Decane having a specific gravity (at 23°C) of 0.7298 and not highly volatile (b.p. 174°C) at room temperature. The use of highly volatile solvent will introduce inaccuracy in the results since appreciable loss of solvent will occur during weighings.

Swelling tests were carried out on 25 mm square samples, cut from 1 mm moulded sheet. The pre-weighed samples were swollen in solvent contained in a covered container placed in the dark for about a week, during which the weights of the samples were regularly monitored. The swollen samples were subsequently transferred into fresh solvent and left to stand for several more days. At equilibrium

swelling, the weights of the swollen samples were recorded and samples were dried in a vacuum oven at 60°C. The difference between the weight of swollen and dried samples was taken as the true weight of the solvent imbibed.

During swelling, a small proportion of non-rubbers leached out, since they are soluble in the swelling agent (1). The amount of non-rubbers leached out was very small (about 1%) and no significant effect on the results was expected.

3.2 Experimental Discussion

The objective of the studies was to establish the reliability and accuracy of stress-strain measurements carried out on the testing machine. The tests were checked against the dead loading technique of measurement (except for compressions) and the variability of modulus due to the effect of types of test-piece and anisotropy (87-89) was investigated. All tests were carried out using 25 pphr N330 carbon black filled natural rubber vulcanizates.

3.2.1 Uniaxial extension

3.2.1.1 Effects of measurement techniques

With dead loading techniques, the magnitude of load and extension were measured to a known precision because direct measurements were carried out; the load was measured to about $\pm 0.01N$ and the extension to ± 0.01 mm.

The extensions using dead loading were taken 60 seconds after the addition of load. Variations in modulus due to creep were therefore expected. The increase in strain with time at constant load (i.e. creep) during the first two minutes was difficult to monitor, but the reduction in stress with time (i.e. stress-relaxation) was much easier to measure. When the rates of creep (C_R) and stress relaxation (S_R) are defined respectively by,

$$C_R = \frac{1}{e} \left(\frac{de}{dt} \right)_t \quad (3.1)$$

and

$$S_R = -\frac{1}{\bar{\sigma}} \left(\frac{d\bar{\sigma}}{dt} \right)_e \quad (3.2)$$

Gent (90) showed that, at a given extension e

$$C_R = \alpha S_R \quad (3.3)$$

where

$$\alpha = \frac{\bar{\sigma}}{e \left(\frac{d\bar{\sigma}}{de} \right)_t} \quad (3.4)$$

$\bar{\sigma}$ is the stress per unit unstrained area corresponding to an extension e , t is the relaxation time and $\frac{d\bar{\sigma}}{de}$ is the slope of the stress-extension curve. Knowing α and S_R , the values of C_R can be evaluated.

For our vulcanizates, the reduction in stress during the first 2 minutes was observed to vary from about 2% at low strain to over 8% at high strain (table 3.4). Using equation (3.1), the amount of creep occurring over two minutes was calculated. Over the range of strain investigated, the predicted amount of creep was observed to vary from about 3% to 5% (table 3.4). The reduction in modulus over the strain ranges investigated was therefore expected to be about the same extent as the amount of creep.

Table 3.4 Values of creep calculated from stress-relaxation using conversion factor α at $t = 2$ minutes

Strain %	α	Stress relaxation (measured) %	Creep (calculated) %
20	1.34	2.2	2.9
30	1.44	2.3	3.3
50	1.38	2.5	3.5
70	1.27	2.6	3.3
100	1.12	3.3	3.7
120	1.07	3.9	4.2
150	0.88	5.4	4.8
170	0.77	6.4	4.9
200	0.69	7.5	5.2
250	0.62	8.0	5.0

For tests carried out using the testing machine, the extension was not measured directly; the grip separation was taken as the measure of strain. The accuracy of strain was therefore dependent on whether the sample deformation varies proportionally to the grip separation. The accuracy of load measured using the load cells was about 0.25-0.5% (see section 3.1.3).

(a) Parallel sided dumbbells

A comparison of the modulus obtained from the two techniques of measurement is shown in figure (3.7). The results were for the mean of three readings, and the variability was not more than $\pm 2\%$ from the mean.

At low to moderate strains, fairly close agreement ($\pm 2\%$) was observed between the results obtained using the two techniques of measurement. As indicated above, some differences due to the effects of creep were expected with dead loading techniques, but as figure (3.7) shows, no significant difference in modulus was observed between the two techniques of measurement, suggesting that the variations due to the differences in times of measurement are within the experimental scatter.

At higher strains (>150%), the modulus obtained using the testing machine was found to be lower than those obtained by the dead loading. The differences increased with strain, up to about 350% strain, when the samples slipped out of the grips.

The differences observed could not be due to creep during dead loading measurements as this effect would be to reduce the modulus by no more than 6%.

Extensions of the parallel sided dumbbells on the testing machine were also measured directly from the separation of two

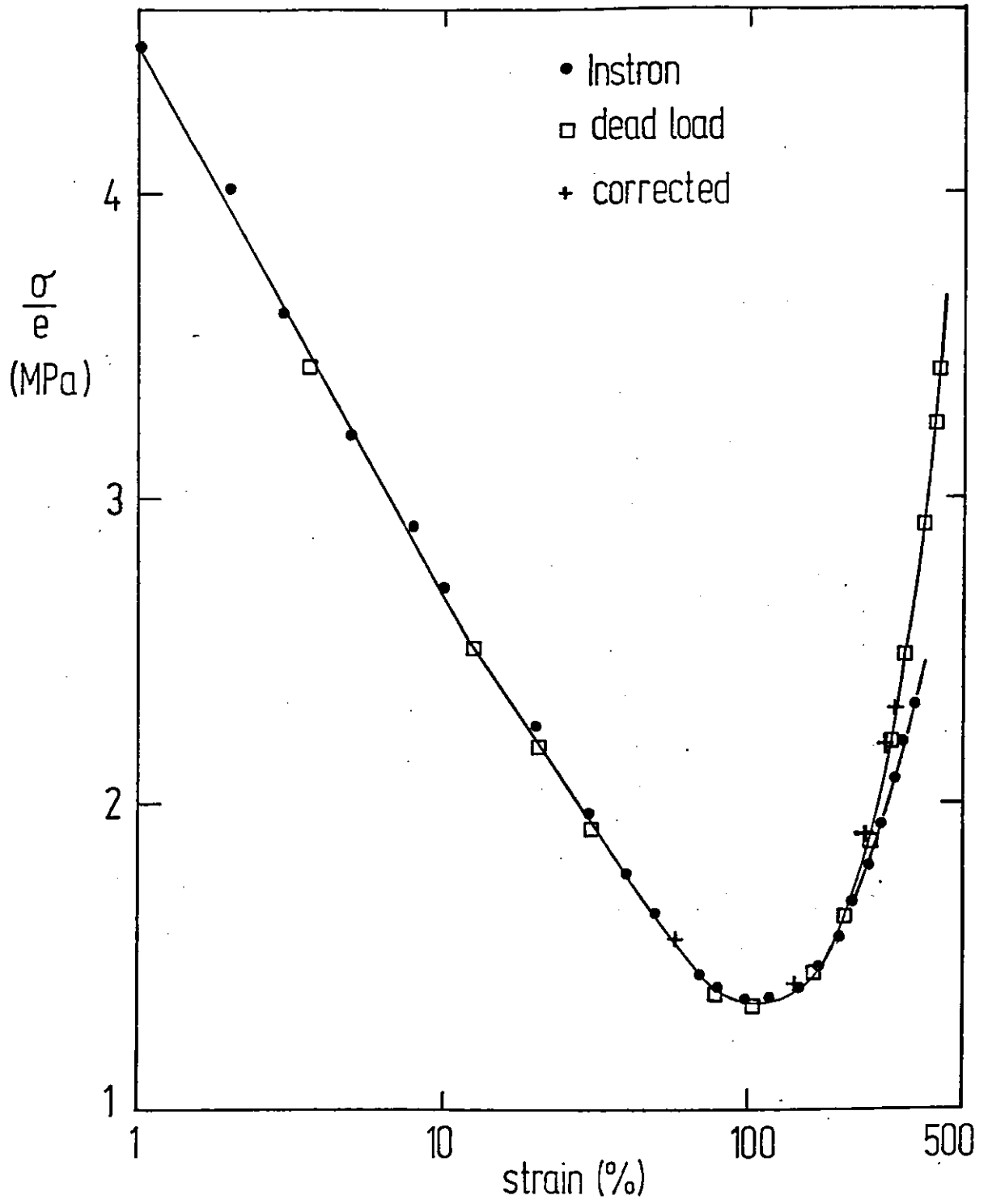


Figure 3.7. Effects of modulus on techniques of measurement for parallel sided dumbbell samples

reference lines on the sample (when the extension was stopped), using a cathetometer. The moduli obtained by this method are given in table 3.5 together with the results obtained using grip separations to determine the strain.

Table 3.5 Effects of sample slippage on modulus

<u>Obtained from Grip Separation</u>		<u>Direct measurement</u>	
e	$\frac{\sigma}{e}$	e	$\frac{\sigma}{e}$
%	(MPa)	%	(MPa)
20	2.24	20	2.24
60	1.53	59	1.55
150	1.41	146.5	1.44
250	1.82	238.5	1.91
300	2.09	283	2.21
320	2.20	303	2.34

Up to 150% strain, no significant difference in strain or modulus was observed between the two sets of results, but at higher strains, the extension given by crosshead separation (column 1) became progressively higher than those measured using the cathetometer (column 3).

The differences in strain measurements observed in table 3.5 were thought to arise from slippage of the sample at the gripped shoulders. When lines were drawn across the parallel strip at the intersections of the shoulders and the strip prior to extension, the lines were observed to be displaced in the direction of tensile force on extension, indicating that the square shoulders were being

pulled out of the grips. This confirmed the view that the differences in strain observed in table 3.5 were due to sample slippage.

Column 4 of table 3.5 gives the values of modulus based on the strain obtained by direct measurement. The results are consistent with those obtained using the dead loading technique, where the strains were also directly measured (figure 3.7, corrected results). This suggests that, if accurate strains were measured, the moduli are independent of measurement techniques.

At low to moderate strains, the moduli obtained by taking the grip separation as the measure of strain are the same as those obtained by direct measurement. At higher strains, sample slippages result in errors in the strain measurement since the grip separation do not represent the true strain. Measurements of the modulus using parallel sided dumbbells on the testing machine are therefore reliable at low to moderate extensions (<150%) before any slippage occurs.

(b) Ring samples

When rings were tested on the testing machine, the stresses did not immediately increase with displacement. A tail or soft lead-in of the load-deflection curves developed during straightening of the rings, resulting in an uncertainty in the origin. Zero deflection was obtained by extrapolating the linear region of the load-deflection curve onto the base line.

All strains were calculated from the mean circumference of the undeformed rings and the results obtained were the means of three readings. At low strains, the results obtained vary by more than $\pm 5\%$ from the mean while at higher strains, they vary by about $\pm 2\%$. When the tests were carried out using the dead loading techniques,

more reproducible results were obtained ($\pm 2\%$ from the mean).

A comparison of moduli obtained using the two techniques of measurement using rings is shown in figure 3.8. At low to moderate strains the moduli obtained using dead loading were considerably higher than those using the testing machine. Only at very high strains ($>200\%$) were the moduli obtained using the two different techniques of measurement within the experimental scatter.

The basic difference between the two techniques of measurement was the measurement of strain. With dead loading, the strains were measured directly and to a known precision, whereas when tests were carried out using the testing machine, settlement of the sample onto the grip resulted in some uncertainty in the strain origin. Considerable systematic errors could be introduced in using linear extrapolation to obtain the strain origin and this may explain the differences in moduli observed at low to moderate strains (fig. 3.8). At very high strains, reasonable agreement was obtained between the two techniques of measurement because small absolute errors in strain did not significantly affect the moduli.

At low to moderate strains, the measurement of moduli using rings was not reliable for tests carried out on the testing machine since the grip separation did not give an accurate measure of strain in the sample. Reliable moduli were only obtained when measurements were carried out using dead loading techniques. Rings therefore proved to be unsuitable for our purpose.

3.2.1.2 Effects of types of test-piece

The samples compared were parallel sided dumbbells, type C dumbbells and rings. The measurements of moduli were carried out using dead loading techniques because the strains were able to be measured to a

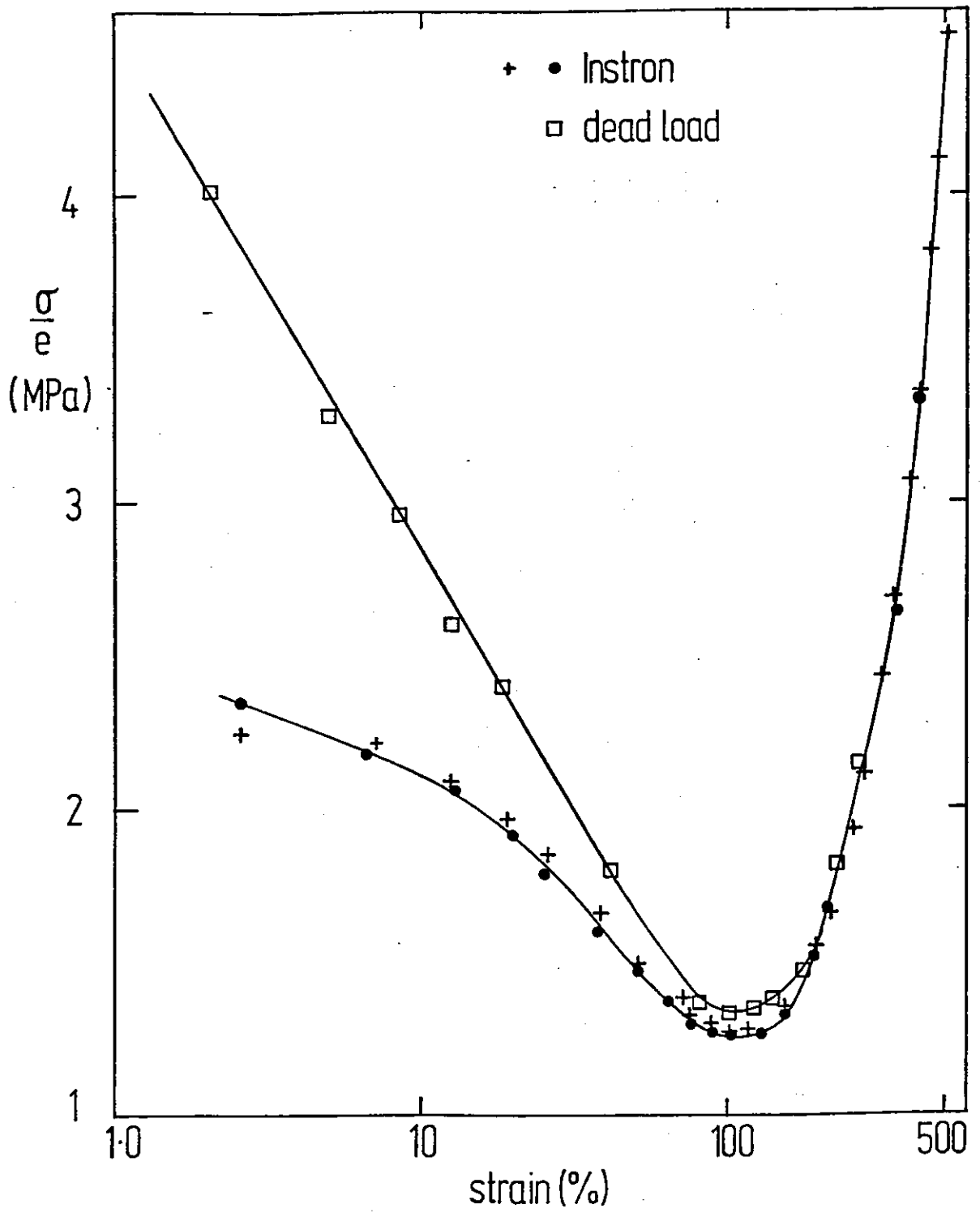


Figure 3.8. Effects of modulus on techniques of measurement for ring samples

known precision with all samples. The results are shown in figure 3.9. All moduli (or $\frac{\sigma}{e}$) values appeared to be within the experimental scatter i.e. no significant difference in modulus was observed between samples of different geometries. This suggests that, when force and deflection are measured accurately, the tensile stress-strain values over the strain range covered are unaffected by the sample geometries.

3.2.1.3 Effects of anisotropy

The effects of anisotropy on modulus was investigated using parallel sided dumbbells diestamped along and perpendicular to the direction of milling. No significant differences between moduli were observed for the two different directions of test, suggesting that the effects of anisotropy on tensile moduli of normally prepared samples were minimal.

3.2.2 Lubricated compression

All tests were carried out using the testing machine and the crosshead separation was taken as the measure of strain. No tailing of soft-lead in of the load-deflection curves was observed during the tests and the errors due to the strain origin were expected to be small.

3.2.2.1 Effects of types of test-piece

The investigations into the effects of types of test-piece on compression modulus were carried out using (a) moulded disks (b) square samples cut from 4.0 mm moulded sheet and (c) disks formed by plying 2.0 mm thick moulded sheet.

Different types of test-piece were used in order (a) to check the effects of sample dimensions on compression modulus since there

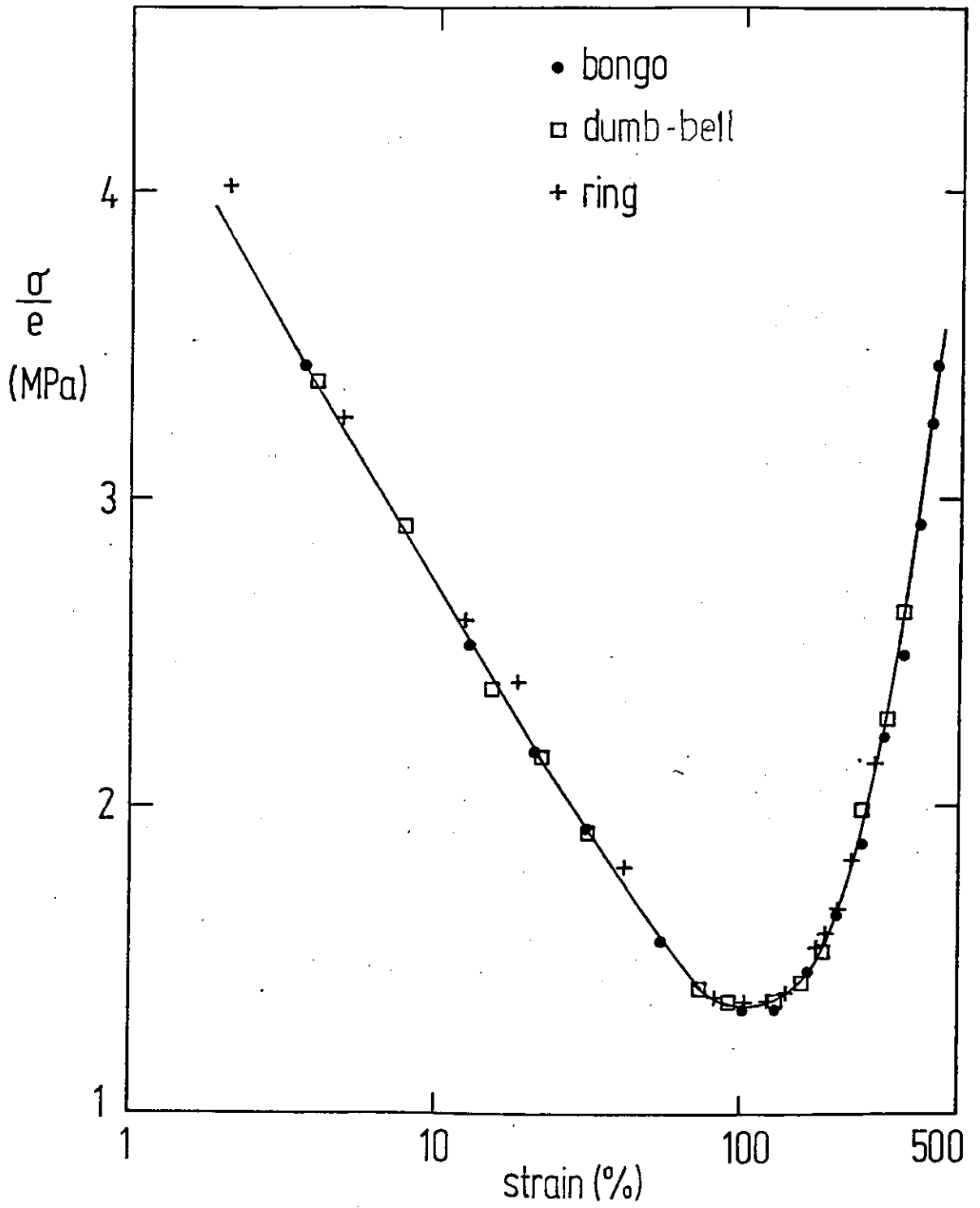


Figure 3.9. Effects of modulus of types of test-piece

was a possibility that the extent of lubrication may vary with sample diameter/size and (b) to use the rubber samples which were obtained from the same sheet as those in tension and simple shear (cold bonded samples).

The results for moulded samples are shown in figure 3.10, where the points are the results obtained from disks and the broken lines are those for square samples cut from moulded sheet (4 mm thick). At low to moderate strains (<50%) the moduli obtained for samples of different geometry were approximately the same but at high strains (>50%), about 15% difference was observed between the lowest and highest value.

With plied-up disks of different diameters about 10% difference in modulus was observed between the highest and lowest values at low to moderate strains (<50%) (fig. 3.11). At higher strains (>50%), the variability observed with plied-up disks was similar to that observed with moulded samples. At all strains, the variability observed followed no specific trend.

It was expected that all plied-up disks would give the same modulus since they were made up of rubbers cut from the same sheet. But as figure 3.11 shows, differences in moduli were observed with sample of different dimensions. The differences were not due to the machine error since a similar effect was not observed with moulded samples which were similarly tested. The possibility was that the scatter was due to the presence of the bonding agents within the samples. No firm evidence could be put forward to support the view but based on the observation that the plied-up samples became distorted after the tests, it was deduced that the bonding agent used was not effective and such an effect may have contributed to the scatter of results observed in figure 3.11.

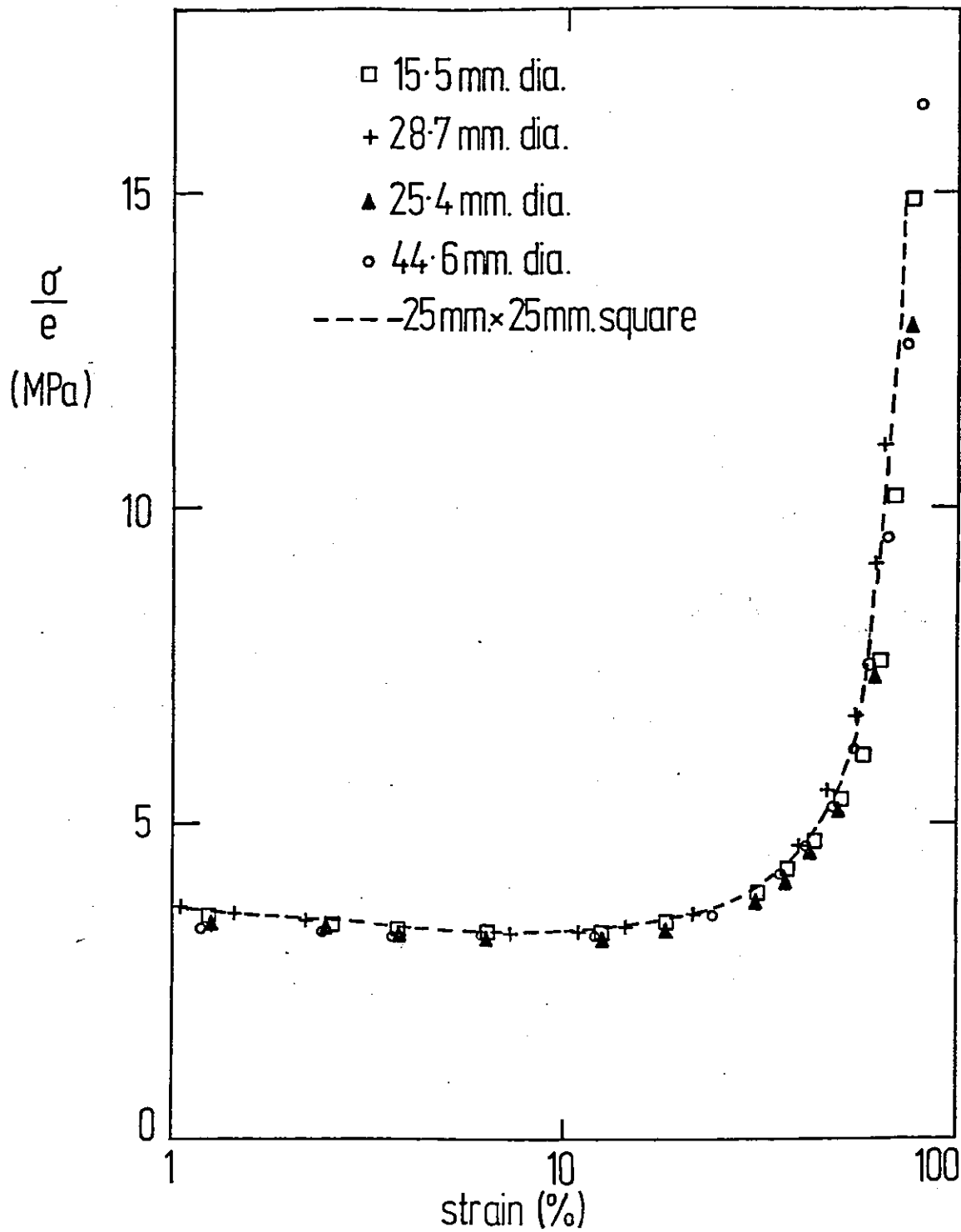


Figure 3.10. Effects of modulus on sample geometry for moulded samples

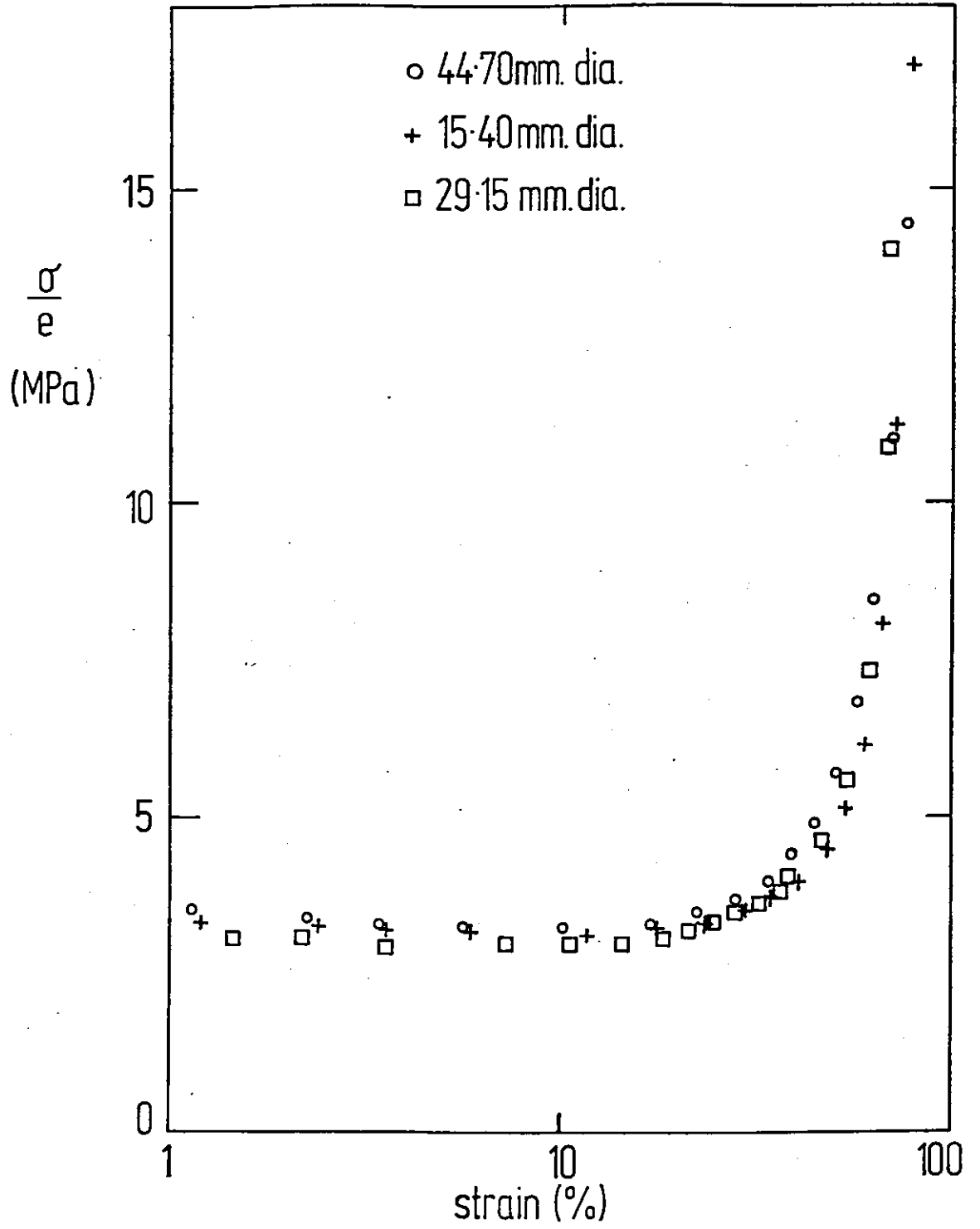


Figure 3.11. Effects of modulus on sample geometry for plied-up samples

The experimental results indicate that the coefficient of friction and so the modulus was unaffected by sample cross-sectional area (i.e. area of contact) when 1:1 volume to volume teepol-water mixture was used as lubricant. Some variability though was observed when plied-up disks were used because the samples were not well bonded. For this study, moulded disks appeared therefore to be the more suitable test-specimens.

3.2.3 Simple shear

The measurements were carried out on the testing machine and the grip separation was taken as the measure of strain. With all samples tested, no tailing of the stress-strain curve was observed and subsequently a clear origin was obtained. The variation in modulus due to errors in selecting the strain origins were consequently expected to be small.

No anisotropic effects were expected with shear samples since the rubber was randomly mixed during the mould filling process. Tests also indicated that when the double shear test-pieces were rotated, no differences in modulus were obtained.

3.2.3.1 Effects of types of test-piece

Experiments on the effects of types of test-piece on shear modulus were carried out using double and quadruple shear samples which were prepared both by moulding and cold bonding.

During deformation, the three metal pieces of the double shear samples were firmly gripped, ensuring the dimension perpendicular to the direction of shear remained unchanged. The samples were therefore subjected to simple shear deformation. With the quadruple shear test-pieces, the metal pieces were unrestrained, and contraction perpendicular to the shear direction

could occur. For samples of about 5 mm thick, the extent of contraction and the variations of shear moduli due to contraction are given in table 3.6.

Table 3.6 Effects of sample contraction (Quadruple shear)

Shear Strain (%)	Reduction in thickness (%)	G_{expt} (MPa)	G_{calc} (MPa)
19	0	0.90	0.90
49	1.2	0.8	0.80
98	1.8	0.73	0.72
146	2.5	0.74	0.73
195	3.9	0.78	0.75
244	5.9	0.91	0.85

The experimental values of shear modulus, (G_{expt}) were obtained by calculating based on the original sample thickness while the values of G_{calc} were obtained based on the deformed thickness. At moderate strains (<150%) the sample contraction and hence the differences between the experimental and calculated values of modulus were not significant (i.e. within experimental scatter). At higher strains (>150%), however the difference between G_{expt} and G_{calc} became detectable.

A comparison between moduli obtained using double and quadruple shear samples is shown in fig. 3.12. Within the strain range covered, it appeared that the types of test-pieces and bonding have no significant effect on the modulus. The contraction of samples in quadruple shear is not large enough to be significant at low to moderate strains (>150%). Thus, for tests at low to

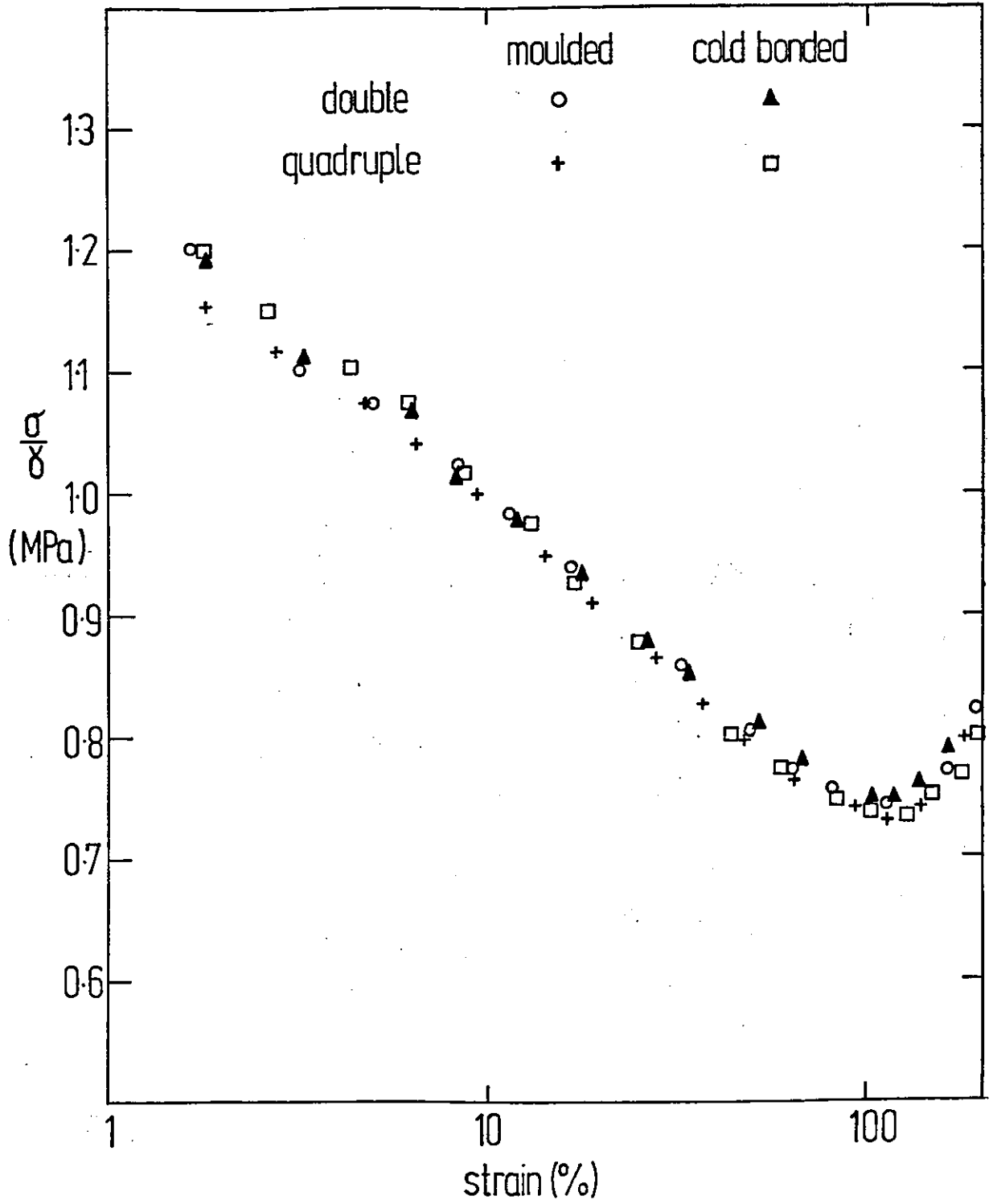


Figure 3.12. Effects of shear modulus on types of test-piece

moderate strains, both the quadruple and double shear samples can be used.

3.3 Conclusion

The section discusses the reliability of the stress-strain measurements carried out on the testing machine using samples of different geometries. For low to moderate strains, (<100%), the following conclusions can be drawn.

(a) In tension, the stress-strain values obtained with the parallel sided dumbbells were more reliable and reproducible ($\pm 2\%$ from the mean) than those obtained from rings. All further tensile tests were therefore carried out on the testing machine using the parallel sided dumbbells.

(b) No significant difference in modulus was obtained with the use of the two different types of shear samples, which were prepared either by cold bonding or moulding. In all cases, the results were within the experimental scatter ($\pm 2\%$ from the mean). However since the cold bonded samples could be more easily made from disks used for compression tests, double shear samples were used for all further tests.

(c) A water-teepol mixture (1:1 by volume) was found to be a good lubricant for the compression tests. Hence, all the lubricated compression tests were carried out using water-teepol as the lubricant.

The moulded samples gave more reliable and reproducible ($\pm 2\%$ from the mean) results than the corresponding plied-up samples. Consequently, further tests were carried out using moulded samples. Since all the moulded samples evaluated gave approximately the same modulus, then for convenience, disks of 25.4 mm in diameter and those

cut from 4.0 mm thick moulded sheet were used because (i) both samples could be bonded onto the double shear end pieces and (ii) tensile tests could also be carried out on the sample obtained from the same sheet. Thus, direct comparison of the stress-strain properties for rubber taken from the same sheet but tested using different modes of deformation could be carried out.

SECTION 4: STRESS-STRAIN RELATIONSHIP FOR FILLED AND
UNFILLED RUBBERS

- 4.1 Introduction
- 4.2 A form of stress-strain relationship
- 4.3 Verification of the stress-strain relationship
 - 4.3.1 The correlation between stress and strain
 - 4.3.2 Comparisons between experimental and predicted values
- 4.4 Physical significance of parameters A, B and C

SECTION 4 STRESS-STRAIN RELATIONSHIP FOR FILLED AND UNFILLED
RUBBERS

4.1 Introduction

There are two main approaches in defining constitutive equations to describe the elastic nature of rubber-like materials. The molecular approach considers the response of the molecular network to deformation. Typically, this is the statistical or Gaussian theory where the parameters are calculated from such quantities as finite molecular length and molecular weight between crosslinks. There is also the phenomenological approach where the elasticity theory was derived from entirely mathematical considerations. The theories of Mooney, Rivlin and Valanis-Landel, are among those which are derived based on the phenomenological approach.

The statistical theory does not satisfactorily describe the stress-strain behaviour of rubber. The phenomenological theories, were able to describe the stress-strain behaviour of rubber fairly accurately. However, those theories were based on the assumption that the stresses are uniquely determined by the strain imposed. This assumption is valid provided that there is complete reversibility and no hysteresis occurs. With rubber-like materials in general, the assumption can be challenged on three grounds. Firstly the stresses on extension and retraction cycles are not identical and a significant proportion of the energy input is lost on retraction. Secondly the stresses are dependent on the strain history i.e. stress relaxation occurs with rubber resulting in variation of stresses with time.

The third factor concerns the effects of stress-softening, which give rise to a rubber requiring a greater stress to produce a given elongation on its first extension than during subsequent extension (91, 92). This phenomenon is exhibited by both filled and unfilled rubbers. On these grounds, it is clear that the assumption of stresses being uniquely determined by the imposed strains cannot be justified.

The theories of rubber elasticity are also based on the assumption that the sample is isotropic in the undeformed state. The assumption may be valid when the samples are at an equilibrium state of strain. However, all previous theories were tested using samples which were subjected to cyclic deformations to a relatively high strain prior to the test i.e. the samples were conditioned. The prestretching process can result in stress-softening, the effect of which may vary along the three different principal directions. Anisotropy may consequently be induced during conditioning cycles, making the assumption of isotropy invalid.

Even though there are uncertainties about the assumptions made, the phenomenological theories are still used for the prediction of the stress-strain characteristics of rubbers. As indicated by Tschoegl (34) and James, Green and Simpson (93) the most promising and widely used approach is that which involve the strain invariants, I_1 and I_2 , and which is basically that suggested by Rivlin (28,29). The prediction of stress using the theory of Rivlin involves the partial derivatives, $\frac{\partial W}{\partial I_1}$ and $\frac{\partial W}{\partial I_2}$, which are obtained from biaxial strain measurements. As indicated by Rivlin, determinations of $\frac{\partial W}{\partial I_1}$ and $\frac{\partial W}{\partial I_2}$ are subject to large experimental errors because they

involve the inverse term $(\lambda_1^2 - \lambda_2^2)^{-1}$ (see equation (2.41)). The errors are magnified as λ_1 and λ_2 tend to equality. In the limiting case, when $\lambda_1 = \lambda_2$ and $t_1 = t_2$, the values of $\frac{\partial W}{\partial I_1}$ and $\frac{\partial W}{\partial I_2}$ are indeterminate. Consequently the calculated values of $\frac{\partial W}{\partial I_1}$ and $\frac{\partial W}{\partial I_2}$ for values of λ_1 and λ_2 which are nearly equal are subject to large errors. At low stresses, the values of these partial derivatives are also likely to be subject to large errors because the probable errors in t_1 and t_2 are more nearly absolute in value than proportional to the magnitudes of t_1 and t_2 .

The relation between λ_1 and λ_2 at constant I_1 and I_2 is shown in figure 4.1. During the determination of $\frac{\partial W}{\partial I_1}$ and $\frac{\partial W}{\partial I_2}$, one of the strain invariants is kept constant while the other is varied, by increasing or decreasing λ_1 and λ_2 , the variation of which follows the curves in figure 4.1. If there is any irreversibility with the test samples, two different stresses and consequently two different values of $\frac{\partial W}{\partial I_1}$ and $\frac{\partial W}{\partial I_2}$ will be obtained at the same strain. The theory of Rivlin however considers $\frac{\partial W}{\partial I_1}$ and $\frac{\partial W}{\partial I_2}$ as material constants which only depend on strain; two different values at a fixed strain are therefore unacceptable. Thus if the deformation is irreversible, the theory of Rivlin cannot adequately describe the stress-strain behaviour of rubber.

The stress-strain relationship in tension or compression obtained from the phenomenological theory of Rivlin may be expressed as:

$$\frac{\sigma}{\lambda - \lambda^{-2}} = 2 \left(\frac{\partial W}{\partial I_1} + \frac{1}{\lambda} \frac{\partial W}{\partial I_2} \right) \quad (4.1)$$

and in simple shear, it may be written in the form,

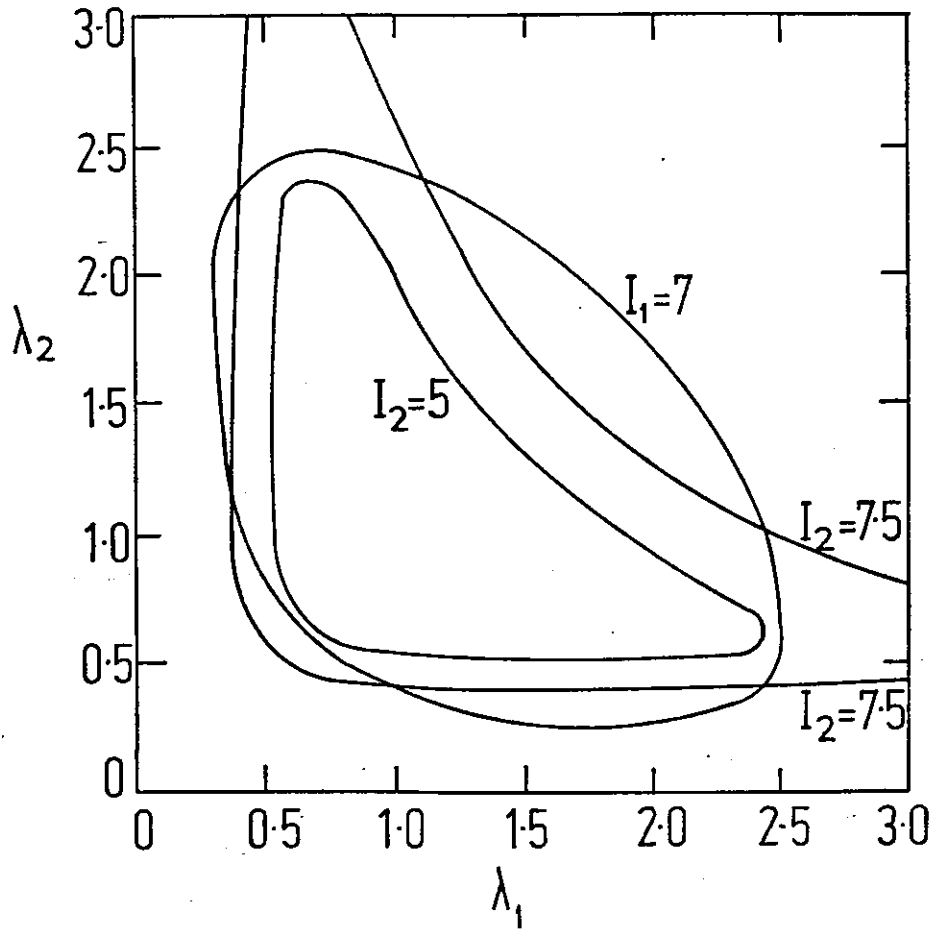


Figure 4.1. Relation between λ_1 and λ_2
at constant I_1 and I_2 (28)

Explanatory note

The theory of Rivlin expresses the stored energy function, W as a function of $\frac{\partial W}{\partial I_1}$ and $\frac{\partial W}{\partial I_2}$. If W is strongly dependent on I_1 and I_2 , the moduli in tension, compression (H) and simple shear (G) cannot be simply related because the contributions due to I_1 and I_2 will be different for different types of strain. Only if W is a function of I_1 or I_2 are the moduli likely to be related.

Previous work (94) had suggested that the stored energy function for the three simple modes of deformation considered was dependent only on I_1 , and the contribution due to I_2 was small. If this were true, then the moduli in tension, compression and simple shear should be equal if the strains at which they were measured gave equal values of I_1 . For convenience and because $(I_1-3)^{\frac{1}{2}}$ is equal to the shear strain (equation 2.39), this function was used.

Comparing the moduli at equal values of I_1 can also reveal any dependence of W on I_2 . If $\frac{\partial W}{\partial I_1}$ is dependent on I_2 and/or the contribution due to $\frac{\partial W}{\partial I_2}$ is not small, differences in the values of H and G at equal $(I_1-3)^{\frac{1}{2}}$ will be observed.

$$\frac{\sigma}{\gamma} = 2 \left(\frac{\partial W}{\partial I_1} + \frac{\partial W}{\partial I_2} \right) \quad (4.2)$$

Knowing $\frac{\partial W}{\partial I_1}$ and $\frac{\partial W}{\partial I_2}$, stress-strain behaviour in tension, compression or shear can be calculated using equation (4.1) and (4.2) respectively.

The terms $\frac{\partial W}{\partial I_1}$ and $\frac{\partial W}{\partial I_2}$ have been found to vary with both I_1 and I_2 (30,31). Several attempts have been made to quantify these partial derivatives. For unfilled rubbers, Obata, Kawabata and Kawai (30) expressed the values of $\frac{\partial W}{\partial I_1}$ and $\frac{\partial W}{\partial I_2}$ in terms of I_1 and I_2 , namely,

$$\frac{\partial W}{\partial I_1} = a_0 + \frac{a_1}{(I_1-3)^2} - \frac{a_2(I_2-3)}{(I_1-3)^{2.5}} \quad (4.3)$$

$$\frac{\partial W}{\partial I_2} = A_0 + \frac{A_1}{(I_2-3)} + \frac{2a_2}{3(I_1-3)^{\frac{1}{2}}}$$

where a_0 , a_1 , a_2 , A_0 and A_1 are constants for a particular rubber.

Using equation (4.3) and the values of the constants given by Obata et al, stresses at defined strains were calculated for tension,

compression and shear deformations using the Rivlin's equation (equation

4.1 and 4.2). The results obtained, expressed as $\frac{\sigma}{\lambda-\lambda^{-2}}$ (or H) and

$\frac{\sigma}{\gamma}$ (or G) Vs $(I_1-3)^{\frac{1}{2}}$ are shown in figure 4.2. For the three modes of deformation considered, values of H and G predicted at equal $(I_1-3)^{\frac{1}{2}}$ are

not identical. At moderate strains $(I_1-3)^{\frac{1}{2}} > 1.0$ for instance, the

modulus in tension was about 50% higher than in compression and such

differences were not observed in practice (94). At low strains, values

of H (in tension/compression) and G (in shear) rose sharply such that

the calculated values of modulus below 20% shear strain (or $I_1-3)^{\frac{1}{2}} < 0.2$)

Note (refer to figure 4.2)

The values predicted by the relationships of Obata et al and James and Green are represented by points in order to enable comparison to be made between the moduli in tension, compression and simple shear at specified $(I_1-3)^{\frac{1}{2}}$ values. The broken line represents typical values of moduli obtained experimentally on a vulcanizate similar to that of James and Green.

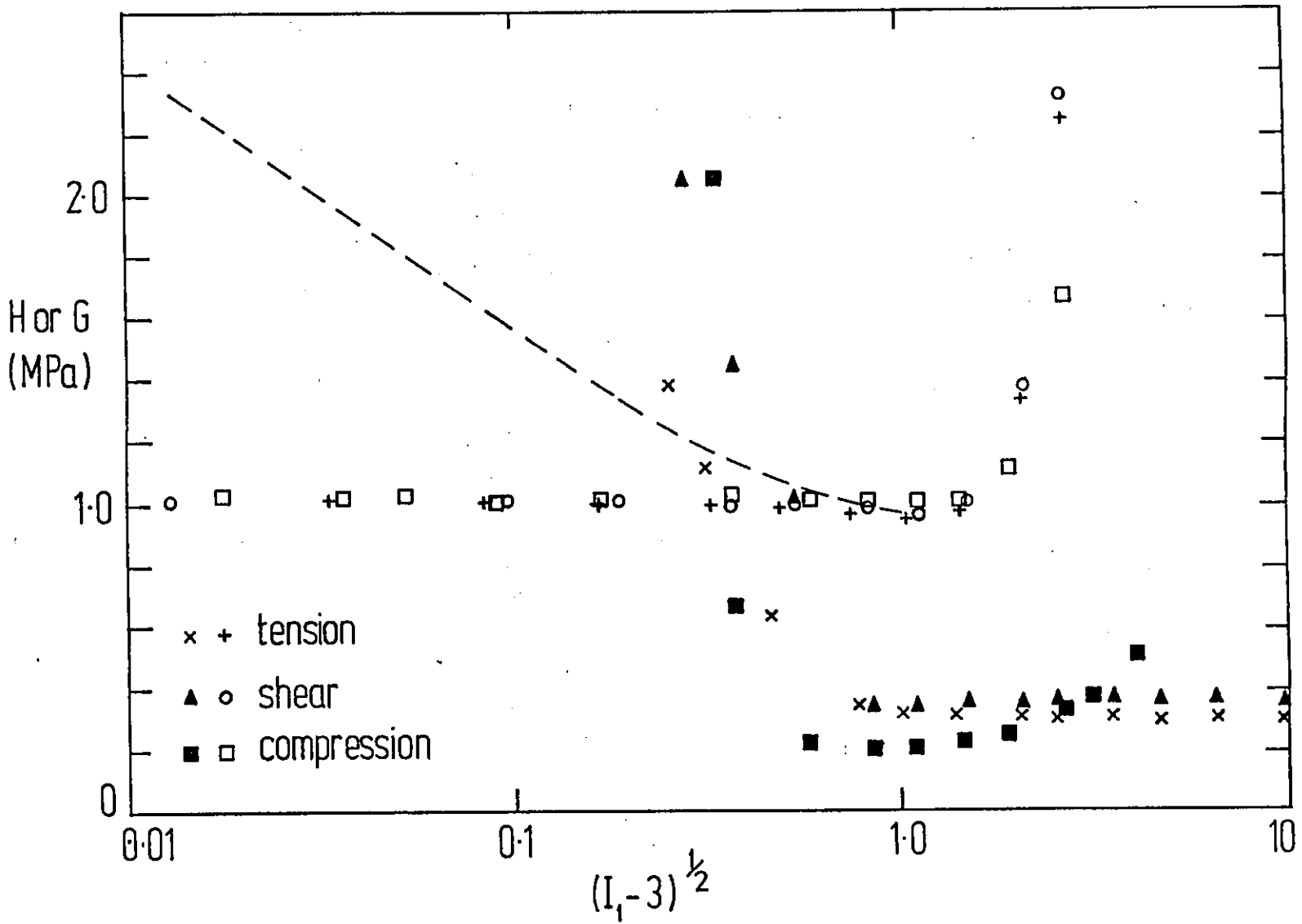


Figure 4.2. Shear, tensile and compressive moduli as a function of $(I_1 - 3)^{1/2}$ (x, \blacktriangle , \blacksquare , Obata's et al; +, o \square - James and Green)

became extremely high. At very high strains, on the other hand, the moduli remained fairly independent of strain. No sign of the sharp up-turn in the plots of G or H Vs $(I_1-3)^{\frac{1}{2}}$, which occurs in practice, was observed. The predicted values are therefore inconsistent with the experimental observations and the values of $\frac{\partial W}{\partial I_1}$ and $\frac{\partial W}{\partial I_2}$ obtained using the Obata relationship are considered inadequate.

James and Green (95) developed an empirical relationship for the calculation of the values of $\frac{\partial W}{\partial I_1}$ and $\frac{\partial W}{\partial I_2}$ which takes the form,

$$\frac{\partial W}{\partial I_1} = C_{10} + 2C_{20}(I_1-3) + 3C_{30}(I_1-3)^2 + C_{11}(I_2-3) \quad (4.4)$$

$$\text{and } \frac{\partial W}{\partial I_2} = C_{01} + C_{11}(I_1-3)$$

where $C_{10}, C_{20}, C_{30}, C_{11}, C_{01}$ and C_{11} are constants for a particular rubber. Using equation (4.4), values of $\frac{\partial W}{\partial I_1}$ and $\frac{\partial W}{\partial I_2}$ for the James and Green rubber (i.e. Natural rubber + 40 phr N330 black) were calculated. The relative contributions of the terms given in equation (4.4) relative to C_{10} for $\frac{\partial W}{\partial I_1}$ and to C_{01} for $\frac{\partial W}{\partial I_2}$ for simple extension are shown in table 4.1. The contributions to $\frac{\partial W}{\partial I_1}$ at low strain ($\lambda < 2.0$) appear to be mainly due to the constant C_{10} , since the terms involving C_{20}, C_{11} and C_{30} are very small. At higher strains ($\lambda > 2.0$) the contribution from the C_{10} term becomes insignificant due to the increase in the term involving C_{30} , the increase of which is due to the $(I_1-3)^2$ term. The value of $\frac{\partial W}{\partial I_1}$ is therefore dependent mainly on the $3C_{30}(I_1-3)^2$ term at high strains.

The partial derivative, $\frac{\partial W}{\partial I_2}$ is given as a sum of two terms, but as table 4.1 shows, the term involving C_{11} is negative.

Table 4.1. Relative Contribution of the terms given by James
and Green formula for simple extension

λ	$\frac{\partial W}{\partial I_1}$				$\frac{\partial W}{\partial I_2}$	
	C_{10} (MPa)	$\frac{2C_{20}(I_1-3)}{C_{10}}$	$\frac{3C_{30}(I_1-3)^2}{C_{10}}$	$\frac{C_{11}(I_2-3)}{C_{10}}$	C_{01} (MPa)	$\frac{C_{11}(I_1-3)}{C_{01}}$
1.01	0.47	-5.55×10^{-6}	5.72×10^{-10}	-2.74×10^{-5}	0.041	-3.17×10^{-5}
1.05	"	-3.4×10^{-4}	2.15×10^{-6}	-1.65×10^{-4}	"	-1.75×10^{-3}
1.10	"	-1.32×10^{-3}	3.23×10^{-5}	-6.19×10^{-3}	"	-7.56×10^{-3}
1.50	"	-2.72×10^{-2}	1.39×10^{-2}	-1.04×10^{-2}	"	-1.56×10^{-1}
2.0	"	-9.45×10^{-2}	1.63×10^{-1}	-2.94×10^{-2}	"	-5.51×10^{-1}
3.0	"	-3.13×10^{-1}	1.81	-7.11×10^{-2}	"	-1.79
4.0	"	-6.32×10^{-1}	7.45	-1.17×10^{-1}	"	-3.61
5.0	"	-1.05	20.49	-1.65×10^{-1}	"	-6.0
7.0	"	-2.17	87.51	-2.57×10^{-1}	"	-12.41

Effectively $\frac{\partial W}{\partial I_2}$ depends only on the C_{01} at low strains ($\lambda < 1.5$) but becomes negative at higher strains ($\lambda > 1.5$).

The total stress depends on both $\frac{\partial W}{\partial I_1}$ and $\frac{\partial W}{\partial I_2}$, but since the two terms which constitute $\frac{\partial W}{\partial I_2}$ are very small, then only the value of $\frac{\partial W}{\partial I_1}$ is significant. The latter only depends on the C_{10} term at low strain and the term involving C_{30} at high strain, as indicated above. Thus using the James & Green formula, the modulus may effectively be approximated to a constant at low strains ($\lambda < 1.5$) and to a term depending on $(I_1 - 3)^2$ at high strains ($\lambda > 1.5$).

Predictions of modulus in tension, compression and simple shear deformations using the James & Green formulae for natural rubber filled with 40 phr N330 black are shown in figure 4.2 (top curve). At all strains, the moduli in the three modes of deformation considered are approximately equal, which is consistent with the experimental observation (94). However in practice, at low to moderate strains ($(I_1 - 3)^{\frac{1}{2}} < 1.0$), the moduli are dependent on strain. This can be clearly seen from the results obtained in tension for a rubber of similar stiffness, which are plotted together in figure 4.2 (broken line) where the modulus progressively decreases with strain at low to moderate (before the up-turn in stress-strain curve).

It may be argued that with the James and Green data, the modulus is independent of strain at low to moderate strains because the samples were subjected to cyclic deformations prior to the tests (i.e. the sample was conditioned). As a result, carbon black agglomerate structures were broken down by the applied strain. Such arguments are however not justified since when natural rubber filled with 40 phr N347 black were subjected to ten cyclic deformations, the moduli are still dependent on strain (fig 4.3). The moduli at low strains are higher than those at high strains ($(I_1 - 3) > 1.0$).

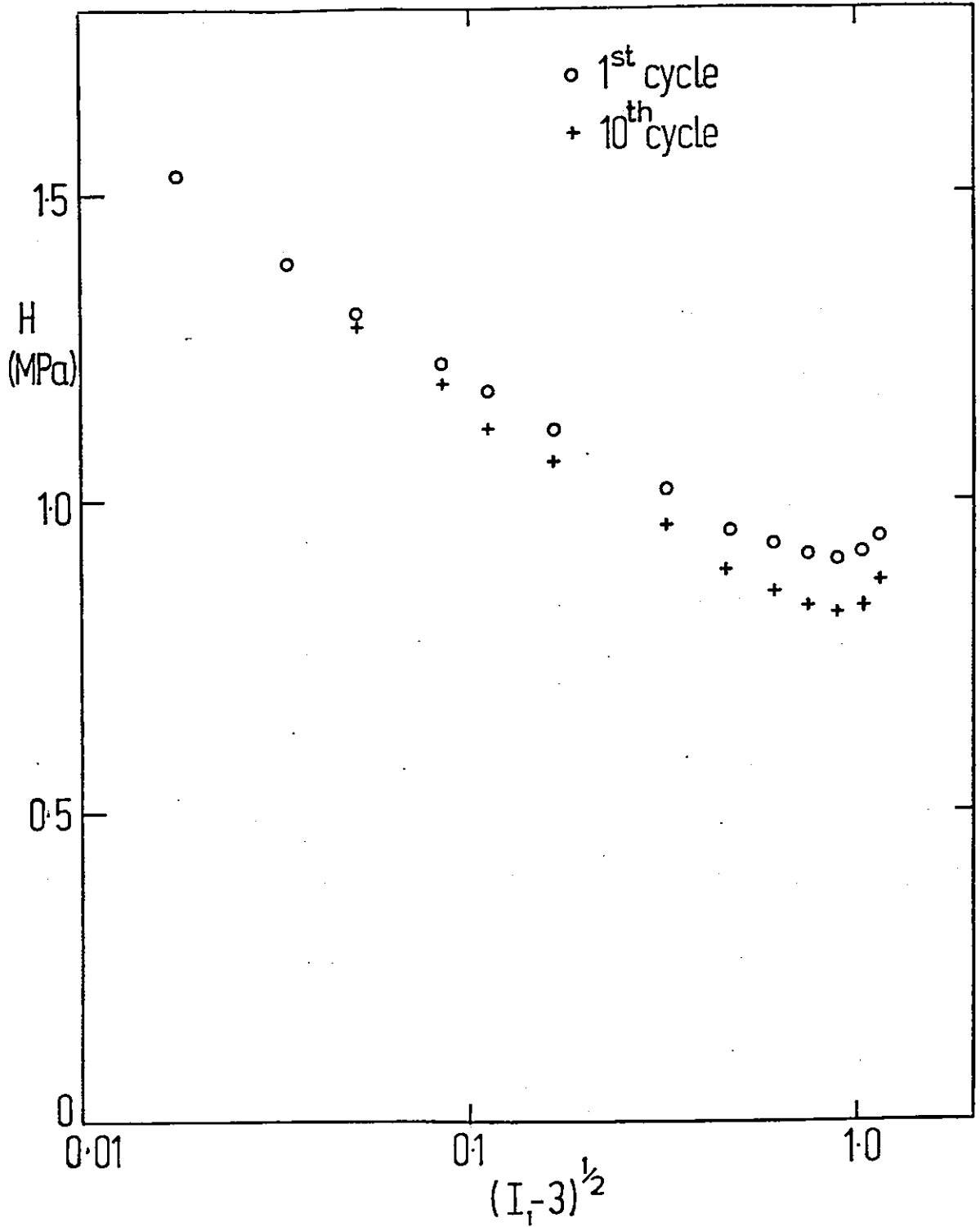


Figure 4.3. Effects of cyclic deformations on tensile modulus of 40 pphr N347 filled natural rubbers

The type of carbon black used for the samples which were subjected to cyclic deformations has about the same structure (as denoted by DBPA values) as that used by James & Green and the cyclic deformations were expected to give similar effects. However as figure 4.3 shows, the results obtained are not consistent with those predicted by the James & Green formula. Thus even though the James & Green formula may predict the same values of modulus in tension and compression (H) to that in simple shear (G), the constant moduli obtained at low to moderate strains does not conform to experimental observations. The equations of James & Green are therefore not adequate for the description of stress-strain behaviour of rubbers.

Without attempting to calculate the values of the partial derivatives, Gregory (94) studied the stress-strain behaviour of a series of black filled rubbers. At low to moderate strains (before the upturn in the stress-strain curve) the author observed that the values of H in tension and compression are identical to G in shear at equal I_1 . No results were available at higher strains ($(I_1-3)^{\frac{1}{2}} > 1.0$). In order to extend the correlation between tension, compression and shear moduli up to higher strains, similar experiments have been carried out. Typical results are shown in figures 4.4 and 4.5. Figure 4.4 shows the plots of H or G Vs $(I_1-3)^{\frac{1}{2}}$ for rubber containing 25 phr N330 black while figure 4.5 shows similar plots for rubber filled with 60 phr N347 black. At low to moderate strains, ($(I_1-3)^{\frac{1}{2}} < 1.0$), both figures show the values of H in tension and compression to be approximately the same as the shear modulus, G. At higher strains however ($(I_1-3)^{\frac{1}{2}} > 1.0$), differences were observed between the moduli in the three modes of deformation considered. The tensile modulus, H

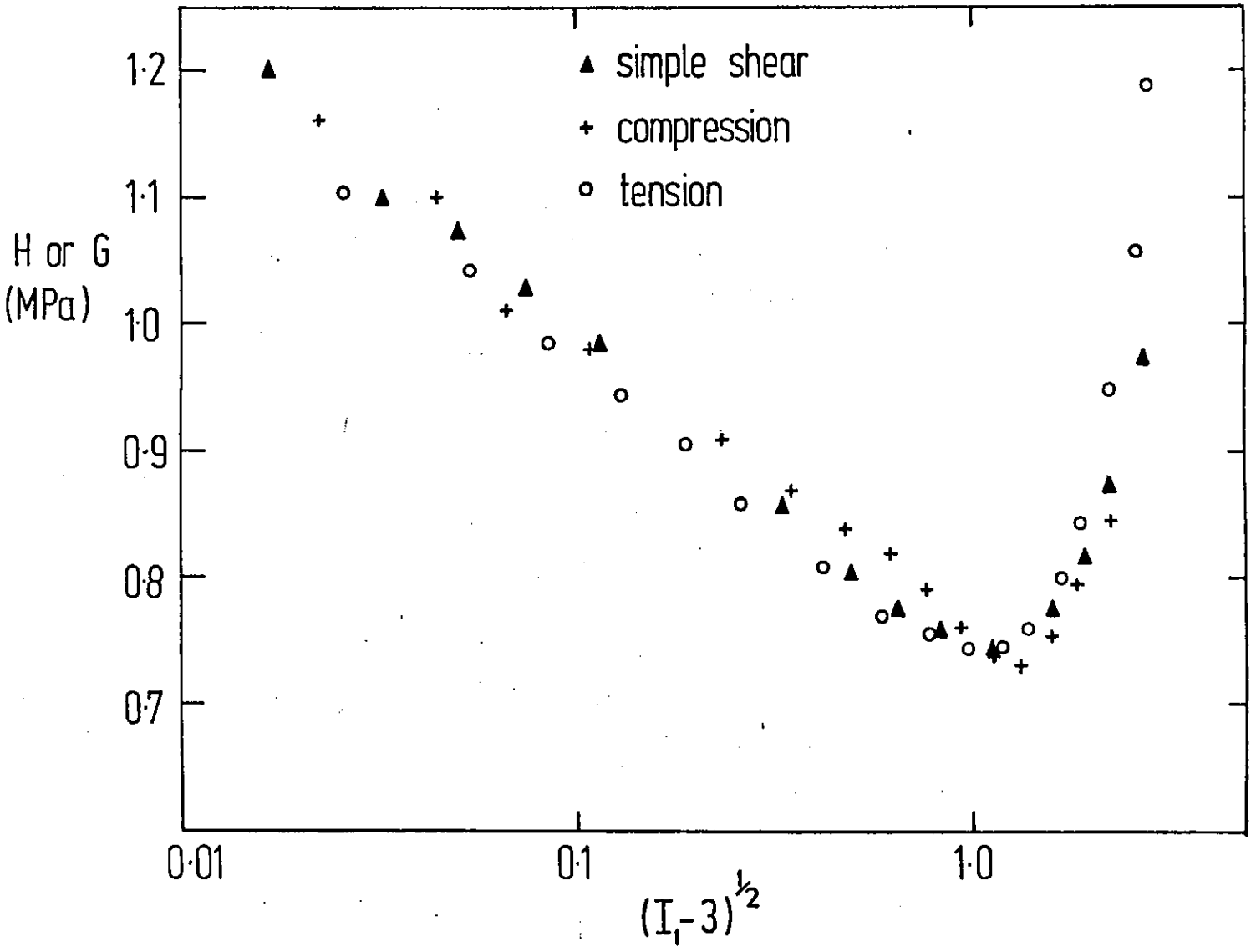


Figure 4.4. Shear, tensile and compressive moduli as a function of $(I_1 - 3)^{1/2}$ for 25 pphr N330 filled rubbers

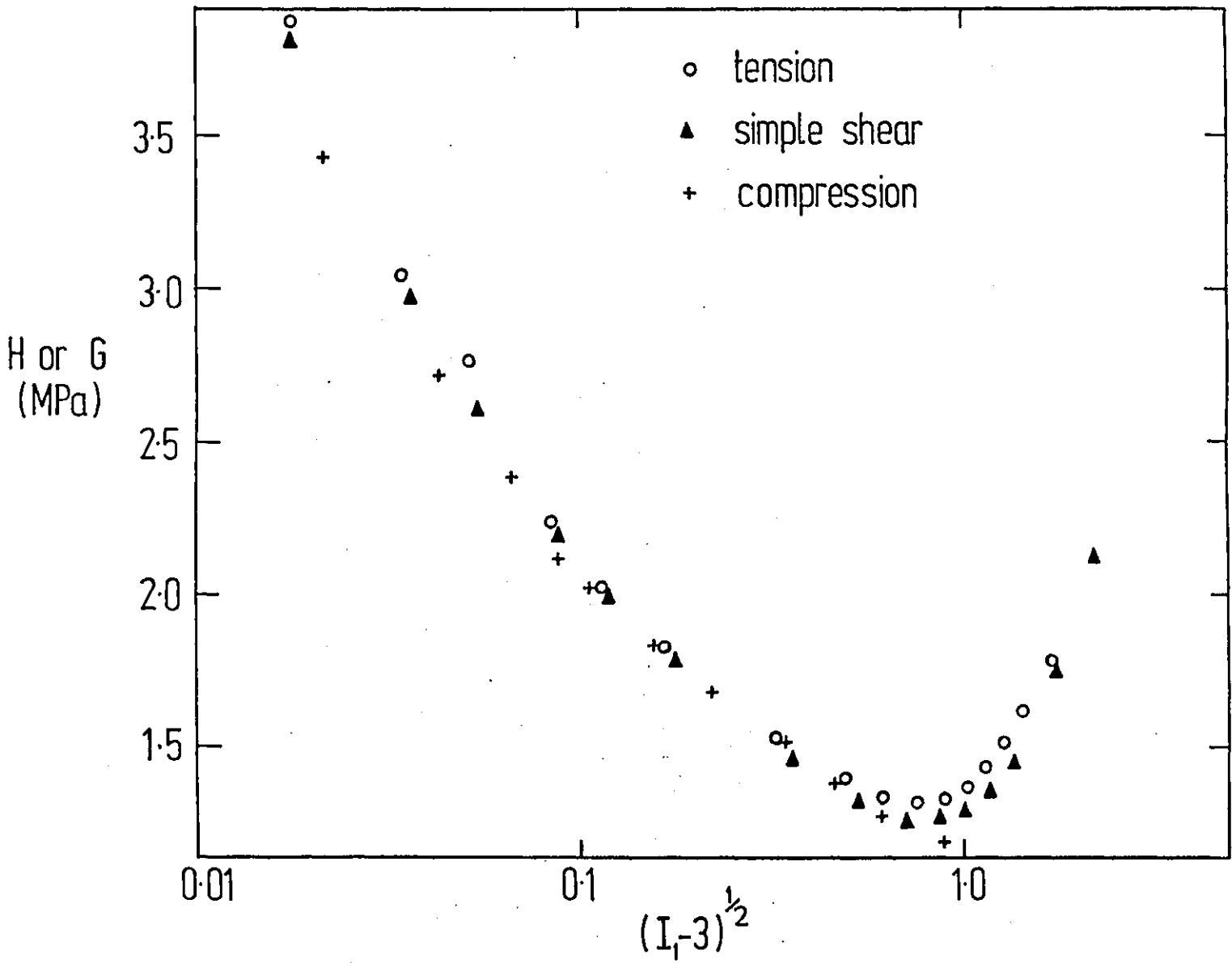


Figure 4.5. Shear, tensile and compressive moduli as a function of $(I_1 - 3)^{1/2}$ for 60 pphr N347 filled rubbers.

for instance, was about 10% higher than the shear modulus at $(I_1-3)^{\frac{1}{2}} = 3.0$, and the differences appeared to increase with strain. Data at very high strain for compressive deformation are not available because of experimental difficulties. The simple relationship between H in tension and compression and G in shear only exists at low to moderate strains.

The values of H and G are given by equations (4.1) and (4.2) respectively. For H to be identical to G, two explanations are suggested.

(a) The term $\frac{\partial W}{\partial I_2}$ is much less than $\frac{\partial W}{\partial I_1}$ and $\frac{\partial W}{\partial I_1}$ is independent of I_2 as suggested by Gregory. This reduces equations (4.1) and (4.2) respectively to

$$\begin{aligned} H &\approx 2\left(\frac{\partial W}{\partial I_1}\right) \\ G &\approx 2\left(\frac{\partial W}{\partial I_1}\right) \end{aligned} \tag{4.5}$$

Experimental evidence tends to suggest that, for both unfilled (30,31) and filled rubbers (95), $\frac{\partial W}{\partial I_1}$ is much greater than $\frac{\partial W}{\partial I_2}$ and the approximation given by equation (4.5) may be justified.

(b) Alternatively, the agreement between H and G observed at moderate strain may suggest that, when expressed as a function of I_1 , the values of $\frac{\partial W}{\partial I_1}$ and $\frac{\partial W}{\partial I_2}$ for different modes of deformation may compensate each other so as to give the values of $\frac{\sigma}{\lambda-\lambda^{-2}}$ in tension and compression to be approximately equal to $\frac{\sigma}{\gamma}$ in simple shear.

Whichever reason is correct, the agreement observed in practice between H and G suggests that at moderate strain, serious errors are not introduced if one assumes that the moduli in tension, compression and shear are only a function of I_1 .

4.2 A form of stress-strain relationship

Assuming that, at low to moderate strains, the moduli in tension, compression and simple shear are a function only of I_1 , then we may write, for simple extension or compression.

$$\sigma_T = F(I_1)(\lambda - \lambda^{-2}) \quad (4.6)$$

and for simple shear

$$\sigma_S = F(I_1)\gamma \quad (4.7)$$

where $F(I_1)$ is a term which is a function of the strain invariant I_1 . It follows that, if $F(I_1)$ is known, the stress-strain behaviour in tension, compression and simple shear can be predicted.

Let us consider a simple shear deformation. When the shear stresses are plotted against shear strain, the relationship is linear at moderate strains (fig. 4.6). The linear region may be expressed as,

$$\sigma_S = A\gamma + k \quad (4.8)$$

where A is the modulus at high strain and k is a constant. At low strain however, equation (4.8) cannot be applicable since the predicted shear stress does not approach zero at limiting shear strain. To accommodate the behaviour at low strains, the value of k may take the form,

$$k = f(\gamma)\gamma \quad (4.9)$$

where $f(\gamma)$ is a function which decreases with shear strain. The simplest possible form of $f(\gamma)$ which gives the required decrease in $f(\gamma)$ with increasing γ , but which provides a finite value of $f(\gamma)$ at zero strain is:

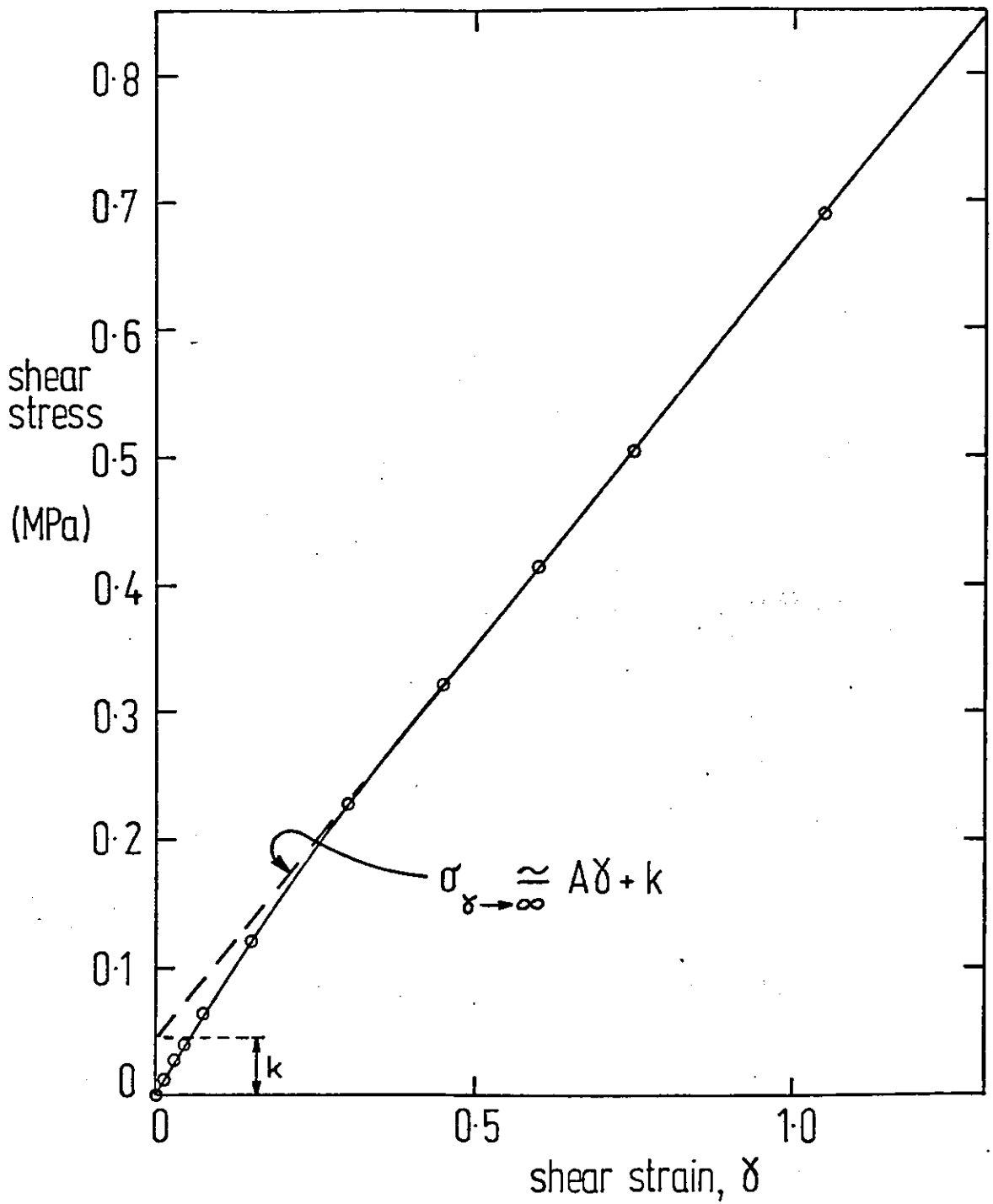


Figure 4.6. Shear stress as a function of shear strain for rubbers filled with 25 phr N330 black

$$f(\gamma) = \frac{1}{B\gamma + C} \quad (4.10)$$

where B and C are constants.

Shear strain is related to the strain invariant I_1 by,

$$\gamma = (I_1 - 3)^{\frac{1}{2}} \quad (4.11)$$

Substitution of equation (4.11) into (4.10) gives,

$$f(\gamma) = \frac{1}{B(I_1 - 3)^{\frac{1}{2}} + C} \quad (4.12)$$

From equations (4.8), (4.9) and (4.12), it follows that the shear stress may be expressed as:

$$\sigma_s = \left(A + \frac{1}{B(I_1 - 3)^{\frac{1}{2}} + C} \right) \gamma \quad (4.13)$$

The plots of $\frac{\sigma_T}{\lambda - \lambda^{-2}}$ Vs $(I_1 - 3)^{\frac{1}{2}}$ were found to be approximately the same as the corresponding plots of $\frac{\sigma}{\gamma}$ Vs $(I_1 - 3)^{\frac{1}{2}}$ for low to moderate strains, suggesting that the function $F(I_1)$ for simple extension and compression is the same as that for simple shear.

It follows that a more appropriate form of equation (4.13), which is applicable to the three modes of deformation considered will be

$$\sigma = \left(A + \frac{1}{B(I_1 - 3)^{\frac{1}{2}} + C} \right) f(\epsilon) \quad (4.14)$$

where $f(\epsilon) = \lambda - \lambda^{-2}$ for tension or compression and $f(\epsilon) = \gamma$ for simple shear.

4.3 Verification of the stress-strain relationship

4.3.1 The correlation between stress and strain

The relationship given by equation (4.14) is applicable to tension, compression and simple shear, but verification was carried out on rubbers subjected to tensile deformation because, experimentally, tensile tests are much easier to perform than shear or compression. Furthermore, repeat tests can be carried out for rubbers originating from the same source (i.e. same moulded sheet), thus reducing variability.

In tension, equation (4.14) may be written as,

$$H = A + \frac{1}{B(I_1-3)^{\frac{1}{2}} + C} \quad (4.15)$$

where $H (= \frac{\sigma}{\lambda-\lambda^{-2}})$ is an elastic modulus which depends on the three unknown constants, A, B and C. Rearranging equation (4.15) gives,

$$(H-A)^{-1} = B(I_1-3)^{\frac{1}{2}} + C \quad (4.16)$$

If equation (4.16) is valid, then plots of $(H-A)^{-1}$ Vs $(I_1-3)^{\frac{1}{2}}$ should be linear with a slope B and an intercept C.

In principle, A can be estimated from the limiting value of $\frac{d\sigma}{d(\lambda-\lambda^{-2})}$ at high strain. For lightly filled (≤ 20 phr black) rubbers, a fairly good estimation of A can be obtained graphically, but for unfilled rubbers estimation of A becomes difficult and inaccurate because the slope of σ Vs $\lambda-\lambda^{-2}$ plots at high strains does not reach a limiting value. For heavily filled rubbers on the other hand, the on-set of non-affine deformation at relatively low strain makes determination of $\frac{d\sigma}{d(\lambda-\lambda^{-2})}$ difficult.

Taking $\frac{d\bar{\sigma}}{d(\lambda-\lambda^{-2})}$ as the linear portion of $\bar{\sigma}$ Vs $\lambda-\lambda^{-2}$, curves (as value of A) plots of $(H-A)^{-1}$ Vs $(I_1-3)^{\frac{1}{2}}$ were made.

Typical results are shown in figures 4.7 and 4.8 and this suggests that equation (4.15) gives a good description of the stress-strain behaviour for the low to moderate strain region.

It may be noted that straight lines were only obtained from the plots of $(H-A)^{-1}$ Vs $(I_1-3)^{\frac{1}{2}}$ in the region before the upturn in the stress-strain curve, or in the region of affine deformation because the proposed relationship (equation 4.15) was derived based on the stress-strain behaviour in this region.

The linearity of the plots of $(H-A)^{-1}$ Vs $(I_1-3)^{\frac{1}{2}}$ are sensitive to changes in A, particularly at high strains where H approaches A. An accurate determination of A is therefore required in order to get an accurate value of B and C. Since graphical determination of A was inaccurate, a statistical technique using the method of least squares was subsequently used to obtain parameters A, B and C. In the analyses, variables H and $(I_1-3)^{\frac{1}{2}}$ were known, but parameter A was unknown. In order to obtain parameters A, B and C by this method, values of A were fed into equation (4.16) at an incremental step of 0.01 MPa. As a first approximation, a limiting value of $\frac{d\bar{\sigma}}{d(\lambda-\lambda^{-2})}$ was taken as the value of A. The values of A, B and C which correspond to the maximum correlation coefficients were taken to be the best fit to the experimental data.

Typical values of parameters A, B and C and the corresponding maximum correlation coefficients obtained are shown in tables 4.2 to 4.5. For unfilled rubbers of different crosslink density (table 4.2), the maximum correlation coefficients of the range 0.9934 - 0.9990 were obtained. For sulphur cured rubbers, the values of the maximum

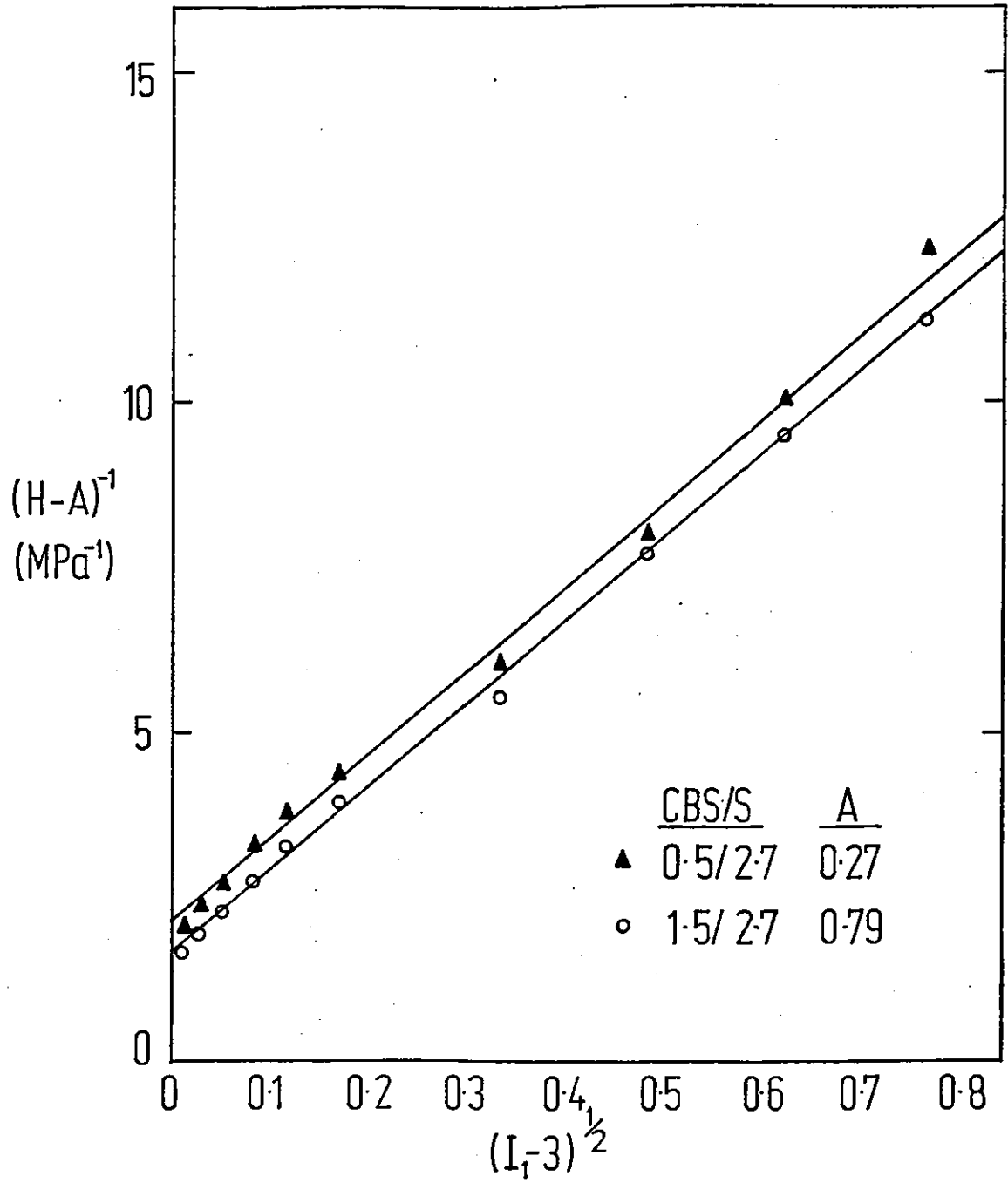


Figure 4.7. $(H-A)^{-1}$ as a function of $(I_1-3)^{\frac{1}{2}}$ for rubbers filled with 20 pphr N347 black

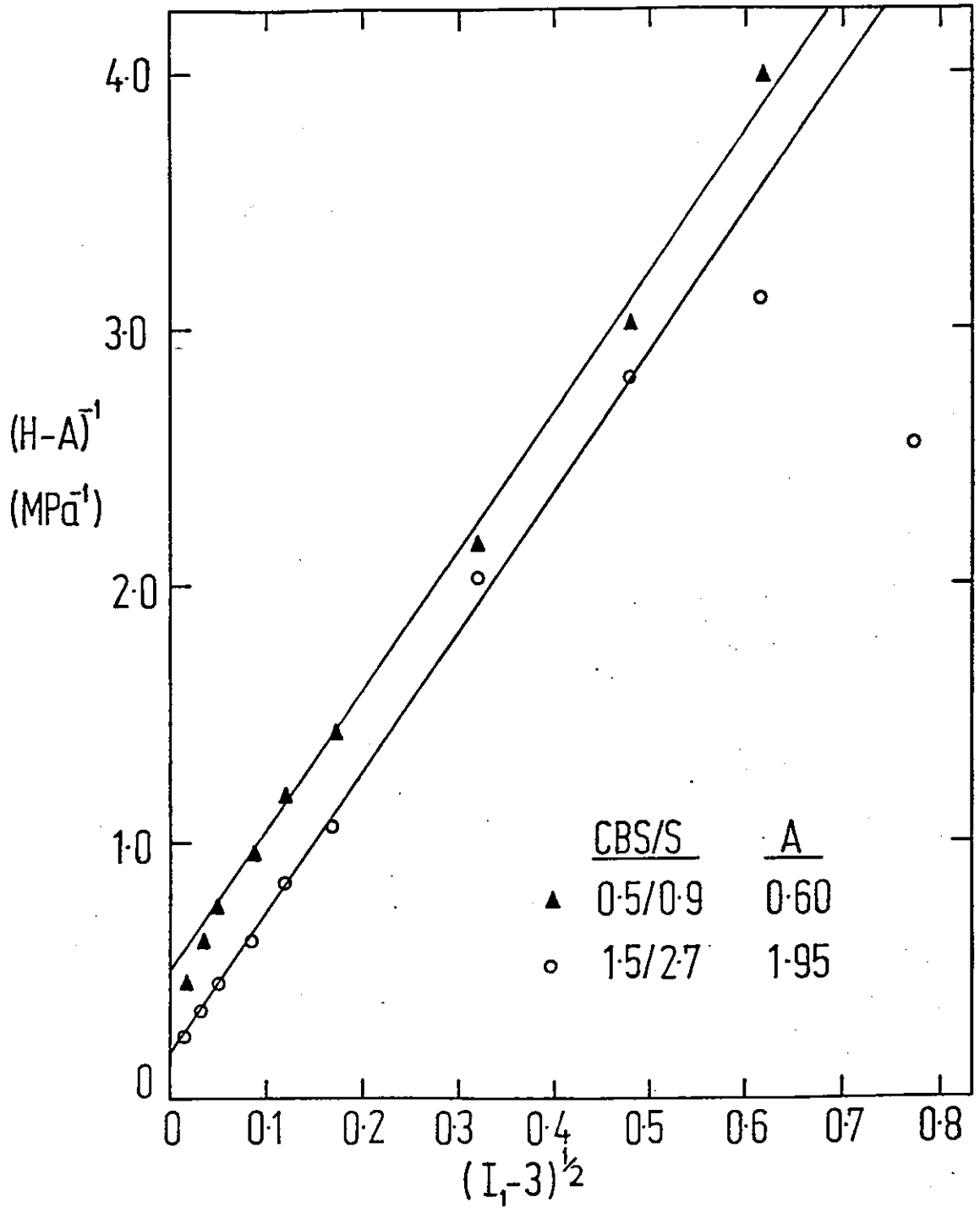


Figure 4.8. $(H-A)^{-1}$ as a function of $(I_1-3)^{1/2}$ for rubbers filled with 60 pphr N347 black.

TABLE 4.2: VALUES OF A, B AND C FOR UNFILLED RUBBERS
(SULPHUR AND PEROXIDE SYSTEMS)

CBS/S Ratios pphr	A (MPa)	B (MPa ⁻¹)	C (MPa ⁻¹)	Max. correlation coefficient
0.25/0.45	0.081	5.78	5.55	0.9990
0.5/0.9	0.150	4.73	5.37	0.9983
0.75/1.35	0.215	3.30	5.07	0.9983
1.0/1.8	0.270	2.86	5.06	0.9983
1.25/2.25	0.355	4.29	5.73	0.9976
1.5/2.7	0.45	6.83	5.74	0.9934

DCP pphr

1	0.207	7.31	6.41	0.9962
2	0.326	3.40	5.35	0.9973
3	0.504	6.67	7.23	0.9964
4	0.698	6.56	5.90	0.9965

correlation coefficients seem to improve with decreasing crosslink density (i.e. lower sulphur content) and averaged about 0.9975. For peroxide cured rubbers, the maximum correlation coefficients averaged about 0.9966, which was comparable to that of the corresponding sulphur system.

Typical values of the correlation coefficients for filled rubbers are given in tables 4.3 to 4.5. For rubbers filled with N550 black and crosslinked using the sulphur vulcanizing system (semi-EV), maximum correlation coefficients from 0.9944 to 0.9992 were obtained. The correlation coefficients appeared to be generally better for those containing 60 phr black than those containing 20 phr black. The maximum correlation coefficients of rubbers filled with the N347 black and crosslinked using the sulphur vulcanizing system (semi-EV) ranged from 0.9940 to 0.9998, with less heavily filled rubbers (e.g. 20 phr black) having higher correlation coefficients than the heavily filled rubbers. The peroxide cured rubbers showed equally good maximum correlation coefficients, ranging from 0.9943 to 0.9999 (table 4.4).

Generally it was observed that lightly filled and unfilled rubbers gave relatively poor (~ 0.99) maximum correlation coefficients compared to heavily filled (> 20 phr black) rubbers. For over 200 rubbers tested, the maximum correlation coefficients obtained varied from 0.9934 to 0.9999, which is fairly good and these results showed that the plots of $(H-A)^{-1}$ Vs $(I_1-3)^{\frac{1}{2}}$ were linear and that equation (4.15) is valid.

4.3.2 Comparison between experimental and predicted values

Equation (4.14) gives the value of H or G as a function of $(I_1-3)^{\frac{1}{2}}$, with parameters A, B and C as constants. For either tension, compression or simple shear, values of A, B and C for a particular

TABLE 4.3: VALUES OF A, B AND C FOR SULPHUR CURED N550 BLACK
FILLED RUBBERS

Black Loadings pphr	CBS/S Ratios pphr	A (MPa)	B (MPa ⁻¹)	C (MPa ⁻¹)	max correlation coefficient
20	0.25/0.45	0.08	7.17	2.89	0.9984
	0.5 /0.9	0.26	9.79	2.71	0.9988
	0.75/1.35	0.35	4.91	3.53	0.9944
	1.0 /1.8	0.56	11.4	3.90	0.9987
	1.25/2.25	0.63	11.22	3.56	0.9983
	1.5 /2.7	0.79	15.12	3.61	0.9981
40	0.25/0.45	0.148	8.47	1.97	0.9986
	0.5 /0.9	0.405	12.04	1.50	0.9975
	0.75/1.35	0.590	10.08	1.49	0.9976
	1.0 /1.8	0.790	11.82	1.51	0.9986
	1.25/2.25	0.965	11.18	1.52	0.9988
	1.5 /2.7	1.125	14.8	2.29	0.9975
60	0.25/0.45	0.208	8.74	1.25	0.9992
	0.5 /0.9	0.54	8.60	1.162	0.9992
	0.75/1.35	0.93	11.06	0.794	0.9991
	1.0 /1.8	1.10	7.45	0.918	0.9987
	1.25/2.25	1.48	8.73	0.688	0.9997
	1.5 /2.7	1.51	10.22	0.613	0.9990

TABLE 4.4: VALUES OF A, B AND C FOR SULPHUR CURED N347 BLACK
FILLED RUBBERS

Black Loadings pphr	CBS/S Ratios pphr	A (MPa)	B (MPa ⁻¹)	C (MPa ⁻¹)	max correlation coefficient
20	0.25/0.45	0.10	10.46	2.99	0.9995
	0.5 /0.9	0.275	9.30	2.52	0.9994
	0.75/1.35	0.460	10.22	2.33	0.9991
	1.0 /1.8	0.52	9.33	2.26	0.9997
	1.25/2.25	0.675	13.93	2.34	0.9989
	1.5/ 2.7	0.800	12.94	2.08	0.9993
40	0.25/0.45	0.093	8.63	1.61	0.9993
	0.5 /0.9	0.360	8.15	0.93	0.9989
	0.75/1.35	0.580	7.65	0.71	0.9996
	1.0 /1.8	0.760	8.07	0.77	0.9990
	1.25/2.25	0.930	8.09	0.57	0.9995
	1.5 /2.7	1.130	9.09	0.41	0.9982
60	0.25/0.45	0.320	7.63	0.53	0.9966
	0.5 /0.9	0.615	5.94	0.43	0.9985
	0.75/1.35	0.970	5.38	0.31	0.9995
	1.0 /1.8	1.350	7.13	0.17	0.9981
	1.25/2.25	1.570	5.0	0.19	0.9995
	1.5 /2.7	2.05	7.67	0.068	0.9940

TABLE 4.5: VALUES OF A, B AND C FOR PEROXIDE CURED N550 AND
N347 BLACKS FILLED RUBBERS

Black Loading pphr	Dicumyl Peroxide pphr	A (MPa)	B (MPa ⁻¹)	C (MPa ⁻¹)	max correlation coefficient
20 FEF	1	0.248	14.75	4.39	0.9982
	2	0.470	23.43	4.53	0.9991
	3	0.620	15.30	4.93	0.9998
	4	0.820	25.75	3.67	0.9998
40 FEF	1	0.380	13.45	2.42	0.9991
	2	0.670	17.85	2.01	0.9995
	3	0.920	17.15	2.01	0.9997
	4	1.205	19.07	1.50	0.9995
60 FEF	1	0.510	10.45	1.23	0.9996
	2	0.910	12.06	0.80	0.9997
	3	1.285	15.25	0.70	0.9997
	4	1.640	16.36	0.57	0.9998
20 HAF-HS	1	0.26	10.60	3.09	0.9997
	2	0.46	12.93	3.30	0.9997
	3	0.60	17.39	2.63	0.9986
	4	0.87	27.92	2.40	0.9998
40 HAF-HS	1	0.37	10.13	1.20	0.9993
	2	0.64	12.54	0.87	0.9943
	3	0.95	12.80	0.72	0.9999
	4	1.18	14.15	0.69	0.9997
60 HAF-HS	1	0.58	8.25	0.63	0.9989
	2	1.01	8.23	0.43	0.9993
	3	1.37	8.61	0.43	0.9994
	4	1.74	10.21	0.30	0.9994

rubber were the same since H and G were identical at equal $(I_1-3)^{\frac{1}{2}}$. Hence knowing the values of A, B and C for any one mode of deformation, prediction of stress-strain values in other modes of deformation can be made.

Values of A, B and C were obtained using a method of least squares from data obtained in simple extension. With these values of A, B and C, prediction of tensile, compressive and shear moduli were made using equation (4.15). Typical results are shown in figure 4.9 to 4.11, where the continuous lines represent the predicted values and the points were the experimental values.

In tension (fig. 4.9), good agreement was obtained between the experimental and predicted values, with the latter differing with the former by not more than 3%. For both unfilled and filled rubbers.

Comparisons between the experimental and predicted compressive moduli are shown in figure 4.10. The agreement observed was also reasonably good, with the predicted values differing by not more than 5% from the experimental values for all rubbers tested.

For simple shear deformations (fig. 4.11), the agreement observed between the experimental and predicted moduli was similar to those observed with compression, with the latter differing from the former by not more than 5%. The agreement appears to be better with heavily filled rubbers (60 phr N347) than with lightly filled rubbers.

At low to moderate strains (i.e. before the upturn in stress-strain curve) equation (4.14) has been shown to give a good description of the stress-strain behaviour of both filled and unfilled rubbers crosslinked with different vulcanizing systems. The shear and compressive moduli were able to be predicted using the data from

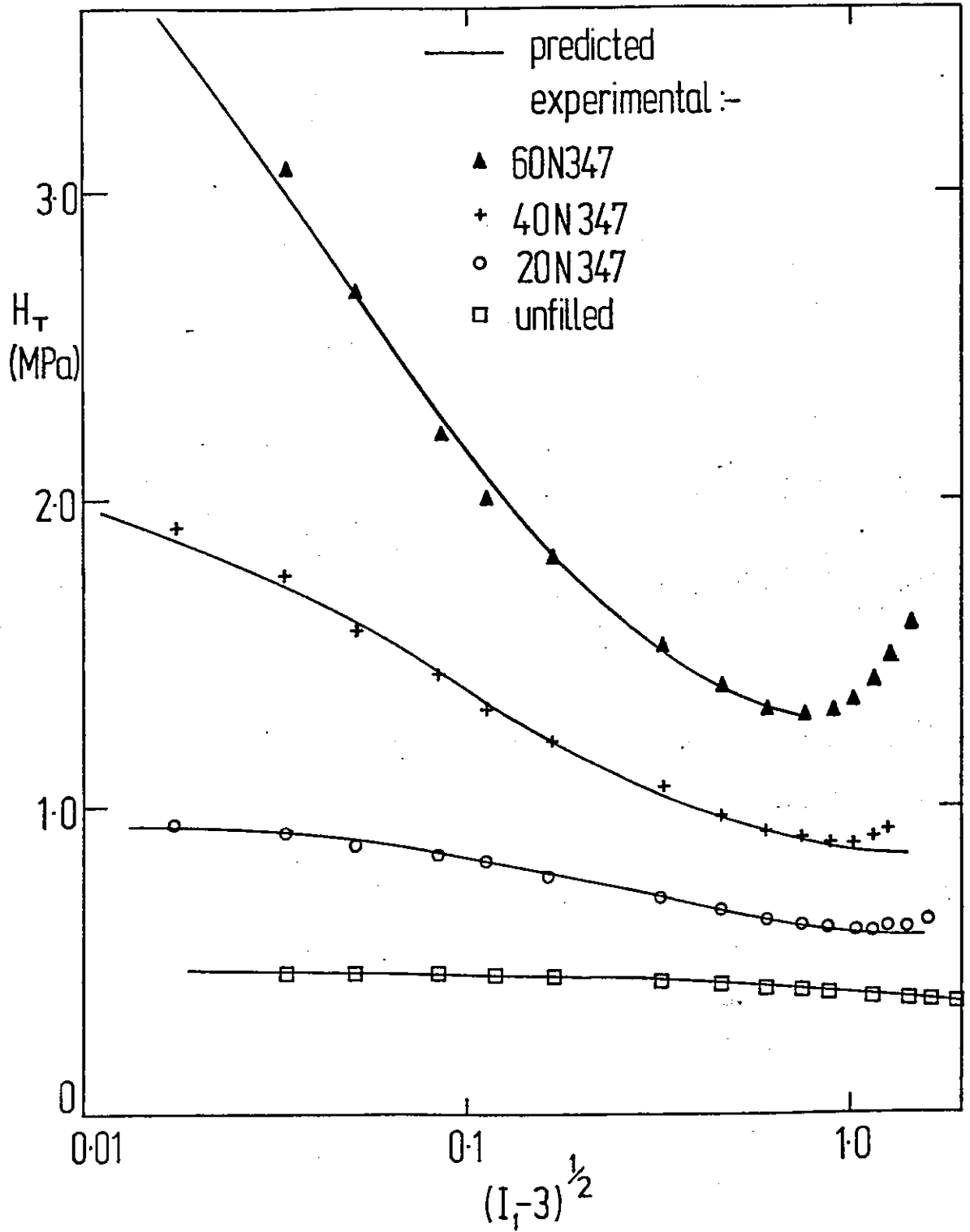


Figure 4.9. Comparison between experimental and predicted tensile moduli

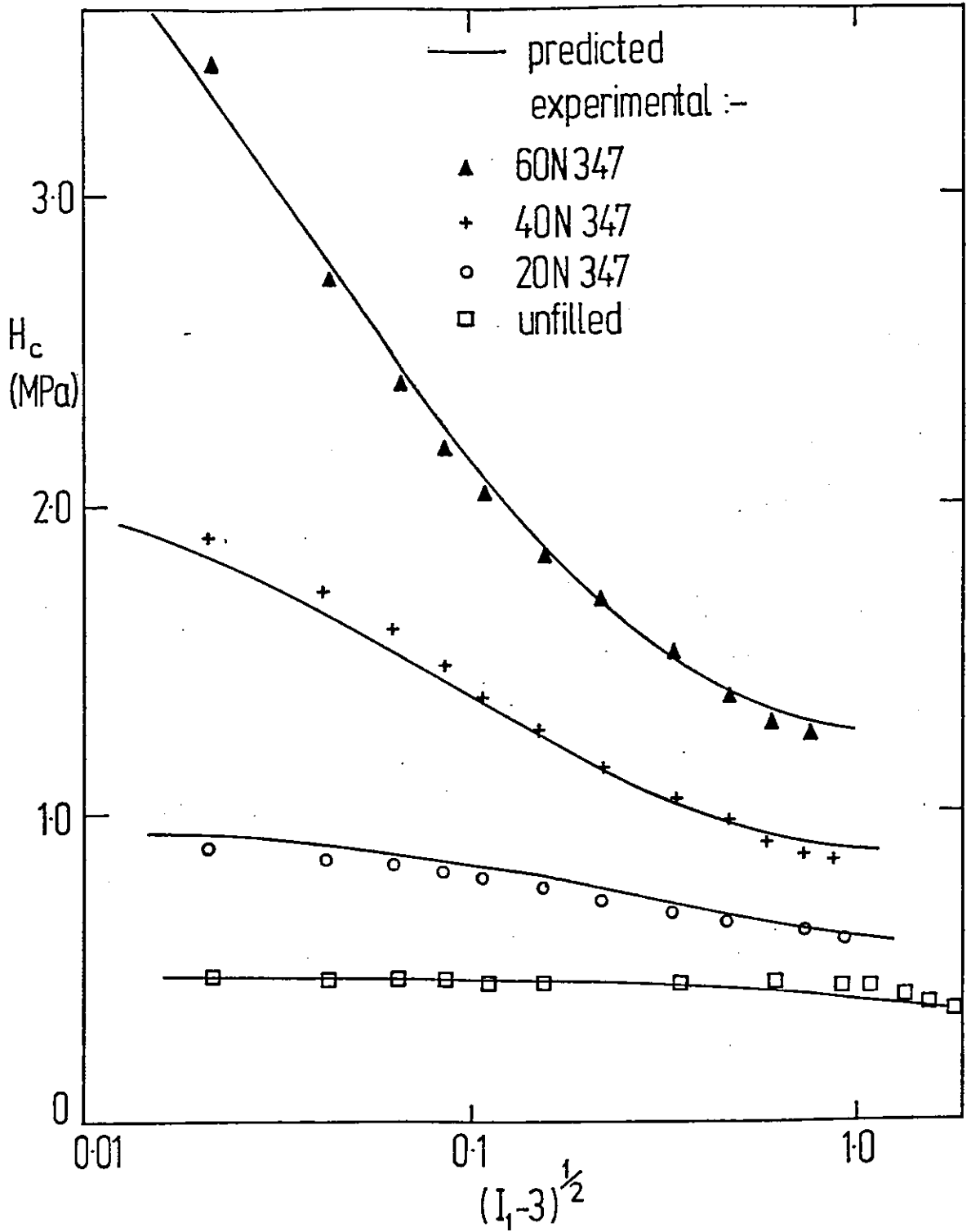


Figure 4.10. Comparison between experimental and predicted compressive moduli

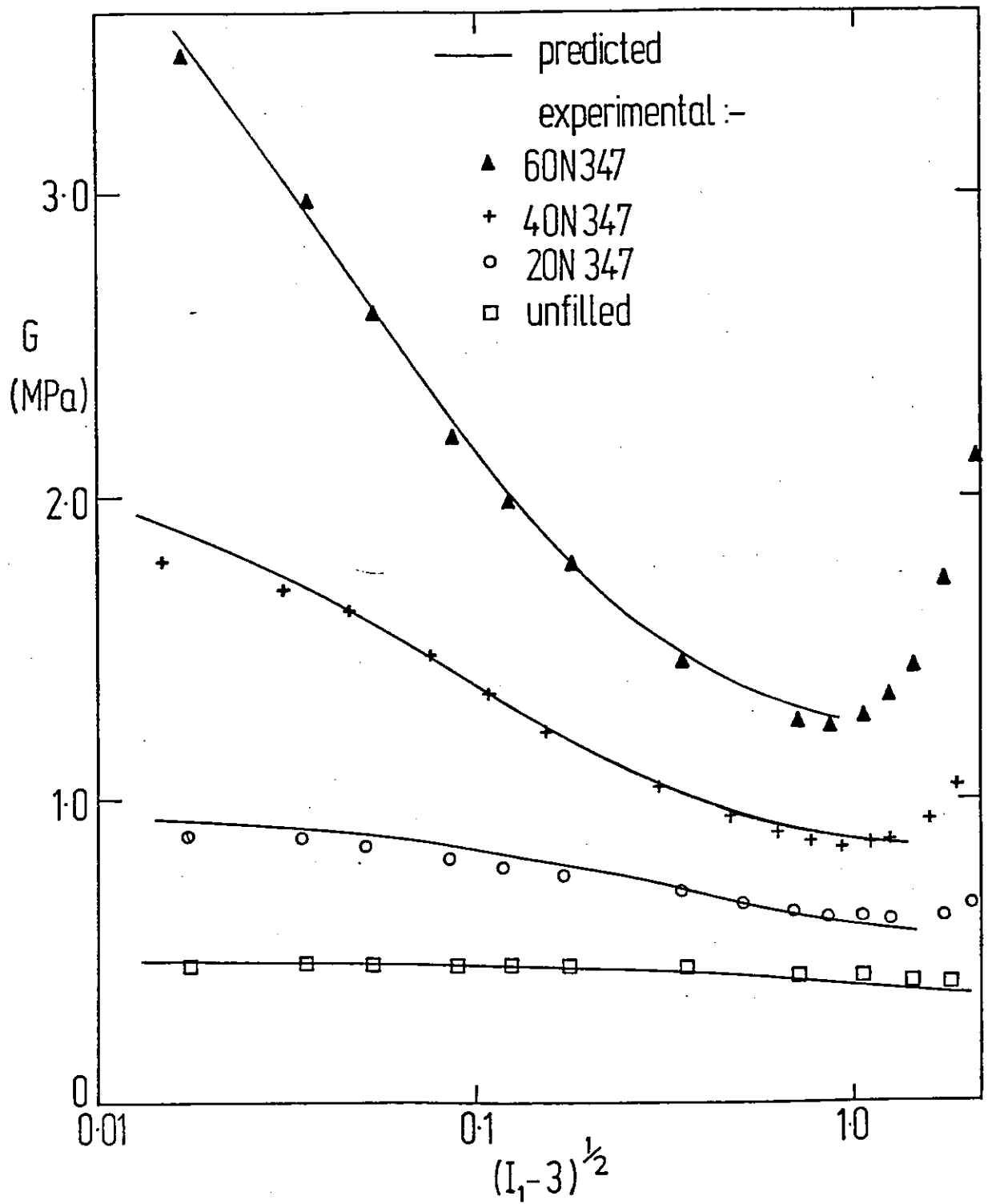


Figure 4.11. Comparison between experimental and predicted shear moduli

simple extension to within 5%, and this will enable tests in different modes of deformation to be rationalized and simplified. The proposed equation is also more useful than the available stress-strain relationship because it is applicable to filled rubbers and it correctly predicts the non-linear stress-strain behaviour in simple shear.

4.4 Physical significance of A, B and C

The proposed relationship between stress and strain takes the form,

$$H \text{ or } G = A + \frac{1}{B(I_1-3)^{\frac{1}{2}} + C} \quad (4.17)$$

where $H = \frac{\sigma}{\lambda - \lambda^{-2}}$, $G = \frac{\sigma}{\gamma}$ and A, B and C are constants. The limiting conditions for the proposed relationship are:

$$(a) \text{ as } (I_1-3)^{\frac{1}{2}} \rightarrow 0, \quad H_0 = A + \frac{1}{C} \quad (4.18)$$

$$\text{and } (b) \text{ as } (I_1-3)^{\frac{1}{2}} \rightarrow \infty, \quad H_\infty = A$$

The parameter A is equivalent to H_∞ or G_∞ , the modulus at high strain. According to Payne (79,80), G_∞ is the value of shear modulus which is independent of strain at sufficiently high strains i.e. at strain greater than those needed to breakdown any structure of carbon black.

The difference in modulus, $H_0 - H_\infty = \frac{1}{C}$ gives the value of the change in modulus with strains, which in the literature is given as $G_0 - G_\infty$. This term has been attributed to the structural effect of carbon black agglomeration i.e. $G_0 - G_\infty$ arises from the breakdown of the carbon black agglomerate structures. Since $\frac{1}{C}$ is equal to $G_0 - G_\infty$, the former describes the extent of breakdown of carbon black structure due to the effects of strains.

From equations (4.17) and (4.18), it is clear that the term involving parameter B is negligible at the limiting strains. However in between the two strain limits, parameter B gives a significant effect since it is associated with the strain invariant, I_1 . The

modulus contribution from the $B(I_1-3)^{\frac{1}{2}}$ term decreases with strain while that of A and $\frac{1}{C}$ are constant. Thus parameter B may be associated with the manner in which H_0 changes to H_∞ .

SECTION 5: EFFECTS OF COMPOUNDING ON PARAMETERS A, B AND C

5.1 Introduction

5.2 Parameter A

5.2.1 Effects of crosslink density

5.2.2 Effects of carbon black

5.2.3 The enhancement of crosslink density

5.3 Parameter C

5.3.1 Effects of crosslink density

5.3.2 Effects of interparticle distance

5.3.3 A combined function of crosslink density
and interparticle distance

5.4 Parameter B

SECTION 5 EFFECTS OF COMPOUNDING ON PARAMETERS A, B AND C

5.1 Introduction

For the three simple modes of deformation considered in this thesis, namely simple extension, lubricated compression and simple shear, the moduli at low to moderate strains were observed to conform with the relation,

$$H \text{ or } G = A + \frac{1}{B(I_1 - 3)^{\frac{1}{2}} + C} \quad (5.1)$$

where A, B and C are constants. In order to characterise H or G, factors affecting these constants have to be known.

The amount and types of compounding ingredients are the most important factors affecting the modulus of a rubber, hence the effects of compounding on A, B and C were investigated in this section.

5.2 Parameter A

5.2.1 Effects of crosslink density

With rubbers crosslinked using the sulphur vulcanizing system, parameter A was found to be linearly related to the concentration of sulphur (or phr sulphur) for both filled and unfilled rubbers (fig. 5.1 and 5.2). The correlation coefficients for the relationship of A to sulphur concentration were found to be more than 0.99 suggesting that the relationship between the variables plotted was close. Coran (96) has shown that the crosslink density of a rubber is proportional to the square root of the product of the sulphur and accelerator concentrations. It follows that, with a constant accelerator: sulphur ratio, the crosslink density will be proportional

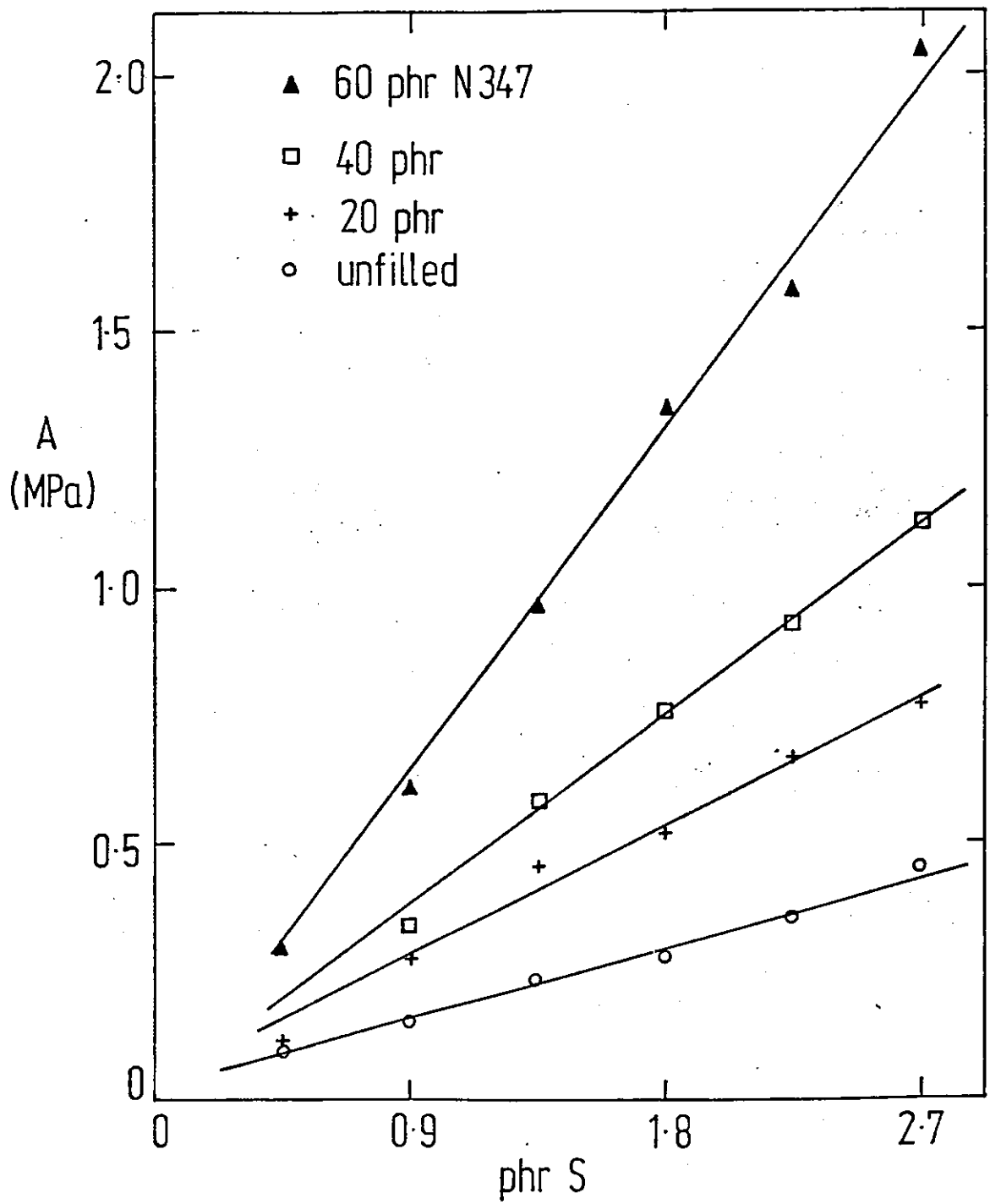


Figure 5.1. Parameter A as a function of (phr S) for unfilled and rubbers filled with N347 black

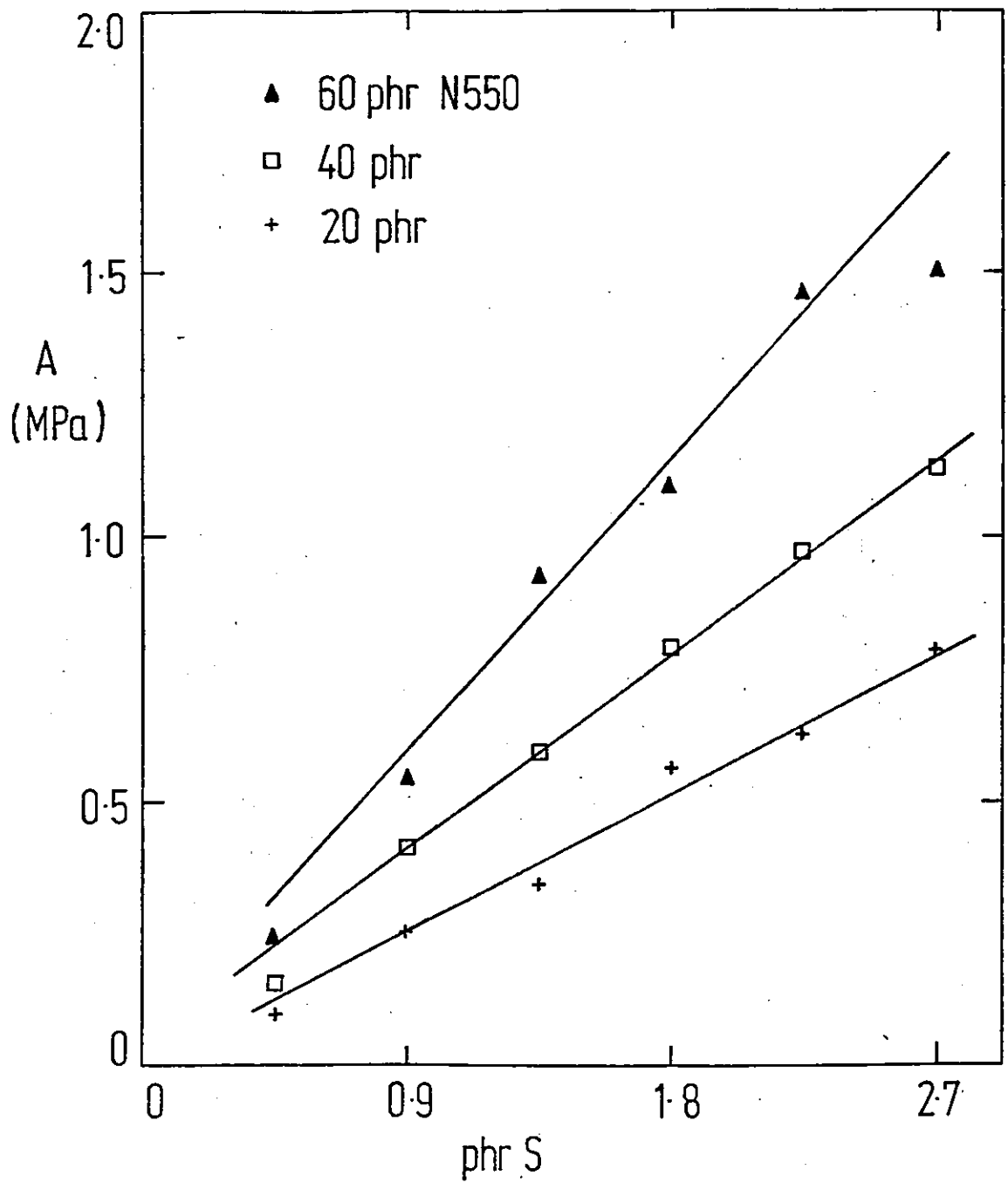


Figure 5.2. Parameter A as a function of (phr S) for rubbers filled with N550 black

to the sulphur concentration. This implies that for rubbers crosslinked using sulphur vulcanizing systems, the parameter A is proportional to crosslink density.

For rubbers crosslinked using the peroxide vulcanizing system (DCP) results obtained indicate that A is also linearly related to the concentration of dicumyl peroxide for both filled and unfilled rubbers (fig. 5.3 and 5.4), with correlation coefficients of more than 0.99. Assuming that the crosslink density of the peroxide cured rubbers is proportional to the concentration of dicumyl peroxide used, then the parameter A is proportional to crosslink density for the peroxide cured rubbers.

The statistical theory relates the nominal stress to the extension ratio in simple extension by,

$$\bar{\sigma} = NkT(\lambda - \lambda^{-2}) \quad (5.2)$$

where N is the number of chains per unit volume, k is the Boltzmann constant and T is the absolute temperature. Separation of the proposed equation (4.12) gives

$$\bar{\sigma} = A(\lambda - \lambda^{-2}) + \frac{1}{B(I_1 - 3)^{\frac{1}{2}} + C} (\lambda - \lambda^{-2}) \quad (5.3)$$

Ignoring the second term on the right hand side of equation (5.3) comparison of equations (5.2) and (5.3) suggests that A to be equal to NkT.

Assuming that A may be equated to NkT, then values of A at the test temperature may be calculated for peroxide cured rubbers, assuming that (a) all dicumyl peroxide is used for the crosslinking process (b) one molecule of dicumyl peroxide crosslinks two molecules of rubber hydrocarbon and (c) rubber has an infinite molecular weight.

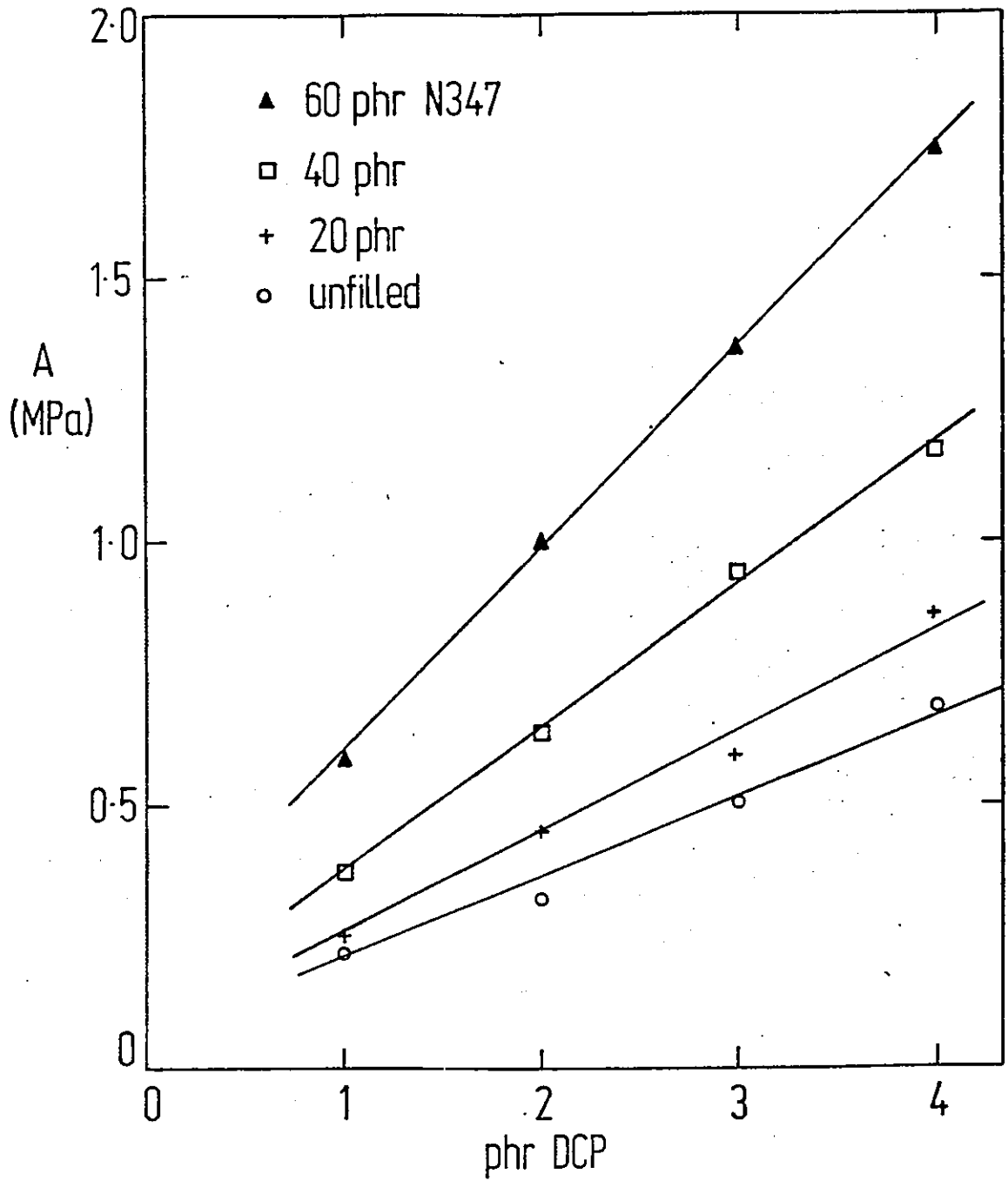


Figure 5.3. Parameter A as a function of phr DCP for unfilled and rubbers filled with N347 black

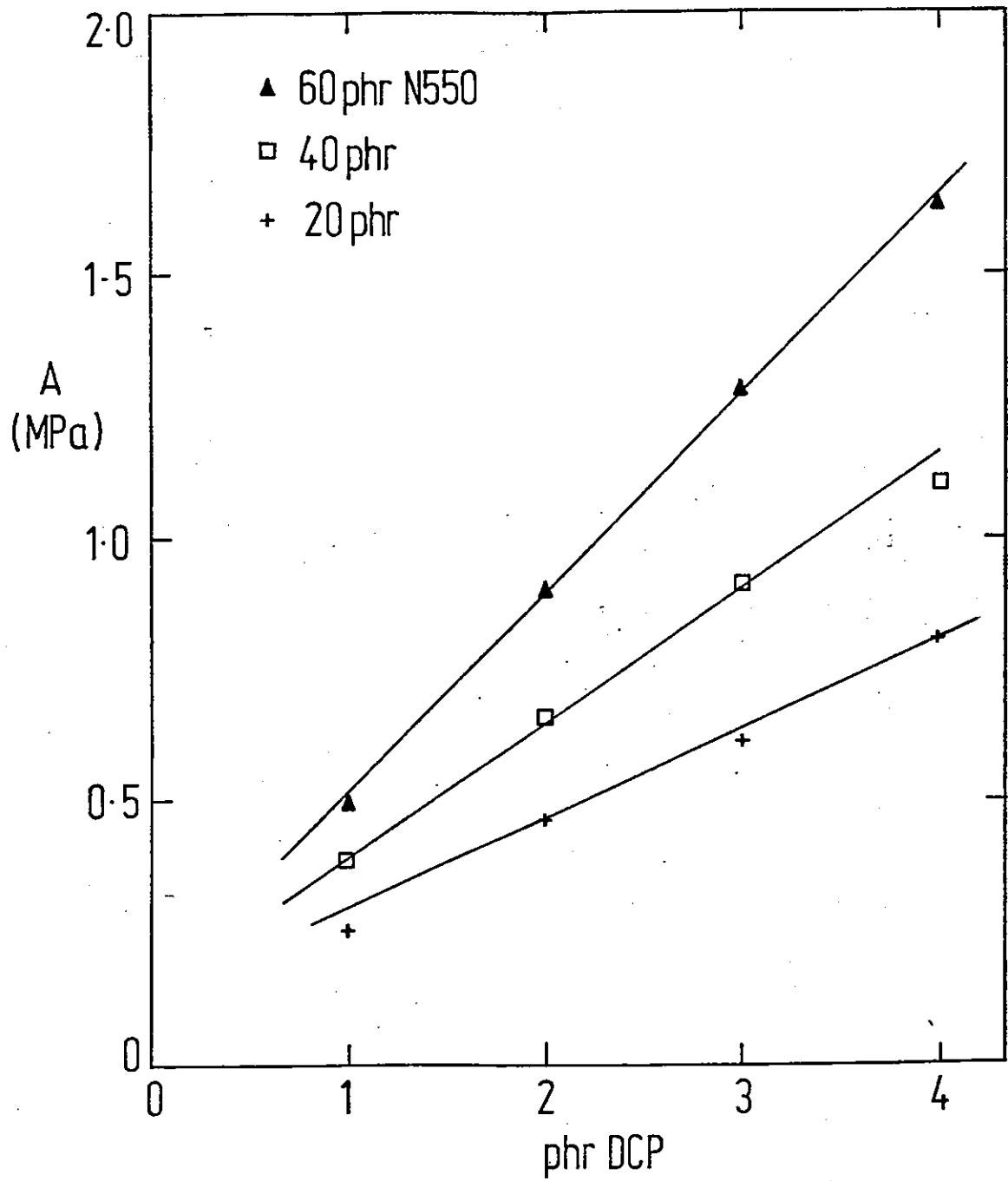


Figure 5.4. Parameter A as a function of phr DCP for rubber filled with N550 black

Taking $T = 296 \text{ K}$ and $\rho = 0.96 \text{ gm/cm}^3$, the calculated values of A are compared with the experimental results in table 5.1.

Table 5.1. Experimental and Calculated Values of A

Dicumyl peroxide (pphr)	1	2	3	4
Experimental A (MPa)	0.207	0.326	0.504	0.695
Calculated A (MPa)	0.171	0.343	0.514	0.685

Except for that of the lowest level of dicumyl peroxide (i.e. 1 pphr), the calculated values of A were within 10% of the experimental values. The good agreement observed between the experimental and the calculated values of A suggests that parameter A is equal to the NkT term of the statistical theory.

5.2.2. Effects of carbon black

Carbon black increases the stiffness of rubbers and thus the value of A . The extent of increase in the stiffness or the value of A depends, in part, on the amount of carbon black used. With the results obtained, parameter A was observed to be non-linearly related to the volume fraction of black, ϕ .

The non-linear increase in modulus with increasing concentration of carbon black is usually described by the use of the Guth-Gold (63) type of hydrodynamic equation. (Section 2.2). When the same principle is applied to the increase in A for a filled rubber relative to that of an unfilled rubber (A_0), the Guth-Gold type of equation takes the form:

$$A = A_0 (1 + \alpha \phi + \beta \phi^2) \quad (5.4)$$

where α and β are constants associated with the shape factor and occluded volume effects. Rearranging equation (5.4) gives:

$$\frac{\left(\frac{A}{A_0} - 1\right)}{\phi} = \alpha + \beta \phi \quad (5.5)$$

If equation (5.5) is valid, then plots of $\left(\frac{A}{A_0} - 1\right) / \phi$ Vs ϕ should be a straight line of slope β and intercept α , the constants of which should be the same for rubbers filled with the same type of carbon black since the constants are functions of occluded volume and shape factor. However, as figure 5.5 shows, the values of α and β were independent of the types of carbon black but depend on the vulcanizing systems used. This suggests that the difference in shape factor and occluded volume of carbon black gives no significant change in the values of the slope and intercept of the $\left(\frac{A}{A_0} - 1\right) / \phi$ Vs ϕ plots. Hence it must be assumed that other factors, in addition to the volume filling effects, determined the stiffening effects of carbon black.

Several authors (97-99) have reported that there were differences between the cure efficiency of black filled peroxide and sulphur cured rubbers. Kraus (97) for instance stated that the incorporation of 50 phr N330 black resulted in a 40% increase in the crosslinking efficiency for the sulphur cured rubbers, while for the corresponding peroxide cured rubbers, the author obtained a maximum apparent "black contribution" of about 20%. Porter (99) reported that the presence of carbon black in the N-cyclohexyl benzothiazole-2-sulphenamide (CBS) accelerated sulphur vulcanizing system increased the crosslinking efficiency of rubber, but with the peroxide vulcanizing system, particularly at higher crosslink density, it tends to suppress it.

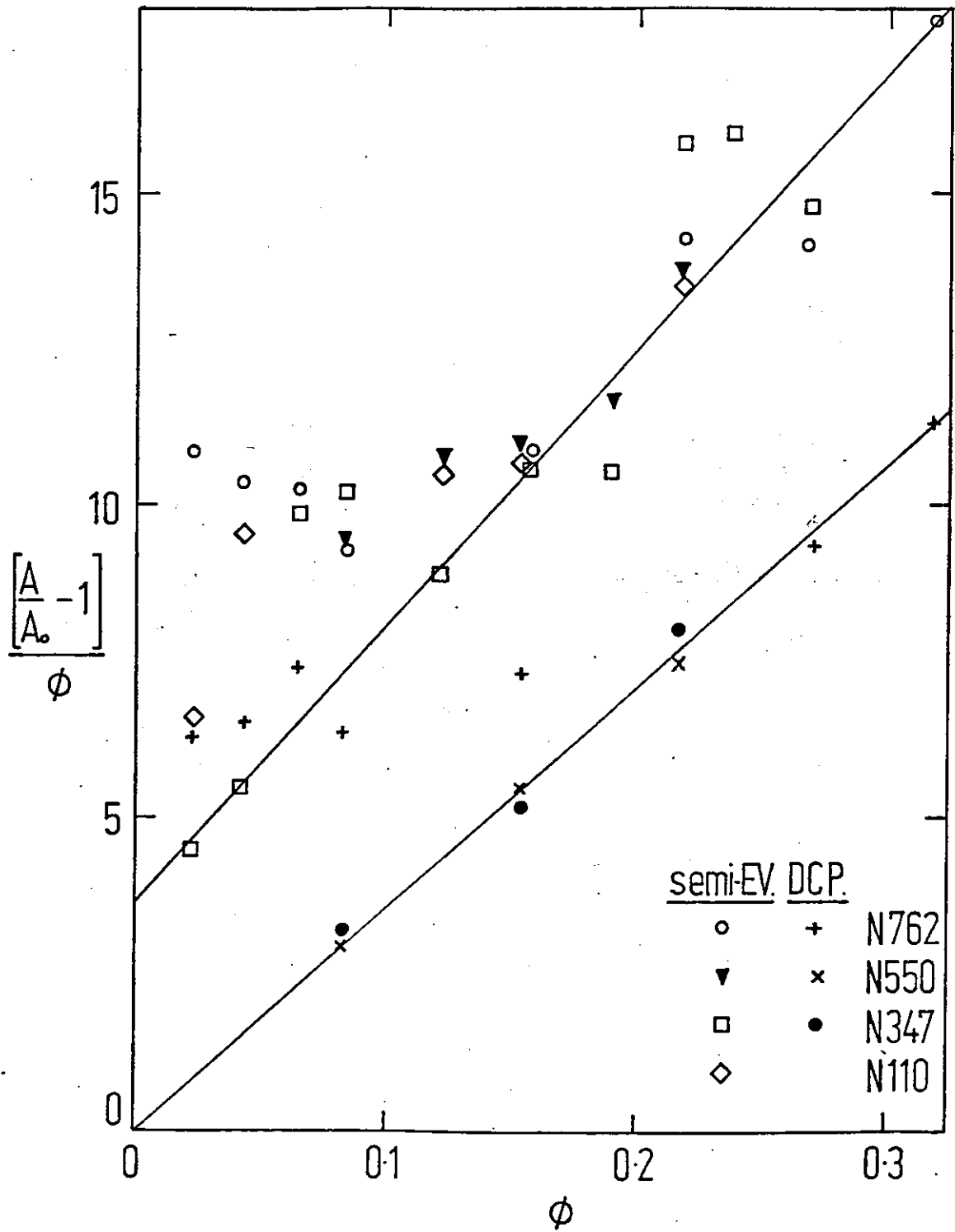


Figure 5.5. $\frac{A}{A_0} - 1$ as a function of ϕ for rubbers

filled with different blacks and crosslinked using different vulcanizing systems

Based on these reports, it is likely that the differences observed between the results for rubbers crosslinked using the peroxide and sulphur based vulcanizing systems shown in figure 5.5 were due to the differences in their cure efficiencies.

If the presence of carbon black alters the crosslink density of the sulphur and peroxide cured rubbers, then equation (5.4) does not adequately describe the stiffening effects of carbon black. To take into account the changes in the rubber matrix, it is proposed that equation (5.4) takes the form

$$A = A_0 F(\phi)(1 + \alpha \phi + \beta \phi^2) \quad (5.6)$$

where $F(\phi)$ is a function which is associated with the change in modulus of the rubber matrix due to the presence of carbon black, which may be different for different vulcanizing systems. If $F(\phi)$ and $F'(\phi)$ are the functions for peroxide and sulphur cured rubbers respectively, then

$$\left(\frac{A}{A_0}\right)_{\text{CBS/S}} = \frac{F'(\phi)}{F(\phi)} \left(\frac{A}{A_0}\right)_{\text{DCP}} \quad (5.7)$$

where the ratios $\left(\frac{A}{A_0}\right)_{\text{CBS/S}}$ and $\left(\frac{A}{A_0}\right)_{\text{DCP}}$ are those for rubbers crosslinked using sulphur and peroxide vulcanizing systems respectively.

There is no evidence to indicate if the differences in the crosslinking efficiencies between the peroxide and sulphur based vulcanizing systems were due to either an enhancement of the crosslinking for the latter or the suppression of the former or both. However since we are interested in the differences between the crosslinking efficiencies of the two vulcanizing systems, then for

simplicity, it is assumed that the crosslink density of the peroxide cured rubbers is independent of filler loading. The modulus of filled rubbers crosslinked using dicumyl peroxide is then given by,

$$A = A_0 (1 + \alpha \phi + \beta \phi^2) \quad (5.8)$$

For the corresponding sulphur vulcanizing system, we may therefore write,

$$\frac{\left(\frac{A}{A_0}\right)_{\text{CBS/S}}}{F'(\phi)} = (1 + \alpha \phi + \beta \phi^2) \quad (5.9)$$

where $(1 + \alpha \phi + \beta \phi^2)$ is the scaling factor due to the volume filling effects of the black. Using equation (5.9), values of $F'(\phi)$ for rubbers crosslinked using sulphur vulcanizing systems may be estimated using the experimental values of A and A_0 and the values of α and β for the corresponding rubbers crosslinked using the peroxide vulcanizing system.

For rubbers crosslinked using the sulphur vulcanizing system (i.e. CBS/S), results (table 5.2) show that $F'(\phi)$ increases with black loading up to about 20 pphr, after which it remains fairly constant. At black loadings of more than 10 pphr, about 40-50% increase in the $F(\phi)$ value was observed. The function $F'(\phi)$ appears to be independent of crosslink density and the type of black used.

The determination of the crosslink density of filled rubbers and hence the term $F(\phi)$ could not be made directly because no direct technique is available. For unfilled rubbers, the number of crosslinks present can be determined from equilibrium swelling data using the Flory-Rehner equation (100), relating the volume fraction of rubber (V_r)

Table 5.2: Values of $F'(\phi)$ for sulphur (semi-EV) cured rubbers

CBS/S ratios (pphr)	Black Loading (pphr)										
	Types of Black		5	10	20	30	40	50	60	70	80
0.5 /0.9	N550		0.98	1.25	1.38	1.49	1.45	1.36	1.35	-	-
0.75/1.35			-	-	1.29	1.55	1.47	1.62	1.62	-	-
1.0 /1.8			1.13	1.32	1.65	1.61	1.56	1.49	1.53	-	-
1.25/2.5			-	-	1.43	1.50	1.48	1.39	1.58	-	-
1.5 /2.7			0.98	1.16	1.40	1.41	1.34	1.29	1.26	-	-
0.5 /0.9	N347		1.11	0.93	1.43	1.27	1.28	1.15	1.54	1.94	1.47
0.75/1.35			1.05	1.04	1.59	1.43	1.44	1.38	1.69	1.73	1.45
1.0 /1.8			1.09	1.21	1.62	1.39	1.55	1.46	1.87	1.55	1.42
1.25/2.25			0.99	1.29	1.41	1.45	1.42	1.37	1.68	1.43	1.39
1.5 /2.7			1.07	1.10	1.35	1.31	1.34	1.28	1.71	1.30	1.27
1.0 /1.8	N110		1.12	1.33	1.49	1.49	1.45	-	1.48	-	-

and the molecular weight between crosslinks (M_c), namely

$$M_c = -\rho V_r \frac{1}{3} [\ln(1-v_r) + v_r + \chi v_r^2] \quad (5.10)$$

where ρ is the density of the rubber, V is the molar volume of solvent and χ is the solvent-rubber interaction parameter. In the presence of fillers, equation (5.10) fails because swelling is also restricted by the fillers and the value of V_r will not represent that of the rubber matrix. However if the equivalent value of V_r for the rubber matrix is known, value of M_c and hence the crosslink density ($\eta = \frac{\rho}{M_c}$) can be calculated.

The dependence of degree of restriction of swelling on the volume fraction of filler has been quantitatively investigated by Kraus (97) and Lorenz and Park (98). The Kraus investigations were based on a model which assumed that the rubber molecules covering the surfaces of filler particles were not displaced by swelling agents, and were not able to swell at all. Away from these layers, restriction to swelling was assumed to decrease with distance from the filler surfaces, until at a certain distance, the rubber matrix swelled normally, that is, to the extent of the corresponding unfilled rubber. Using different polymers, several sulphur vulcanizing systems and solvents and different crosslink density Kraus obtained the relation,

$$\frac{V_{r_0}}{V_r} = 1 - [3c(1-v_{r_0})^{\frac{1}{3}} + v_{r_0} - 1] \frac{\phi}{1-\phi} \quad (5.11)$$

where V_{r_0} and V_r are the volume fractions of rubber matrix for unfilled and filled rubbers respectively and c is a constant for a given filler. Lorenz and Park on the other hand considered restricted

swelling of the rubber matrix in the neighbourhood of filler particles. The zones nearest to filler particles were considered to exhibit the smallest swelling and zones sufficiently far from filler particles exhibited the same swelling as the unfilled rubber. For N330 black filled natural rubber, Lorenz and Park found that their results followed an empirical relationship,

$$\frac{Q}{Q_0} = a e^{-z} + b \quad (5.12)$$

where Q and Q_0 refer to the weights of the swelling agent imbibed per unit weight of rubber matrix in filled and unfilled rubbers, z is the weight of filler per unit weight of rubber matrix and a and b are constants.

Equations (5.11) and (5.12) were derived assuming that the presence of carbon black did not influence the crosslink density of the rubber. If, however, the presence of filler influences the crosslink density of rubber, then the restriction of swelling will be due to one or more of the following three causes:

(a) The filler may cause an increase in crosslinking efficiency of the vulcanizing agents, thus giving additional chemical crosslinks.

(b) The filler may restrict swelling of rubber because of adhesion of rubber to filler surfaces either by physical adsorption or through the formation of rubber to filler bonds.

(c) The filler may alter the affinity of swelling agent for rubber.

If the same type of carbon black and swelling agent are used, then the contributions to swelling from factors (b) and (c) for rubber crosslinked using different vulcanizing agents will be about

the same. Any difference in swelling will be only due to factor (a).

The results obtained from the swelling tests were analysed in accordance with the treatment put forward by Kraus and Lorenz and Park. The equation due to Kraus (equation 5.11) predicts a linear dependence of $(1 - \frac{V_{r_0}}{V_r})$ on $(\frac{\phi}{1-\phi})$ but results obtained did not conform to equation (5.11). Similar observations were made by Porter (99).

When the results were analysed in accordance with the relation due to Lorenz and Park, they conformed with equation (5.12) in that a linear dependence of $\frac{Q}{Q_0}$ on e^{-z} was obtained (fig. 5.6). The values of $\frac{Q}{Q_0}$ at equal e^{-z} were different for rubbers crosslinked using different crosslinking systems; the values for rubber crosslinked using the EV and peroxide systems were approximately the same, but both were higher than for the corresponding rubbers crosslinked using the semi-EV and conventional systems, which were also approximately the same. The two linear equations representing rubbers crosslinked using the EV or the peroxide systems and the Semi EV or the Conventional Systems are, respectively,

$$\frac{Q}{Q_0} \text{ DCP, EV} = 0.41 e^{-z} + 0.59 \quad (5.13)$$

$$\frac{Q}{Q_0} \text{ Semi-EV, Conv.} = 0.56 e^{-z} + 0.44 \quad (5.14)$$

The difference in the slopes between equations (5.13) and (5.14) was about 38%, the difference of which was due to the differences in restriction to swelling. These differences were consistent with the results obtained earlier, where the values of $F'(\phi)$ for the

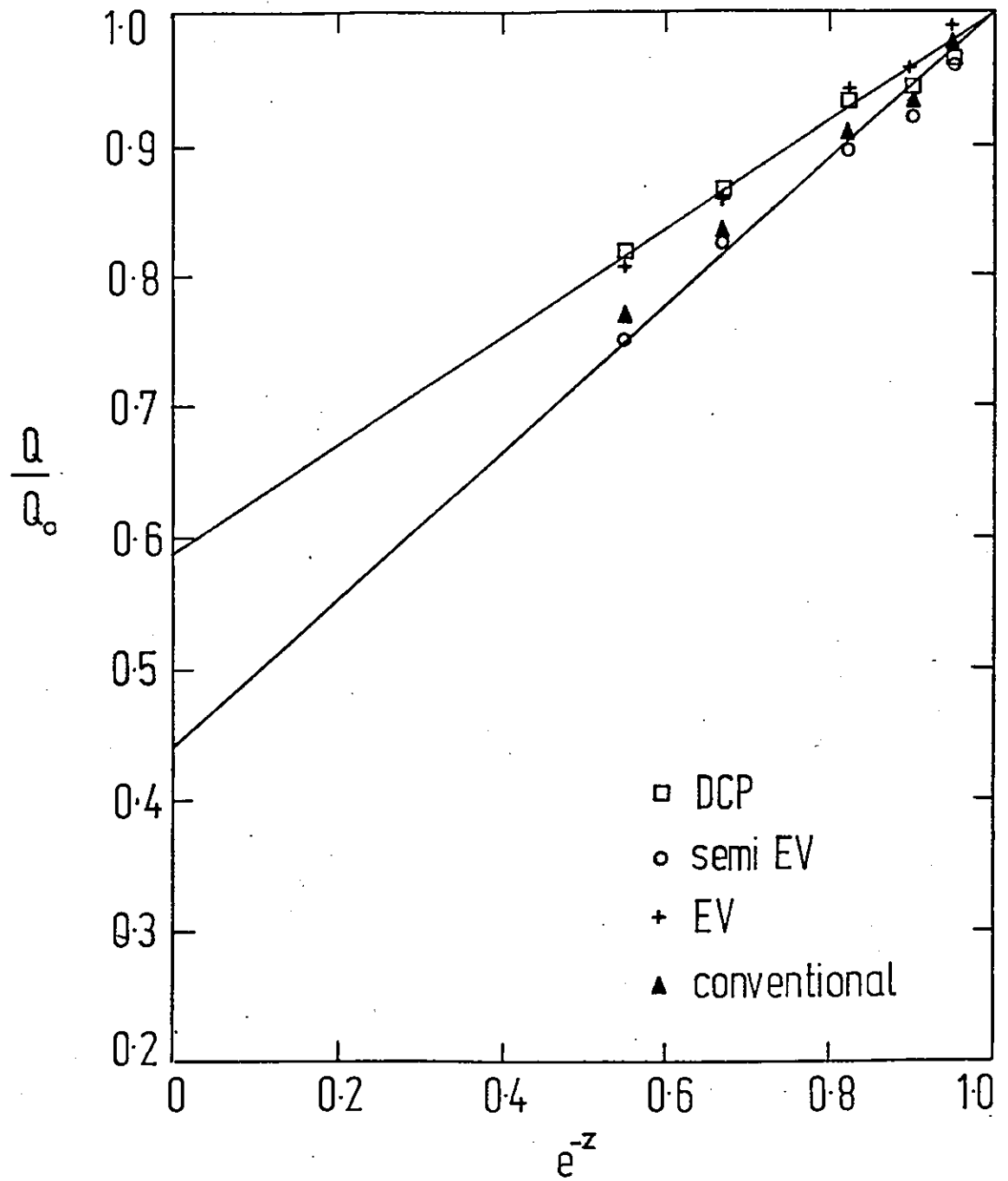


Figure 5.6. $\frac{Q}{Q_0}$ as a function of e^{-z} for rubbers filled with N347 black

sulphur cured rubbers were about 40% higher than for the corresponding peroxide cured rubbers.

To accommodate the changes in the rubber matrix, it is proposed that the Lorenz and Park equation be modified to,

$$Q = Q_m (a e^{-z} + b) \quad (5.15)$$

where Q_m replaces Q_o and a and b are constants. The parameter Q_m is defined as,

$$\begin{aligned} Q_m &= \frac{\text{Weight of solvent imbibed}}{\text{Weight of rubber matrix}} \\ &= \frac{\rho_s}{\rho} \left(\frac{1}{V_r} - 1 \right) \end{aligned} \quad (5.16)$$

where ρ_s is the density of solvent and V_r is the volume fraction of the rubber matrix.

For rubbers crosslinked using the peroxide vulcanizing system, if the presence of carbon black is assumed to have no influence on the crosslink density of the rubber matrix, then (from equation 5.13),

$$Q_m = \frac{Q}{0.41 e^{-z} + 0.59} \quad (5.17)$$

Using the experimental values of Q , values of Q_m were calculated. For the peroxide cured rubbers used, values of Q_m of filled rubbers were observed to approximately the same as the equivalent unfilled rubber, in accordance with the assumption made (table 5.3).

The values of Q_m for the corresponding rubbers crosslinked using the sulphur systems were calculated based on the values of a and b (of equation 5.15) for that of the peroxide cured rubbers. Using the calculated values of Q_m , values of V_r were obtained using

Table 5.3: Influence of carbon black on crosslink density of rubbers crosslinked using different vulcanizing systems

Black loading (pphr)		Unfilled	5	10	20	40	60
Peroxide system	Q	1.54	1.49	1.46	1.45	1.33	1.26
	Q_m	1.54	1.52	1.52	1.57	1.54	1.55
	$M_c \times 10^{-3}$ (gm/mole)	4.98	4.87	4.87	5.12	4.97	5.01
	$\eta \times 10^4$ (moles/cc)	1.93	1.97	1.97	1.87	1.93	1.92
EV system	Q	1.97	1.95	1.90	1.85	1.68	1.59
	Q_m	1.97	1.99	1.97	2.0	1.95	1.95
	$M_c \times 10^{-3}$ (gm/mole)	7.55	7.71	7.60	7.78	7.42	7.43
	$\eta \times 10^4$ (moles/cc)	1.27	1.25	1.27	1.23	1.29	1.29
Semi-EV system	Q	1.85	1.79	1.70	1.66	1.53	1.39
	Q_m	1.85	1.82	1.77	1.79	1.77	1.71
	$M_c \times 10^{-3}$ (gm/mole)	6.81	6.62	6.32	6.42	6.31	5.91
	$\eta \times 10^4$ (moles/cc)	1.41	1.45	1.52	1.50	1.52	1.62
Conventional system	Q	1.72	1.68	1.61	1.56	1.42	1.32
	Q_m	1.72	1.72	1.68	1.69	1.65	1.62
	$M_c \times 10^{-3}$ (gm/mole)	5.98	5.97	5.75	5.82	5.56	5.43
	$\eta \times 10^4$ (moles/cc)	1.60	1.61	1.67	1.65	1.73	1.77

equation (5.16). These values of V_r , which were for the rubber matrix of filled rubbers, were used for the calculations of M_c (and η) using equation (5.10) by taking $\chi = 0.41$ (102,103). For rubbers crosslinked using an EV (CBS/S) system, the calculated values of M_c and crosslink density were observed to be independent of black loading (table 5.3). This indicates that the crosslinking efficiency of an EV system was not affected by the presence of carbon black.

For rubbers crosslinked using the conventional and semi-EV systems, the M_c was observed to vary with carbon black loading (table 5.3). Assuming that the crosslink density of the unfilled rubber (η_0) represents the crosslink density of the rubber matrix unaffected by the presence of carbon black, then for rubber crosslinked using the semi-EV or conventional systems, a 60 phr N347 black gave rise to about 10 to 15% higher crosslinking efficiency compared to the corresponding rubber crosslinked using an EV or peroxide system. For the four different types of vulcanizing systems used, the variation in crosslink density of rubbers, plotted as $\frac{\eta}{\eta_0}$ Vs ϕ are shown in figure 5.7. Some scatter of results was observed, but essentially the values of $\frac{\eta}{\eta_0}$ for rubbers crosslinked using the semi-EV and conventional systems were linearly related to the volume fraction of carbon black (ϕ).

There could be two possible reasons for the increase in crosslink density of rubbers crosslinked using the semi-EV/conventional vulcanizing systems over that of the peroxide vulcanizing system. Firstly, carbon black could act as a catalyst for the vulcanization reactions and secondly carbon black itself could react with the sulphur pendent groups present along the rubber main chain. Both mechanisms will result in more efficient vulcanization.

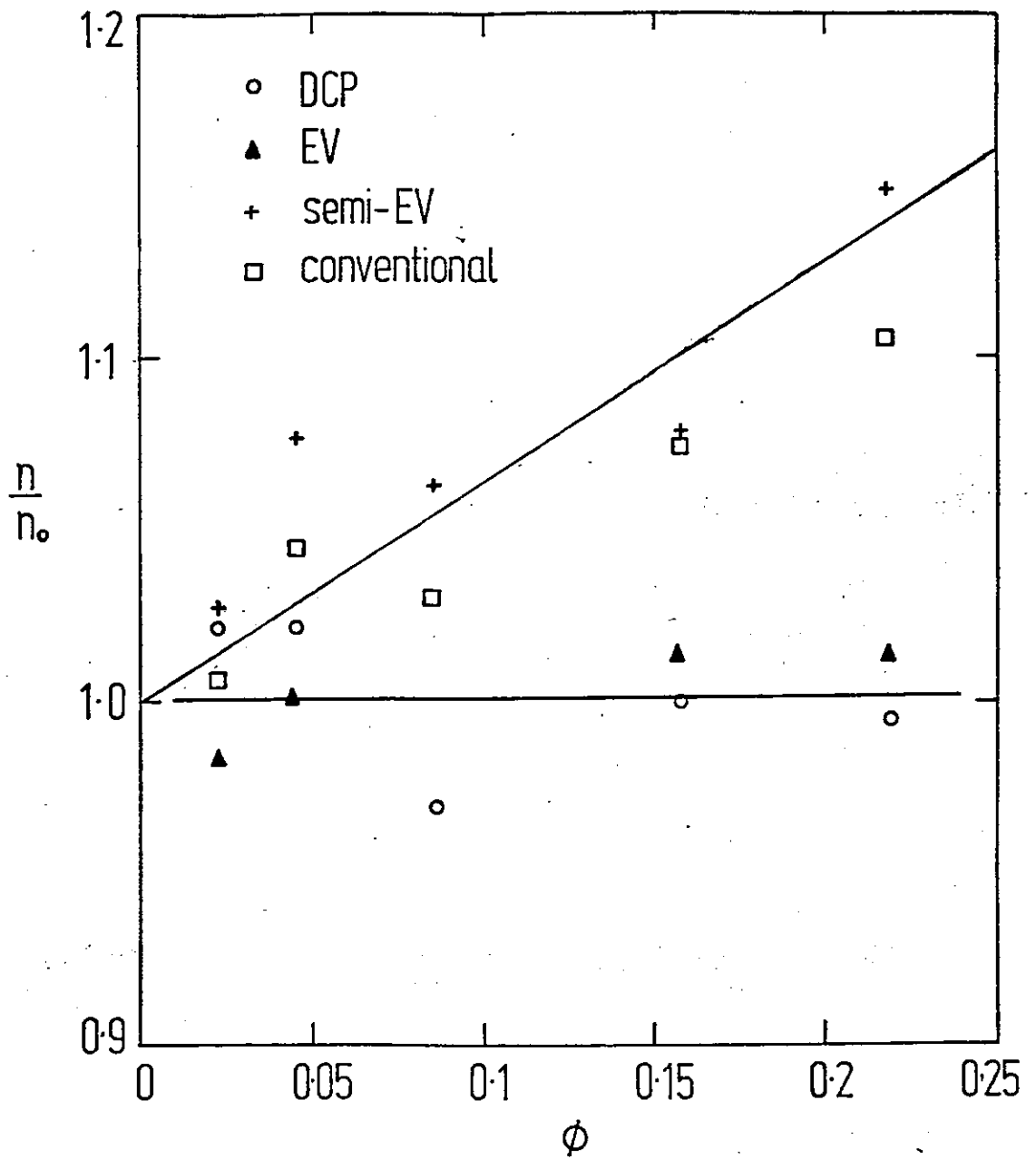
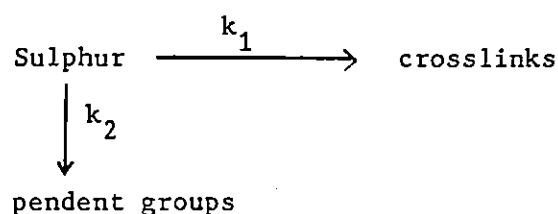


Figure 5.7. Values of $\frac{\eta}{\eta_0}$ as a function of ϕ for rubbers filled with N347 black and crosslinked using different vulcanizing systems.

The chemistry of sulphur vulcanization of natural rubber (104) is complex, but it is known that during vulcanization processes, sulphur may form crosslinks and pendent or side groups. In crosslinks, sulphur may be present as monosulphide, disulphide or polysulphide, while as side groups, it may be as pendent sulphides, or cyclic mono- and disulphides (fig. 1.1). The first possibility involves catalysis of the vulcanization process by carbon black. If the presence of carbon black catalyses crosslink formation, then more crosslinks will be formed. On the other hand if carbon black catalyses the formation of sulphidic pendent groups, then comparatively less crosslinks will be formed. Assuming that, during vulcanization,



where k_1 and k_2 are rate constants. The rate of formation of either crosslinks or pendent groups will depend on k_1 and k_2 respectively and the concentration of the two products formed is related to the rate constants by,

$$[\text{Crosslinks}] = \frac{k_1}{k_2} [\text{pendent groups}]$$

and the total number of crosslinks formed = $[\text{sulphur}] \left[\frac{k_1}{k_1 + k_2} \right]$.

If the presence of carbon black catalyses crosslink formation, then

$$\text{Total number of crosslinks formed} = [\text{sulphur}] \left[\frac{k_1'}{k_1' + k_2} \right]$$

where k_1' is the rate constant for the formation of crosslinks in the presence of carbon black.

The ratio of the modulus of the rubber matrix (A_m) to that of the unfilled rubber (A_o) may be expressed as,

$$\frac{A_m}{A_o} = \frac{A}{1 + \alpha \phi + \beta \phi} \alpha \left[\frac{k_1'}{k_1' + k_2'} \right] \left[\frac{k_1 + k_2}{k_1} \right] \quad (5.18)$$

which gives $\frac{A_m}{A_o}$ to be independent of crosslink density (or sulphur concentration), but increases with k_1' . The limiting value of $\frac{k_1'}{k_1' + k_2'}$ is unity, representing the saturation value of $\frac{A_m}{A_o}$ but this is not consistent with the results shown in figure 5.7 where for up to $\phi = 0.22$ no limiting value was observed. This suggests either that the increase in crosslink density is not due to catalysis of crosslink formation reaction by carbon black or the saturation condition has not been reached with the concentrations of filler used.

The second possibility requires that the reactive functional groups present on the carbon black surfaces react with the sulphidic pendent groups. This type of reaction will result in a rubber-sulphur-carbon black type of network, which consequently depends on the availability of both the functional groups and the sulphidic pendent groups. For this type of reaction, two cases are possible, depending on whether the concentration of sulphidic pendent groups are greater or less than the reactive functional groups. (a) If the concentrations of reactive functional groups on the carbon black surfaces are much more than those of the sulphidic pendent groups, the networks form will not increase with carbon black loading but (b) if the reactive functional groups are much fewer than the sulphidic pendent groups, the networks form will increase with carbon black loading. Results obtained (fig. 5.7) showed a linear increase

of crosslink density with the volume fraction of carbon black, indicating that the more probable reaction is that of case (b).

It thus appears that both reactions are possible and there is no evidence to suggest whether the first or second reaction mechanisms is more probable.

5.2.1.3. The enhancement of crosslink density

The Guth-Gold equation which is used to predict the modulus of filled rubber relative to that of the unfilled rubber was derived based on the assumption that the presence of fillers does not enhance the crosslink density of the rubber matrix. To take into account the change in the crosslink density of rubber, it is proposed that the equation be modified to,

$$A = A_m (1 + \alpha \phi + \beta \phi^2) \quad (5.19)$$

where A_m is the modulus of the rubber matrix. Using the values of M_c given in table 5.3, values of A_m were calculated (table 5.4).

Contrary to that observed earlier (fig. 5.5), when these values of A_m were used in the Guth-Gold equation instead of A_o , values of $(\frac{A}{A_m} - 1)/\phi$ at equal value of ϕ for the four different vulcanizing systems used were approximately the same (fig. 5.8). This suggests the proposed equation (5.19) is valid and A_m should be used in place of A_o in order to account for any change in the crosslink density of the rubber matrix.

Even though the modulus A can satisfactorily be described using equation (5.19), the coefficients α and β did not appear to conform to the Guth-Gold equation; equation (2.60) predicts much lower moduli than the experimental values (fig. 5.8). The use of the Guth

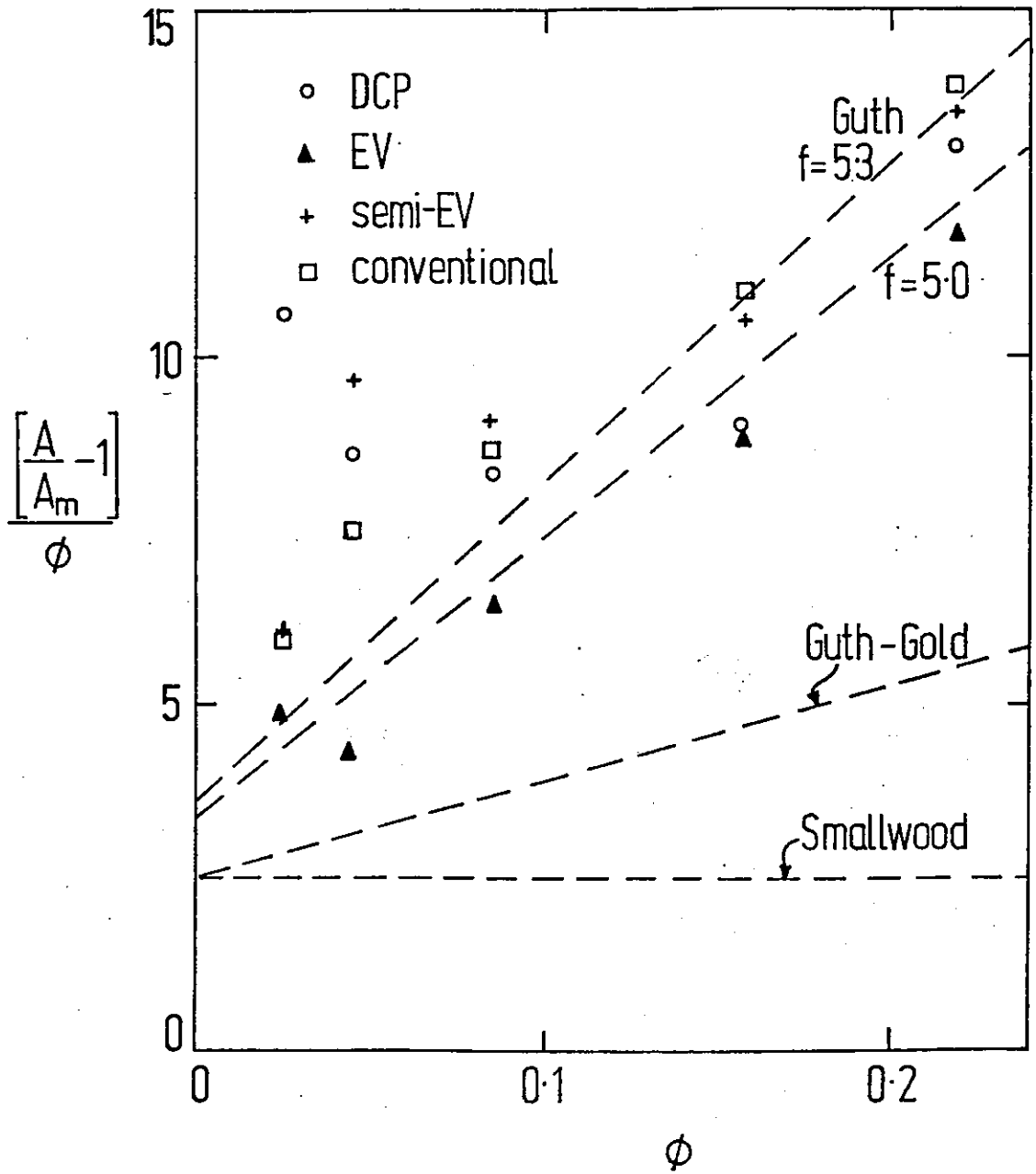


Figure 5.8. $\frac{A}{A_m} - 1$ as a function of ϕ for N347 black filled rubbers crosslinked using the four different vulcanizing systems.

Table 5.4: Influence of carbon black on the experimental values of A and of the rubber matrix (A_m)

Black loading (pphr N347)		0	6	10	20	40	60
Peroxide system	A_{expt}	0.51	0.61	0.68	0.79	1.15	1.82
	A_m	0.48	0.49	0.49	0.46	0.48	0.47
EV system	A_{expt}	0.29	0.34	0.37	0.47	0.76	1.14
	A_m	0.31	0.31	0.31	0.30	0.32	0.32
Semi-EV system	A_{expt}	0.34	0.41	0.53	0.66	1.02	1.59
	A_m	0.35	0.36	0.37	0.37	0.38	0.46
Conventional system	A_{expt}	0.40	0.45	0.55	0.71	1.16	1.76
	A_m	0.39	0.40	0.41	0.41	0.43	0.44

equation (2.61) with $f = 5.3$ may be able to fit the experimental data, but such value of f is rather high for most black (67), and consequently it is not favourable.

Lately (67-71) a concept of effective volume of carbon black was introduced where the total volume of 'filler' was assumed to comprise the volume fraction of filler, ϕ , and a proportion of rubber occluded within the black structure which is shielded from deformation. The shielded rubber acts as part of filler rather than part of rubber when subjected to a stress. Medalia (71) showed that about half of the occluded rubber acted as a filler and the effective volume of filler/carbon black (ϕ') was given by (equation 2.63),

$$\phi' = \phi + 0.5 \phi_{\text{occ}} \quad (5.20)$$

where ϕ_{occ} is the volume fraction of occluded rubber, which can be

calculated using equation (2.62). When the values of ϕ' were used in equation (5.19) in place of ϕ , the results obtained (fig. 5.9) were observed to conform with the Guth-Gold equation (equation 2.60), with a slope (β) of about 14 and an intercept (α) of 2.5. This suggests two possibilities: (a) the shape factor f of the Guth equation (2.61) plays an insignificant part in the hydrodynamic equation used for predicting the modulus of filled rubbers and (b) the occluded volume causes the differences between the experimental and those calculated using Guth-Gold/Guth type of equation shown in figure 5.8.

From the preceding discussion, it is clear that, in order to describe the modulus of carbon black filled rubbers over that of the unfilled rubbers, three factors have to be considered. (a) The effects of enhancement of crosslink density due to the presence of carbon black, (b) the effective volume fraction of filler/carbon black and (c) the hydrodynamic effects of the fillers/carbon black. When these factors are taken into consideration, the modulus of filled rubber (A) was found to conform to the equation,

$$A = A_m (1 + 2.5 \phi' + 14.1 \phi') \quad (5.21)$$

where A_m is the modulus of the rubber matrix and ϕ' is the effective volume fraction of filler/carbon black. For rubbers crosslinked using the peroxide and EV vulcanizing systems, results showed that A_m is equal to that of unfilled rubber (A_0), and for rubbers crosslinked using the semi-EV and conventional systems, values of A_m were essentially linearly related to the volume fraction of carbon black.

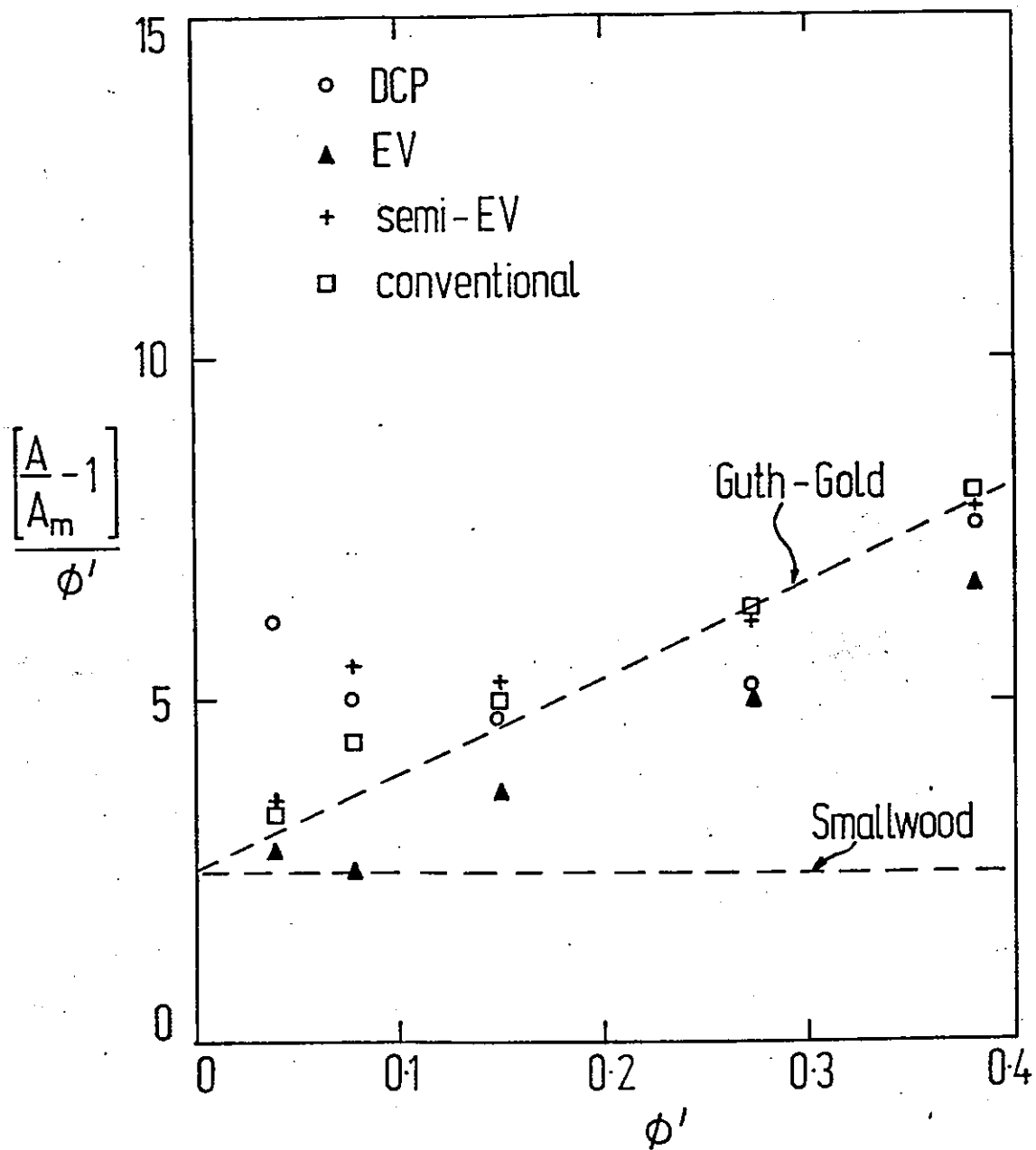


Figure 5.9. $\frac{\left(\frac{A}{A_m} - 1\right)}{\phi'}$ as a function of ϕ' for N347

black filled rubbers crosslinked using four different vulcanizing systems

5.3. Parameter C

5.3.1. Effects of crosslink density

The term $\frac{1}{C}$ has been equated to the $H_o - H_\infty$ term, which has been attributed to the effects of carbon black agglomeration. Payne, Whittaker and Smith (86) showed that $G_o - G_\infty$ (which in the notation used in this thesis is $H_o - H_\infty$) was dependent on carbon black loading but independent of crosslink density of the rubber. Their results appeared to be consistent with the results obtained for rubber filled with N550 black, where the values of $\frac{1}{C}$ were fairly independent of crosslink density (where the crosslink density was assumed to be linearly related to concentration of curatives).

It was observed that the value of C could be related to the ratio of the modulus of filled rubber (A) to that of the rubber matrix (A_m). Thus, neglecting any effects of crosslink density, the value of C for N550 filled rubbers may be written as

$$C = C_o X^{-1} \quad (5.22)$$

where C_o is the value of C for unfilled rubber and $X = \frac{A}{A_m}$. The values of A_m were calculated based on the results obtained in section 5.2.3 using the relation $A = \rho \frac{RT}{M_c}$, where the crosslink density was assumed to be linearly related to the concentration of curatives. Except for rubbers filled with high loading of black (≥ 40 pphr), values of CX for rubbers crosslinked using the sulphur and peroxide based vulcanizing systems were observed to be fairly constant (table 5.5). Similar results were also observed with rubbers filled with N762 black.

For rubbers filled with N347 black, values of C were not independent of crosslink density; $\frac{1}{C}$ increasing linearly with both

Table 5.5: Effects of crosslink density and black loading on parameter C for rubbers filled with N550 black

Black loading (pphr)	CBS/S ratios (pphr)	$\eta \times 10^4$ mole/cc	CX (MPa ⁻¹)	DCP (pphr)	$\eta \times 10^4$ moles/cc	CX (MPa ⁻¹)
Unfilled	0.5/0.9	0.71	5.37	1.0	0.64	6.41
	0.75/1.35	1.06	5.07	2.0	1.28	5.35
	1.0/1.8	1.41	5.06	3.0	1.93	7.23
	1.25/2.25	1.76	5.73	4.0	2.57	5.90
	1.5/2.7	2.12	5.74			
20		0.75	4.02		0.623	6.88
		1.13	4.79		1.25	6.78
	"	1.50	6.46	"	1.87	6.53
		1.88	5.20		2.49	4.77
		2.25	5.41			
40		0.76	3.45		0.64	5.87
		1.14	3.37		1.29	4.25
	"	1.52	3.45	"	1.93	3.87
		1.90	3.38		2.57	2.84
		2.28	4.90			
60		0.81	3.59		0.64	3.98
		1.22	2.83		1.28	2.29
	"	1.62	2.91	"	1.92	1.91
		2.03	2.36		2.56	1.47
		2.43	1.77			

the concentration of sulphur and dicumyl peroxide (table 5.6).

Table 5.6: Effects of crosslink density and black loading on parameter C for rubbers filled with N347 black

Black loading (pphr)	CBS/S ratios (pphr)	$\eta \times 10^4$ moles/cc	CX (MPa ⁻¹)	DCP (pphr)	$\eta \times 10^4$ moles/cc	CX (MPa ⁻¹)
20	0.5/0.9	0.75	4.0	1.0	0.62	5.14
	0.75/1.35	1.13	4.10	2.0	1.25	4.87
	1.0/1.8	1.50	3.54	3.0	1.87	3.32
	1.25/2.25	1.88	3.57	4.0	2.49	3.25
	1.5/2.7	2.25	3.19			
40		0.76	1.91		0.64	2.79
		1.14	1.58		1.29	1.77
	"	1.52	1.26	"	1.93	1.44
		1.90	1.22		2.57	1.27
		2.28	0.89			
60		0.81	1.52		0.64	2.32
		1.22	1.15		1.28	1.39
	"	1.62	0.66	"	1.92	1.23
		2.03	0.69		2.56	0.82
		2.43	0.27			

Thus taking into account both the effects of black loading and crosslink density, equation (5.22) may be written as:

$$C = \frac{C_o X^{-1}}{1+F(\eta, \phi)} \quad (5.23)$$

where $F(\eta, \phi)$ is a parameter which depends on crosslink density and volume fraction of carbon black.

For rubbers crosslinked using the sulphur vulcanizing system, the crosslink density can be varied by varying the proportions of sulphur and accelerator. But if the square root of the product of the concentrations of sulphur and accelerator is kept constant, the crosslink density will be approximately the same (96) and consequently $F(\eta, \phi)$ will be dependent only on ϕ . For rubbers filled with N347 black and crosslinked using conventional, semi-EV and EV vulcanizing systems, results (table 5.7) showed that the values of $\frac{C_o}{CX}$ were approximately the same at equal loading of black.

Table 5.7: Values of $\frac{C_o}{CX}$ for rubbers crosslinked using different vulcanizing systems

		$\frac{C_o}{CX}$		
Vulcanizing systems		Conventional	Semi-EV	EV
Carbon black (pphr)	CBS/S ratios (pphr)	0.6/3.0	1.0/1.8	6.0/0.3
	Unfilled	1.0	1.0	1.0
	5	1.05	0.96	1.01
	10	0.95	0.97	1.28
	20	1.44	1.32	1.32
	40	3.38	3.01	3.31
	60	3.76	4.74	4.96

As indicated in section one, the three different types of vulcanizing systems used give different proportions of mono-, di- and polysulphidic

crosslinks, but since crosslink densities were kept constant, then the values of $\frac{C_0}{CX}$ given in table 3.7 suggest that $F(\eta, \phi)$ is independent of the types of crosslink.

For filled and unfilled rubbers crosslinked using the semi-EV and peroxide systems, the crosslink density of the rubber matrix calculated from the equilibrium swelling data are given in table 5.3. The results are for rubbers crosslinked using a 1.8 pphr sulphur and a 3.0 pphr dicumyl peroxide for the sulphur and peroxide vulcanizing systems respectively. Assuming that the concentrations of the curative are linearly related to the crosslink density, then the crosslink density of the rubber vulcanized using different concentrations of curatives can be calculated. For several rubbers filled with N550 and N347 blacks, the calculated values of crosslink density (η) are given in tables 5.5 and 5.6. When the plots of $\frac{C_0}{CX}$ Vs η were made (fig. 5.10) for rubbers crosslinked using sulphur and peroxide vulcanizing systems, at equal black loadings, the values obtained were approximately the same. The values of C were therefore independent of the vulcanizing systems and this confirmed the view that the agglomeration of carbon black (as reflected by $\frac{1}{C}$ values) is independent of the types of crosslink present but depends on the crosslink density.

5.3.2. Effects of interparticle distance

Since $\frac{1}{C}$ has been associated with agglomeration of carbon black, then as suggested by Voet et. al. (82), the interparticle distance is an important parameter in determining the value of C.

Assuming that the carbon black particles are spherical and if the particles formed a cubic lattice of distance d between the centre of the spheres, then the volume fraction of the particle within the

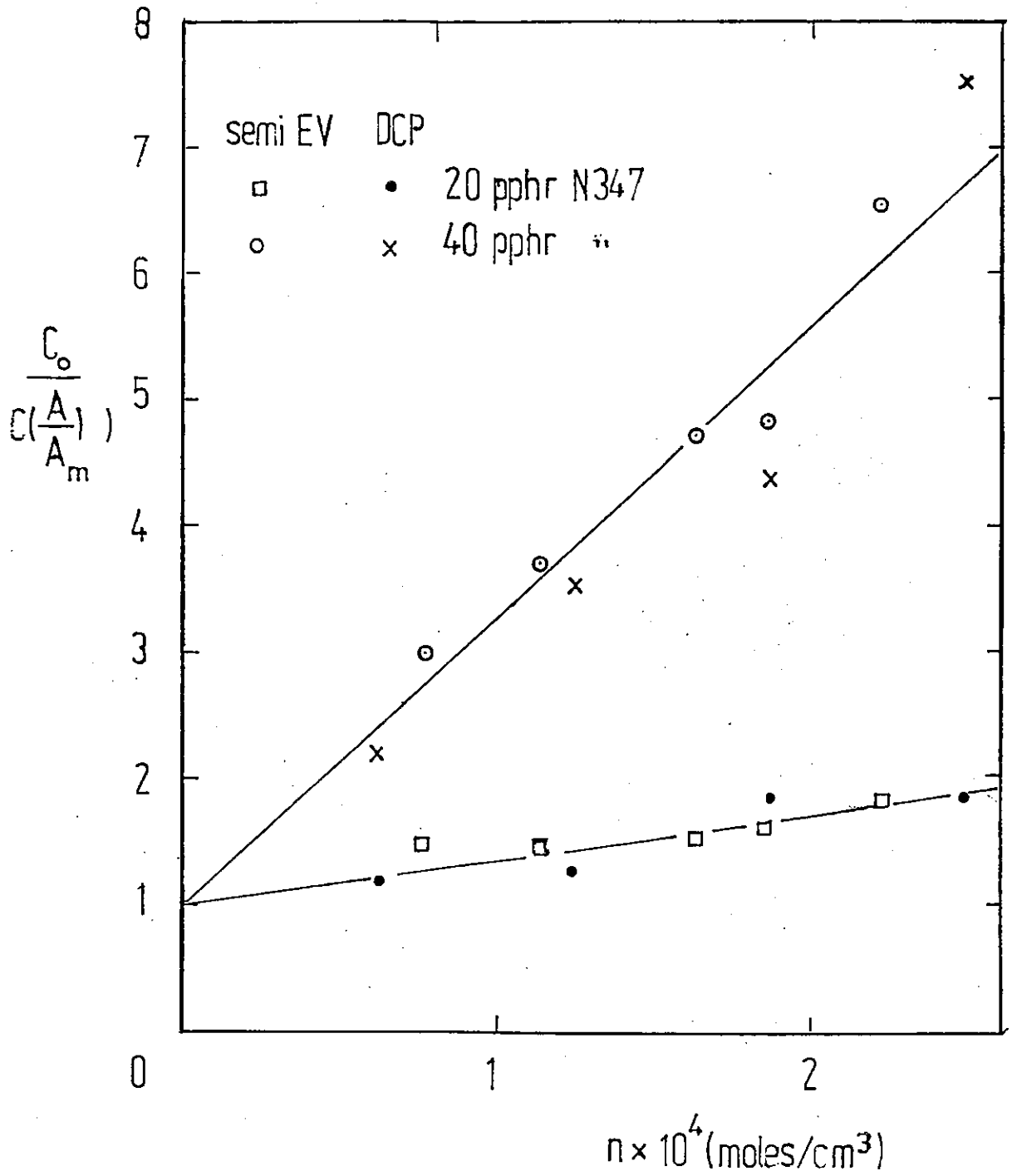


Figure 5.10. Variations of $\frac{C_o}{C(\frac{A}{A_m})}$ with crosslink density for rubbers filled with N347 black

lattice will be

$$\phi = \frac{2 \left(\frac{\pi D^3}{6} \right)}{d^3} \quad (5.24)$$

where D is the diameter of the particle. Rearranging equation (5.24) gives

$$d = \left(\frac{\pi D^3}{3\phi} \right)^{\frac{1}{3}} \quad (5.25)$$

Knowing D and ϕ , the mean interparticle separation d may be calculated.

The parameter C can be expressed as a function of d since the value of $\frac{1}{C}$ has been found to vary with filler loading. When values of $\ln\left(\frac{C_0}{CX}\right)$ were plotted as a function of $\ln\left(\frac{1}{d}\right)$, a linear relation having a slope of about 2.5 was obtained (fig. 5.11), i.e.

$$\frac{C_0}{CX} \propto \left(\frac{1}{d} \right)^{2.5} \quad (5.26)$$

According to Van der Tempel (105), the attractive forces due to Van der Waal's attraction between consecutive particles in a chain is inversely proportional to $d^{2.5}$ which is consistent with equation (5.26). Hence parameter C can be considered to arise from the Van der Waals forces of attraction and this is consistent with the view that the nature of agglomeration of carbon black is essentially resulting from particle attraction.

5.3.3. A combined function of crosslink density and interparticle distance

Equation (5.23) expresses the value of C as a function of crosslink density and volume fraction of black. Since the volume

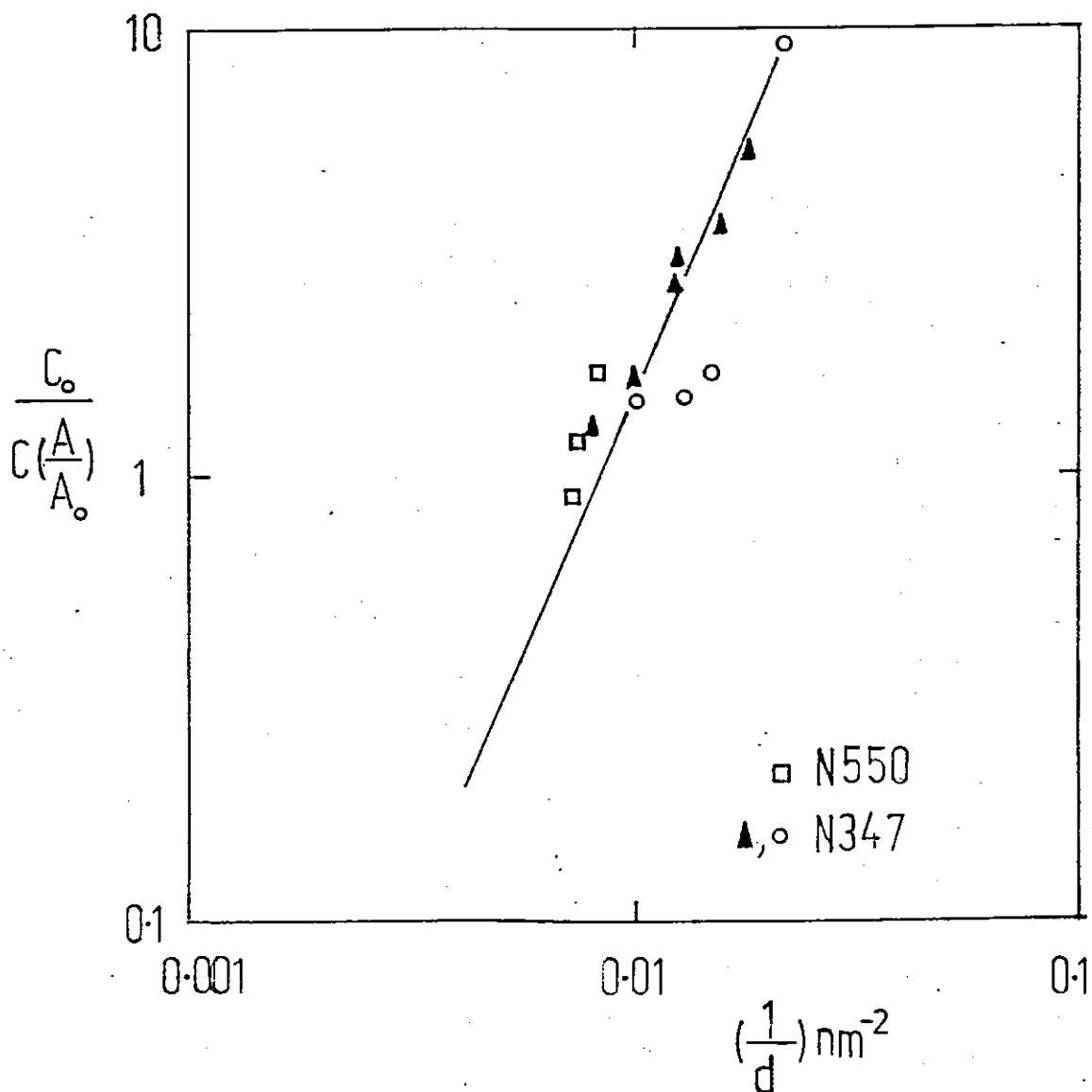


Figure 5.11. $\frac{C_o}{C(\frac{A}{A_m})}$ as a function of the reciprocal of interparticle distance for rubbers crosslinked using the sulphur vulcanizing system

fraction of filler is related to interparticle distance, then equation (5.23) may be more appropriately expressed as a function of crosslink density and interparticle distance, namely

$$\frac{C_o}{CX} = 1 + k.\eta \left(\frac{1}{d}\right)^{2.5} \quad (5.27)$$

where k is a proportionality constant. For rubbers filled with different types of black and crosslinked using the sulphur and the peroxide vulcanizing systems, plots of $\frac{C_o}{CX}$ Vs $\frac{\eta}{d^{2.5}}$ show a reasonable linear relationship (fig. 5.12) suggesting that equation (5.27) is valid. This implies that (a) parameter C depends on the Van der Waals forces of attraction between carbon black particles (b) the reciprocal of C is linearly related to the crosslink density of the rubber matrix and (c) for filled rubber the values of C may be scaled up over that of the rubber matrix in a similar way to that for parameter A.

5.4. Parameter B

Parameter B was observed to be independent of crosslink density but highly dependent on black loadings. The values of B initially increase with increasing black loading up to a maximum after which it starts to decrease.

Rubbers filled with different types of black gave maximum values of B at different black loadings. For instance, rubbers filled with N347 black gave a maximum value of B at lower loading than those filled with N550 black, while those filled with N110 black gave a maximum value of B at lower loading than both the N550 and the N347 black filled rubbers. These differences could be due to the differences in the properties of carbon black, namely (a) the chemistry of the surface groups (b) the structure and (c) the particle size/surface area.

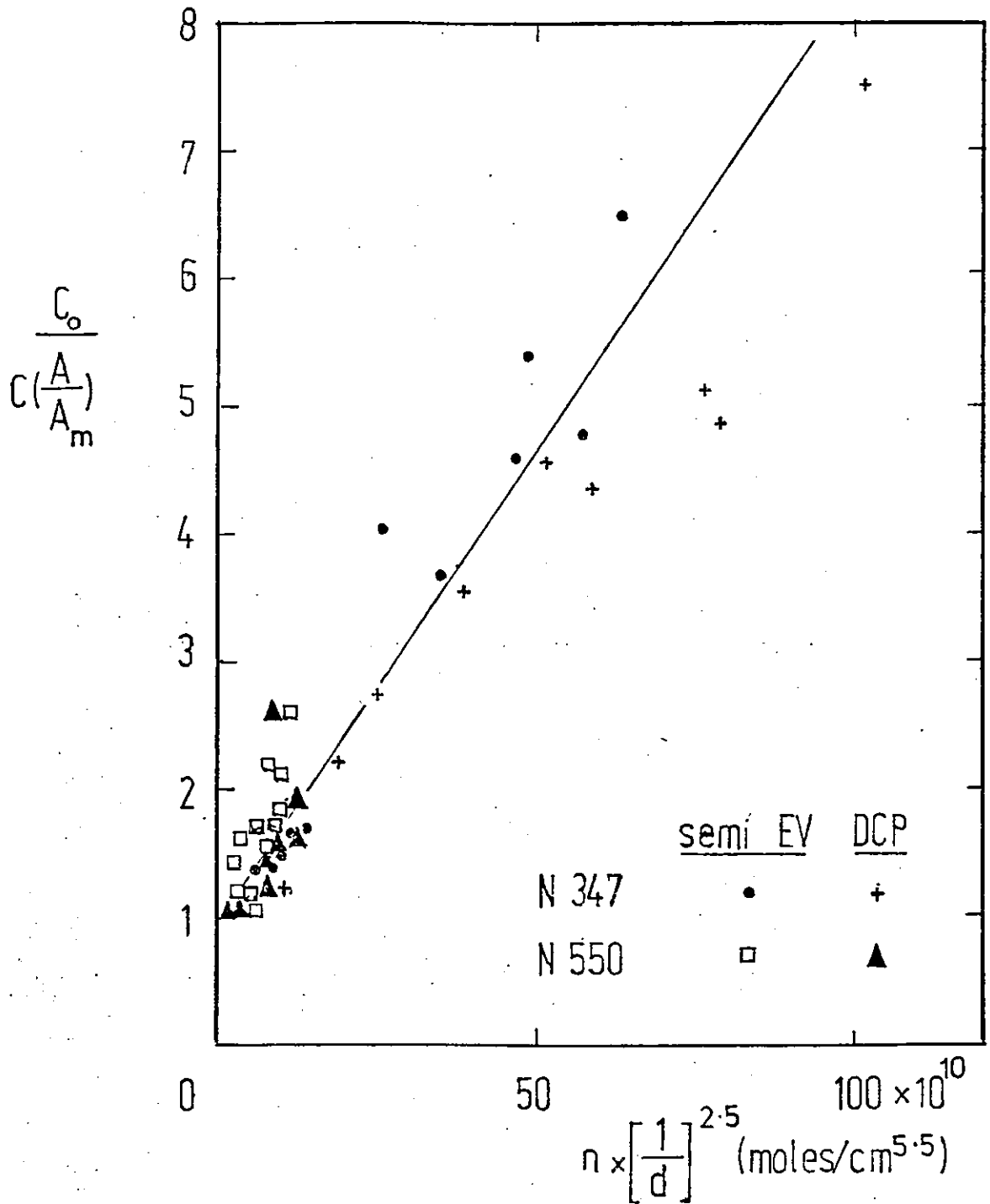


Figure 5.12. $\frac{C_o}{C\left(\frac{A}{A_m}\right)}$ as a function of $n \times \left(\frac{1}{d}\right)^{2.5}$

for rubber of different types and concentrations of crosslink

The chemical reactivity of carbon black, is, for a large part, dependent on the chemical groups on the surfaces, which are introduced during the formation of carbon black. The surface groups are mainly comprised of oxygen and nitrogen, the proportion of which depends on the preparation techniques involved in the production of carbon black. For carbon blacks which undergo the same process of production, the proportions and types of the surface groups are about the same (106). Since the carbon blacks used in this thesis were all prepared by the same technique viz. partial combustion of hydrocarbon in a furnace, then the proportions and types of surface groups present were expected to be about the same. Hence the differences observed with the values of B are unlikely to be associated with the differences in the surface chemistry (factor a).

The agglomerate structure of carbon black influences the modulus/stiffness of rubbers, details of which were discussed earlier. A similar phenomena may also have caused the differences in the maximum values of B observed with rubbers filled with different types of carbon black. However based on the results for rubbers filled with N347 and N550 blacks, which are of about the same structure (as measured by DBPA values), but giving the maximum values of B at different black loading, then it is unlikely that the effects observed were due to differences in the carbon black structure (factor b).

Differences in particle size of fillers caused a variation in the physical properties of rubber (107). The smaller particle (or larger surface area) blacks for instance generally give a higher tensile modulus than the corresponding larger particle blacks. If parameter B is a function of the particle size of filler, then the maximum values of B, at a constant black loading, must be consistent

with the change in particle diameter. For the three different types of carbon black quoted above, their particle diameters are of the order,

$$N110 < N347 < N550$$

Apparently, the maximum values of B for the three different types of black were observed to vary in a similar order, and it is therefore likely that parameter B is a function of carbon black particle size/surface area.

When the values of B were plotted against the product of surface area of carbon black, S and $(\frac{\phi}{1-\phi})$ (where ϕ = volume fraction of black) for all rubbers crosslinked using the sulphur (semi-EV) vulcanizing system, results gave a common curve (fig. 5.13), with the maximum values of B for all rubbers coincide. Similar results were also obtained with rubbers crosslinked using the peroxide system (fig. 5.14), and this suggests that parameter B is more appropriately expressed as a combined function of surface area and volume fraction of black (or more correctly, $\frac{\phi}{1-\phi}$).

The trends for the sulphur (semi-EV) and peroxide cured rubbers in the plots of B Vs $S(\frac{\phi}{1-\phi})$ appear to be similar. Irrespective of the vulcanizing systems used, values of B appeared to be highly dependent on the total surface area of black. Changing the cross-linking system from the semi-EV (CBS/S) to the peroxide system increased the values of B for filled rubbers by about 50% without appreciably affecting those of the corresponding unfilled rubbers.

The dependence of parameter B on the surface area of black suggest the possibility that the former is associated with the carbon black - rubber adhesion or what is commonly known as "bound rubber".

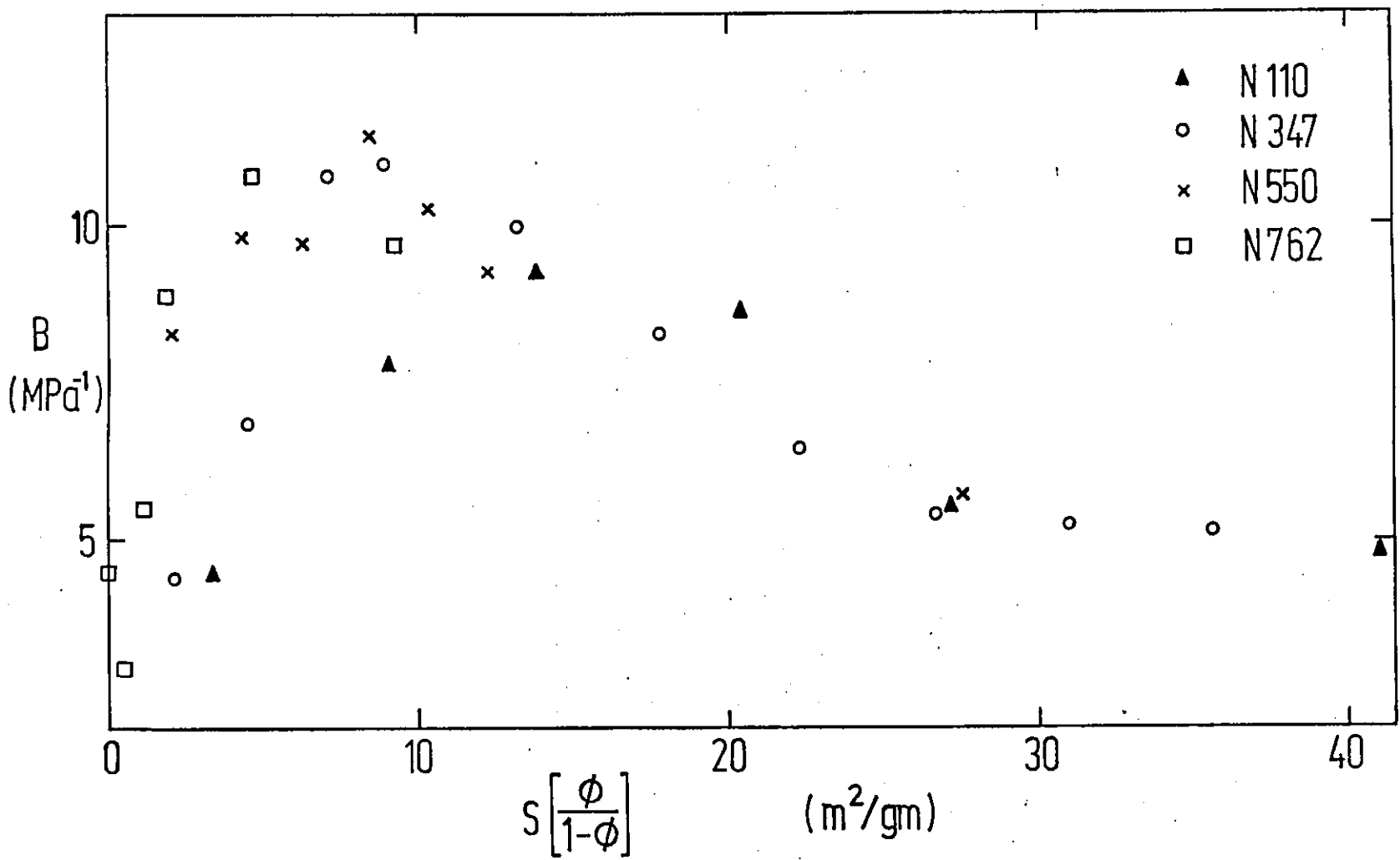


Figure 5.13. Parameter B as a function of $S \left(\frac{\phi}{1-\phi} \right)$ for rubbers filled with different types of black and crosslinked using the sulphur vulcanizing systems

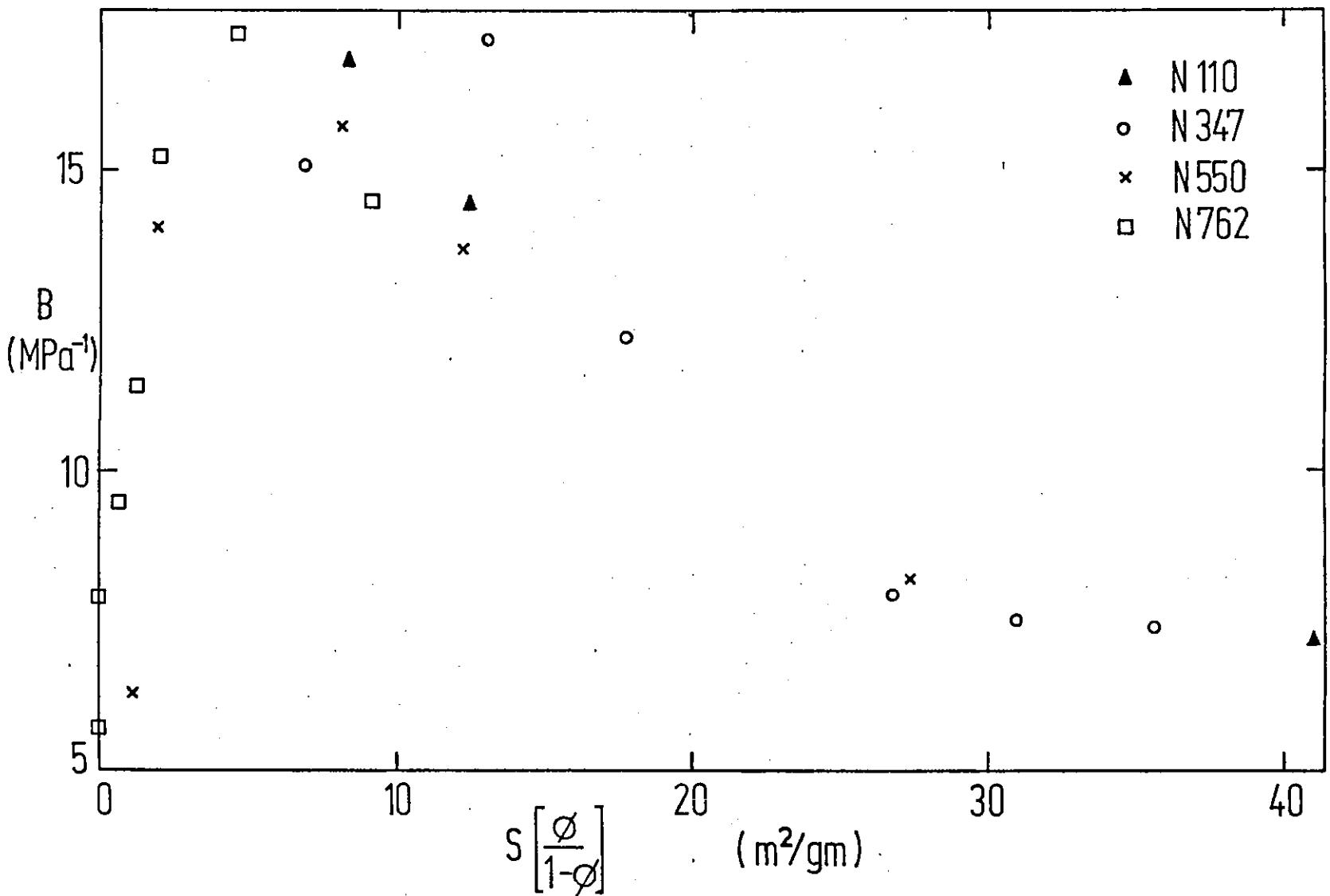


Figure 5.14. Parameter B as a function of $S \left(\frac{\phi}{1-\phi} \right)$ for rubbers filled with different types of black and crosslinked using the peroxide system

Earlier studies (108,109) suggest that bound rubber is proportional to the surface area of carbon black, but later, from an NMR investigation on the interactions between carbon black and rubber, O'Brian et. al. (110) showed that bound rubber is not linearly related to the total surface area of black. The bound rubber was reported to increase initially with $S(\frac{\phi}{1-\phi})$ values but subsequently decreases after reaching a maximum.

The finding of O'Brian is consistent with the plots shown in figures 5.13 and 5.14. The initial increase in the values of B with $S(\frac{\phi}{1-\phi})$ was due probably to the increase in rubber-carbon black contact. At higher loadings of black, the value of B reaches a maximum and then decreases. The decrease, could be due to the tendency of the black presence in rubber to form agglomerates, because such formation reduces the available surface area for the rubber-carbon black interactions.

SECTION 6: SUMMARY AND CONCLUSIONS

SECTION 6. SUMMARY AND CONCLUSIONS

By assuming that the shear modulus is independent of strain at high strains, a semi-empirical relationship consistent with the elasticity theory for the first cycle deformation has been obtained. The relationship appears to be applicable to various types of filled and unfilled rubbers subjected to low to moderate strains. It relates a modulus, H in tension/compression or G in simple shear to a strain invariant I_1 and three material parameters, A, B and C, namely,

$$H \text{ or } G = A + \frac{1}{B(I_1 - 3)^{\frac{1}{2}} + C} \quad 6.1$$

where $H = \frac{\sigma}{\lambda - \lambda^{-2}}$, $G = \frac{\sigma}{\gamma}$, $I_1 = \lambda_1^2 + \lambda_2^2 + \lambda_3^2$ and σ , λ , γ are the nominal stress, extension ratio and shear strain respectively.

At equal I_1 , the modulus H was observed to be identical to G.

The parameter A is the limiting shear modulus at high strain. For unfilled rubber, the parameter A was found to be proportional to the crosslink density of the rubber and approximately equal to the NkT term of the statistical theory of elasticity, suggesting that it arises from the change in the entropy of the network chains during deformation.

The incorporation of carbon black gives a non-linear increase in A with increasing volume fraction of carbon black. The stiffening effect of carbon black is usually explained by the use of the Guth-Gold type of equation, giving the modulus as a function of shape factor, occluded volume and hydrodynamic effects of filler. However with rubbers crosslinked using different vulcanizing systems, the Guth-Gold equation was found to be inadequate for predicting the values of A

for filled rubbers. The discrepancy was attributed to the differences in the crosslinking efficiency of the vulcanizing systems used due to the presence of carbon black. To take into account the change in crosslink density, it is proposed that the Guth-Gold equation be modified to,

$$A = A_m(1 + 2.5 \phi' + 14.1 \phi'^2) \quad (6.2)$$

where A , A_m are the moduli of filled and that of the rubber matrix respectively and ϕ' is the effective volume fraction of carbon black, being taken as the sum of the volume fraction of carbon black (ϕ) and half that of the occluded rubber (ϕ_{occ}).

Assuming that carbon black has no effect on the crosslinking efficiency of the peroxide system, it could be shown that the increase in crosslink density of the corresponding rubbers crosslinked using the semi-EV and conventional N-cyclohexyl benzothiazole-2-sulphenamide accelerated sulphur vulcanizing systems was linearly related to the volume fraction of carbon black. With a 60 pphr N347 black, the increase in crosslink density of rubber crosslinked with the sulphur vulcanizing systems was about 15% higher than the corresponding rubber crosslinked using the peroxide vulcanizing system.

The reciprocal of C is the maximum change in modulus with strain or $G_o - G_\infty$. The values of $\frac{1}{C}$ were observed to be linearly related to the crosslink density but independent of the types of crosslink present. It was also observed to be related to the reciprocal of $d^{2.5}$, where d is the interparticle distance and this suggests that the nature of $\frac{1}{C}$ or the agglomeration of carbon black as essentially resulting from particle separation.

The value of B is negligible at the limiting low and high strains

and it determines the change in modulus with strain between these two limits. It was found to be independent of crosslink density of the rubber matrix, but highly dependent on the total surface area of carbon black. When the values of B were plotted against the product of surface area of carbon black and $(\frac{\phi}{1-\phi})$, it initially increased to a maximum and then decreased to a constant value. The exact significance of B is still obscure but it may be associated with the rubber-filler interactions.

In the study of the stiffening effects of filler, the challenging problem is the development of a more quantitative molecular understanding of the effects of filler in rubber. The proposed relationship enables the stress contributions from the rubber matrix and carbon black be separated, analysed and quantified. A similar analysis was not possible with other established equations and this may constitute an important step in the development of a molecular understanding of the stiffening effects of fillers.

The proposed relationship also enables the prediction of the stress-strain behaviour of rubbers in different modes of deformation to be made from the values of A, B and C obtained from a simple mode of deformation. This will enable the testing of rubbers to be simplified and rationalized.

APPENDIXAssumptions used for the statisticalTheory of Elasticity

- (a) The actual network is replaced by an ideal network in which each segment of a molecule between successive points of cross-linkage is considered to be a freely jointed Gaussian chain and the N chains of network per unit volume has the same contour length.
- (b) In either strained or unstrained states, each junction points of the chain may be regarded as fixed at its mean position.
- (c) There is no change of volume on deformation.
- (d) The effect of deformation is to change the component of the vector of each chain in the same ratio as the corresponding dimension of the bulk materials.
- (e) The entropy of the network is the sum of the entropies of the individual chains.
- (f) The mean square end to end distance for the whole assembly of chains in the unstrained state is the same as for the corresponding sets of free chains.

Assumption (a) was made to avoid mathematical complexity. In actual materials though, the energetic effects of interaction between segments of the same molecules should be taken into account.

The general form of long chain molecules is independent of the precise geometry of the chain provided that the number of bonds, n , about which relatively free rotation can occur is sufficiently large. The geometry of the chain affect the mean square end to end distance $\langle r^2 \rangle$, and provided that the distance between the ends of the chain is not comparable with the fully extended length, nl of the chain (i.e. $r \ll nl$), assumption (a) is valid.

The junction points of the chain are not fixed in space since the molecules themselves are in continuous motion. If the motion of those junction points is taken into consideration, the theory will be more complicated since mobile parts of the chain give entropy contribution. As a result, assumption (b) was made. In reality, only those junction points which are located on the boundary surfaces of the rubber may be regarded as fixed (13), all other junction points are fluctuating. The fluctuating junction points are very much larger in number than the fixed junction points and the assumption that junction points are fixed at its mean position is not justified. Even though the junction points are fluctuating, the overall results may not be significantly different from that which assume that the junction points are fixed since the entropy of the ends of a crosslink (two junction points) have two entropic components, the resultant contribution of which may cancel out.

The assumption that no change in volume occurs on deformation (assumption c) implies that the material is incompressible and the bulk modulus is many fold greater than its shear modulus.

Measurements suggest that the volume changes on deformation is very small (of the order of 10^{-4}), with a Poisson's ratio of about 0.4999 (78, 111, 112). However, for rubber containing filler particles which form vacuoles when the specimen is stretched, dilation is no longer negligible (113).

Assumption (d) is the affine deformation assumption. It is the key assumption in the theory since it relates the deformation of the individual chains to the macroscopic strain in the material. It is justifiable if the fluctuations of the position of junction points (arising from thermal agitation of the associated chains) are neglected and r is much smaller than nl .

The assumption (e) arises from the assumption that the chain is Gaussian and all configurations possess the same energy.

REFERENCES

1. Allen P.W. and Bloomfield G. Chapter 1 in "The Chemistry and Physics of Rubber-like Substances" ed. Bateman L. Maclaren and Sons, London 1963.
2. Fisher H.L. and Gerke R.H. Chapter 3 in "Chemistry and Technology of Rubber" ed. Davis G.C. and Blake J.T., Reinhold, N.Y. 1937.
3. Porter M. Gumi Kunst. (1969), 22(8), 419.
4. Elliott D.J. and Tidd B.K. Prog. Rubb. Technol. (1974), 37, 83.
5. Porter M. Pg. 165 in "The Chemistry of Sulphides" ed. Tobolsky A.V. Interscience Publishers, N.Y. 1968.
6. Bateman L, Cunneen J.I., Moore C.G., Mullins L. and Thomas A.G. Chapter 19 in "The Chemistry and Physics of Rubber-like substances" ed. Bateman L., Maclaren and Sons, London, 1963.
7. Busse W.F. J. Chem. Phys. (1932), 36, 2862.
8. Meyer K.H., Von Susich G., and Valko E.T. Koll. Z. (1932), 59, 208.
9. Guth E. and Mark H., Monats Chem. (1934), 65, 93.
10. Kuhn W. Koll. Z. (1936), 76, 258.
11. Wall F.T. J. Chem. Phys. (1942), 10, 485.
12. Flory P.J. and Rehner J. J. Chem. Phys. (1943), 11, 512.
13. James H.M. and Guth E., J. Chem. Phys. (1943), 11, 455.
14. Treloar L.R.G. Trans. Faraday Soc. (1943), 39, 36, 241.
15. Anthony R.L., Gaston R.H. and Guth E. J. Phys. Chem. (1942), 46, 826.
16. Wood L.A. and Roth F.L. J. Appl. Phys. (1944), 15, 781.
17. Shen M., McQuarrier D.A. and Jackson J.K. J. Appl. Phys. (1967), 38, 791.

18. Flory P.J. Chem. Revs. (1944), 35, 51.
19. Mullins L. J. Appl. Polym. Sci. (1959), 2, 1, 257.
20. Langley N.R. Macromolecules (1968), 1, 348.
21. Ole Kramer, O. Polym. (1979), 20, 1336.
22. Ferry J.D. Polym. (1979), 20, 1343.
23. Love A.E.H. "The Mathematical Theory of Elasticity". 4th Ed., Cambridge University Press, 1927.
24. Treloar L.R.G. Trans. Faraday Soc. (1944), 40, 59.
25. Mooney M.J., J. Appl. Phys. (1940), 11, 582.
26. Gumbrell, S.M., Mullins L. and Rivlin R.S. Trans. Faraday Soc. (1953), 49, 1405.
27. Mark J.E. Rubb. Chem. Technol. (1975), 48, 495.
28. Rivlin R.S. and Saunders D.W. Phil. Trans. R. Soc. (1951), A243, 251.
29. Rivlin R.S. Phil. Trans. R. Soc. (1948), A240, 459; (1948), A241, 379.
30. Obata Y., Kawabata S. and Kawai H. J. Polym. Sci. (1974), A2, 8, 903.
31. Jones D.F. and Treloar L.R-G. J. Phys. D (Appl. Phys.) (1975), 8, 1285.
32. Isihara A., Hashitsuma N. and Tatibana M. J. Chem. Phys. (1951), 19, 1508.
33. Alexander H. Int. J. Engng. Sci (1968), 6, 549.
34. Tschoegl N.W. J. Polym. Sci. (1959), A1, 9.
35. Gent A.N. and Thomas A.G. J. Polym. Sci. (1958), 28, 625.
36. Ogden R.W. Proc. R. Soc. (1972), A326, 565.
37. Valanis K.C. and Landel R.F. J. Appl. Phys. (1967), 38, 2997.

38. Treloar L.R.G. "The Physics of Rubber Elasticity" 3rd Edition, Clarendon Press, Oxford 1975.
39. Tobisch K. Rubb. Chem. Technol. (1980), 53, 836.
40. Arenz R.J. J. Appl. Polym. Sci. (1977), 21, 2453.
41. Vangerko H. and Treloar L.R.G. J. Phys. D. (Appl. Phys.) (1978), 11, 1969.
42. Dannenburg E.M. Rubb. Chem. Technol. (1975), 48, 410.
43. Horn J.B. Chapter 6 in "Rubber Technology and Manufacture" ed. Blow C.M. Newness-Butterworths, London 1977.
44. Donnet J.B. and Voet A. "Carbon black - Physics, Chemistry and Elastomer Reinforcement", Marcel Dekker Inc. N.Y., 1976.
45. Goodwin N. and Park C.R. Ind. Engng. Sci (1968), 20, 621.
46. ASTM test: D2414-79.
47. Brunneuer S.B., Emmett P.H. and Teller E. J. Am. Chem. Soc. (1938), 60, 309.
48. ASTM test: D3765-80.
49. ASTM test: D1510-81.
50. Medalia A.I., Dannenburg E.M., Heckman F.A. and Cotten G.R. Rubb. Chem. Technol. (1973), 46, 1239.
51. Jenson J. and Kraus G. Rubb. Chem. Technol. (1971), 44, 1287.
52. ASTM test: D1765-82.
53. Heizerby and Pahl. Verh. Ver. Behard. Gewerb. (1891), 415; (1892), 25.
54. Ditma H. Gummi Ztg. (1906), 20, 294, 733, 844, 1077.
55. Shepard N.A., Street N.A. and Pack C.R. Chapter 11 in "Chemistry and Technology of Rubber" ed. Davis C.C. and Black J.T., Reinhold, N.Y. 1953.

56. Scott J.R. *Ind. Rubb. J.* (1951), 121, 424, 513.
57. Kraus G. *Rubb. Chem. Technol.* (1965), 38, 1070.
58. Dannenburg E.M. *Rubb. Chem. Technol.* (1975), 48, 410.
59. Medalia A.I. *Rubb. Chem. Technol.* (1978), 51, 437.
60. Gessler A.M., Hess W.M. and Medalia A.J. *Plastics and Rubb.: Processing 1978, Parts III & IV.*
61. Einstein A. *Ann. Physik* (1906), 19, 289; (1911), 34, 1591.
62. Smallwood H. *Rubb. Chem. Technol.* (1945), 18, 292.
63. Guth E. and Gold O. *Phys. Rev.* (1938), 53, 322.
64. Guth E. *Rubb. Chem. Technol.* (1945), 18, 591.
65. Mullins L. and Tobin N.R. *J. Appl. Polym. Sci.* (1965), 9, 2993.
66. Dannenburg E.M., Heckman F.A. and Medalia A.I. *Int. Rubb. Conf., Paris 1970.*
67. Medalia A.I. *J. Coll. Int. Sci.* (1970), 32, 115.
68. Kraus G. *J. Polym. Sci.* (1970), 88, 601.
69. Kraus G. *Rubb. Chem. Technol.* (1971), 44, 199.
70. Sambrook R.W. *J. Inst. Rubb. Ind.* (1970), 4, 210.
71. Medalia A.I., *Rubb. Chem. Technol.* (1972), 45, 1171.
72. Medalia A.I., *Rubb. Chem. Technol.* (1973), 46, 877.
73. Heckman F.A. and Medalia A.I. *J. Inst. Rubb. Ind.* (1969), 3, 66.
74. McDonald G.C. and Hess W.M. *Rubb. Chem. Technol.* (1977), 50, 842.
75. ASTM test: D3493-79.
76. Kraus G. *J. Appl. Polym. Sci.* (1971), 15, 1679.
77. Medalia A.I. *Rubb. Chem. Technol.* (1974), 47, 411.
78. Holownia B.P. *Rubb. Chem. Technol.* (1975), 48, 247.
79. Payne A.R. *J. Appl. Polym. Sci.* (1962), 6, 57, 368.
80. Payne A.R. Chapter 3 in "Reinforcement of Elastomer"
ed. Kraus G. Interscience, N.Y. (1965).

81. Harwood J.A.C. and Payne A.R. *Cashier du Groupe Francois de Rheologie*. N.4. Tome 1 (1967).
82. Voet A., Cook F.R. and Hogue R. *Rubb. Chem. Technol.* (1970), 43, 969.
83. Gessler, A.M. *Rubb. Age*, (1960), 86, 1017; (1960) 87, 64; (1961), 88, 658.
84. Payne A.R. *J. Appl. Polym. Sci.* (1963), 7, 1815.
85. Sircar A.K. and Lamond T.G. *Rubb. Chem. Technol.* (1975), 48, 79.
86. Payne A.R., Whittaker R.E. and Smith J.F. *J. Appl. Polym. Sci.* (1972), 16, 1192.
87. Gurney W.A. and Gough V.E. *Trans. Inst. Rubb. Ind.* (1946), 22, 132.
88. Blow C.M., Demiri, H.B. and Southwart D.W. *J. Inst. Rubb. Ind.* (1974), 8, 244.
89. Wheelan M.A. *Rubb. Chem. Technol.* (1978), 51, 1083.
90. Gent A.N. *J. Appl. Polym. Sci.* (1962) 6(22), 433, 422.
91. Mullins L. *J. Rubb. Res.* (1947), 16, 275.
92. Mullins L. *J. Phys. and Chem.* (1950), 54, 237.
93. James A.G., Green A. and Simpson G.M. *J. Appl. Polym. Sci.* (1975), 19, 2033.
94. Gregory M.J. *Plastics and Rubber: Mat. and Appl.* 1979, Nov.
95. James A.G. and Green A. *J. Appl. Polym. Sci.* (1975), 19, 2319.
96. Coran A.Y. *Rubb. Chem. Technol.* (1964), 673, 37.
97. Kraus G. *Rubb. Chem. Technol.* (1957), 30, 929.
98. Lorenz O. and Park C.R. *J. Polym. Sci.* (1961), 50, 299.
99. Porter M. *Rubb. Chem. Technol.* (1967), 40, 866.
100. Flory P.J. and Rehner J. Jnr. *J. Chem. Phys.* (1943), 11, 521.
101. Kraus G. *J. Appl. Polym. Sci.* (1963), 7, 861.

102. Mullins L. J. Polym. Sci. (1956), 19, 225.
103. Sheehan J. and Bisco A.L. Rubb. Chem. Technol. (1966), 39, 149.
104. Bateman L., Moore C.G., Porter M. and Saville B. Chapter 15 in "The Chemistry and Physics of Rubber-like substances" ed. Bateman L., Maclaren and Sons, London 1963.
105. Van der Tempel M., J. Coll. Sci. (1961), 16, 284.
106. Donnet J.B. and Voet A. "Carbon-black - Physics, Chemistry and Elastomer Reinforcement" Marcel Dekker Inc. N.Y. 1976.
107. Gessler A.M., Hess W.M. and Medalia A.I. Plastics and Rubb.: Processing 1978, Part II.
108. Pliskin I. and Tokita N. J. Appl. Polym. Sci. (1972), 16, 473.
109. Meissner B. Rubb. Chem. Technol. (1975), 48, 810.
110. O'Brien J., Casbell E., Wardell G.E. and McBrierty V.J. Macromolecules (1976), 9, 653.
111. Holf W.L. and McPherson A.T. Rubb. Chem. Technol. (1937), 10, 412.
112. Gee G., Stern J. and Treloar L.R.G. Trans. Faraday Soc. (1950), 46, 1101.
113. Smith T.L. Rubb. Chem. Technol. (1961), 34, 123.
114. James H.M. and Guth E., J. Chem. Phys. (1947), 15, 669.